

Performance Characteristics of Modern Recycled Asphalt Mixes in Missouri, Including Ground Tire Rubber, Recycled Roofing Shingles, and Rejuvenators

Final Report
March 2019

Sponsored by

Midwest Transportation Center
Missouri Dept. of Transportation
Construction & Materials Division
U.S. Department of Transportation
Office of the Assistant Secretary for
Research and Technology



IOWA STATE UNIVERSITY
Institute for Transportation

About MTC

The Midwest Transportation Center (MTC) is a regional University Transportation Center (UTC) sponsored by the U.S. Department of Transportation Office of the Assistant Secretary for Research and Technology (USDOT/OST-R). The mission of the UTC program is to advance U.S. technology and expertise in the many disciplines comprising transportation through the mechanisms of education, research, and technology transfer at university-based centers of excellence. Iowa State University, through its Institute for Transportation (InTrans), is the MTC lead institution.

About InTrans

The mission of the Institute for Transportation (InTrans) at Iowa State University is to develop and implement innovative methods, materials, and technologies for improving transportation efficiency, safety, reliability, and sustainability while improving the learning environment of students, faculty, and staff in transportation-related fields.

ISU Non-Discrimination Statement

Iowa State University does not discriminate on the basis of race, color, age, ethnicity, religion, national origin, pregnancy, sexual orientation, gender identity, genetic information, sex, marital status, disability, or status as a U.S. veteran. Inquiries regarding non-discrimination policies may be directed to Office of Equal Opportunity, 3410 Beardshear Hall, 515 Morrill Road, Ames, Iowa 50011, Tel. 515-294-7612, Hotline: 515-294-1222, email eooffice@iastate.edu.

Notice

The contents of this report reflect the views of the authors, who are responsible for the facts and the accuracy of the information presented herein. The opinions, findings and conclusions expressed in this publication are those of the authors and not necessarily those of the sponsors.

This document is disseminated under the sponsorship of the U.S. DOT UTC program in the interest of information exchange. The U.S. Government assumes no liability for the use of the information contained in this document. This report does not constitute a standard, specification, or regulation.

The U.S. Government does not endorse products or manufacturers. If trademarks or manufacturers' names appear in this report, it is only because they are considered essential to the objective of the document.

Quality Assurance Statement

The Federal Highway Administration (FHWA) provides high-quality information to serve Government, industry, and the public in a manner that promotes public understanding. Standards and policies are used to ensure and maximize the quality, objectivity, utility, and integrity of its information. The FHWA periodically reviews quality issues and adjusts its programs and processes to ensure continuous quality improvement.

Technical Report Documentation Page

1. Report No.	2. Government Accession No.	3. Recipient's Catalog No.	
4. Title and Subtitle Performance Characteristics of Modern Recycled Asphalt Mixes in Missouri, Including Ground Tire Rubber, Recycled Roofing Shingles, and Rejuvenators		5. Report Date March 2019	
		6. Performing Organization Code	
7. Authors William G. Buttlar, James Meister, Behnam Jahangiri, Hamed Majidifard, and Punyaslok Rath		8. Performing Organization Report No.	
9. Performing Organization Name and Address Department of Civil and Environmental Engineering University of Missouri E2509 Lafferre Hall Columbia, MO 65211		10. Work Unit No. (TRAIS)	
		11. Contract or Grant No. Part of DTRT13-G-UTC37	
12. Sponsoring Organization Name and Address Midwest Transportation Center U.S. Department of Transportation 2711 S. Loop Drive, Suite 4700 Office of the Assistant Secretary for Ames, IA 50010-8664 Research and Technology Missouri Dept. of Transportation 1200 New Jersey Avenue, SE Construction & Materials Division Washington, DC 20590 P.O. Box 270 Jefferson City, MO 65102		13. Type of Report and Period Covered Final Report	
		14. Sponsoring Agency Code	
15. Supplementary Notes Visit www.intrans.iastate.edu for color pdfs of this and other research reports.			
16. Abstract A comprehensive laboratory and field investigation was carried out to evaluate the performance of recycled asphalt mixtures in Missouri by researchers at the University of Missouri-Columbia, in collaboration with the Missouri Department of Transportation and the Midwest Transportation Center. Eighteen field sections were evaluated, including a number of sections from the recent Long-Term Pavement Performance (LTPP), Special Pavement Sections (SPS-10) project in Osage Beach, Missouri, which was constructed in 2016. Binder testing and mix performance tests were carried out on field cores and laboratory compacted specimens. Based on the findings of the study, the following conclusions were drawn: (1) Missouri's practices for the responsible and effective use of recycled materials is sound and continues to improve over time. Recent mix designs demonstrate more appropriate balancing between recycled material levels and virgin binder selection, resulting in better performance tests results when compared to older recycled mix designs. (2) Opportunities exist for further improving recycled mix design methods and recycling optimization in Missouri, including (a) moving to higher asphalt binder replacement (ABR) levels, by implementing mixture performance tests (balanced mix design); (b) increasing the use of recycled ground tire rubber (GTR) in Missouri mixes, by using balanced mix design to certify mixes using new, more economical GTR recycling methods, and; (c) researching the use of recycled materials in stone-mastic asphalt (SMA) designs. It is recommended to further evaluate and fine-tune mix performance tests for use in balanced mix design, which is particularly important for modern, heterogeneous recycled mixes.			
17. Key Words binder testing—field cores—field performance—laboratory mixtures— Missouri asphalt mixtures—mixture characterization—performance testing— plant mixtures—RAP—RAS—rejuvenator—rubber		18. Distribution Statement No restrictions.	
19. Security Classification (of this report) Unclassified.	20. Security Classification (of this page) Unclassified.	21. No. of Pages 104	22. Price NA

PERFORMANCE CHARACTERISTICS OF MODERN RECYCLED ASPHALT MIXES IN MISSOURI, INCLUDING GROUND TIRE RUBBER, RECYCLED ROOFING SHINGLES, AND REJUVENATORS

**Final Report
March 2019**

Principal Investigator

William G. Buttlar, Glen Barton Chair in Flexible Pavements
Civil and Environmental Engineering, University of Missouri

Co-Principal Investigator

James Meister, Research Engineer
Civil and Environmental Engineering, University of Missouri

Research Assistants

Behnam Jahangiri, Hamed Majidifard, and Punyaslok Rath

Authors

William G. Buttlar, James Meister, Behnam Jahangiri, Hamed Majidifard, and Punyaslok Rath

Sponsored by

Missouri Department of Transportation,
Midwest Transportation Center, and
U.S. Department of Transportation
Office of the Assistant Secretary for Research and Technology

A report from

Institute for Transportation

Iowa State University

2711 South Loop Drive, Suite 4700

Ames, IA 50010-8664

Phone: 515-294-8103 / Fax: 515-294-0467

www.intrans.iastate.edu

TABLE OF CONTENTS

ACKNOWLEDGMENTS	xi
EXECUTIVE SUMMARY	xiii
1. INTRODUCTION	1
1.1. Overview.....	1
1.2. Literature Review.....	2
1.3. Organization of Report	2
2. MATERIAL SAMPLING AND PROCESSING	3
2.1. Project Selection	3
2.2. Material Sampling.....	5
2.3. Material Storage and Labeling.....	7
2.4. Material Processing.....	8
3. TESTING AND ANALYSIS METHODS	12
3.1. Overview.....	12
3.2. Binder Testing.....	12
3.2.1. Rotary Viscometer Testing	12
3.2.2. Dynamic Shear Rheometer Testing	12
3.2.3. Bending Beam Rheometer Testing	13
3.2.4. Multiple Stress Creep Recovery Test	14
3.3. Mixture Testing.....	15
3.3.1. Disk-shaped Compact Tension Testing	15
3.3.2. Illinois Flexibility Index Testing	19
3.3.3. IDEAL-CT-Index Test.....	20
3.3.4. Hamburg Wheel Track Testing.....	21
3.3.5. DC(T) Creep Testing	22
3.3.6. Indirect Tension (IDT) Creep Compliance and Strength.....	23
4. BINDER RESULTS	27
4.1. Overview.....	27
4.2. Rotational Viscosity Test on Binders	27
4.3. Dynamic Shear Rheometer Test on Binders.....	27
4.4. Bending Beam Rheometer	28
4.5. Multiple Stress Creep Recovery	28
5 .MIXTURE RESULTS	30
5.1. Overview.....	30
5.2. Thermal Cracking Performance Based on DC(T) Fracture Energy.....	32
5.2.1. Field Core Fracture Energy Results.....	32
5.2.2. Plant Mixture Fracture Energy Values Obtained with the DC(T)	34
5.2.3. Laboratory Mixture Fracture Energy Values Obtained with the DC(T).....	36
5.3. Cracking Resistance Using SCB Flexibility Index	37
5.3.1. Field Core Flexibility Index Results.....	38

5.3.2. Plant Mixtures Flexibility Index Results	40
5.3.3. Lab Mixtures Flexibility Index Results	40
5.3.4. Comparing DC(T) and I-FIT Test Results.....	41
5.4. IDEAL CT Index Test	43
5.4.1. Plant Mixture Ideal CT Test Results.....	43
5.4.2. Lab Mixture IDEAL-CT Test Results	45
5.5. Indirect Tension Test Results.....	46
5.6. Hamburg Wheel Track Test Results	48
5.6.1. Field Core Rutting Resistance	48
5.6.2. Field Core Moisture Damage Performance	50
5.6.3. Plant Mixture Rutting Resistance	52
5.6.4. Lab Mixture Rutting Resistance	53
5.7. Hamburg-DC(T) Performance Space Diagram Results.....	54
5.8. Creep Compliance Tests	59
5.8.1. DC(T) Creep Compliance	59
5.8.2. ID(T) Creep Compliance	61
5.9. ANOVA and Tukey Grouping Test.....	62
5.10. IlliTC Modeling	63
6. RUBBER DEMONSTRATION PROJECTS IN MISSOURI.....	67
6.1. Introduction.....	67
6.2. Dry Process Rubber Demonstration Project: I-35, Kansas City, Missouri, Fall 2017.....	67
6.2.1. Binder Test Results	69
6.3. Dry Process Rubber Demonstration Project: I-35, Kansas City, Missouri, Spring 2018.....	70
6.3.1. DC(T) Fracture Energy Test Results of Plant-Produced Mixtures.....	72
6.3.2. SCB Test Results	73
6.3.3. IDEAL Test Results.....	73
6.3.4. Hamburg Wheel Tracking Test Results.....	74
6.4. Summary and Conclusions	75
7. FIELD PERFORMANCE EVALUATION.....	77
7.1. Field Sections Studied and Investigated in this Chapter.....	77
7.2. Relation of Field Performance to Recycling Levels and Performance Tests	83
8. SUMMARY, CONCLUSIONS, AND RECOMMENDATIONS	86
8.1. Summary	86
8.2. Conclusions.....	87
8.3. Recommendations.....	88
REFERENCES	89

LIST OF FIGURES

Figure 2-1. Example of project sampling schematic used to select coring locations: US 54	5
Figure 2-2. Example of project sampling: Magruder Paving, LLC, US 54 near Osage Beach.....	6
Figure 2-3. Example of project coring with full-depth core, left, and asphalt layers only, right.....	6
Figure 2-4. Block saw	9
Figure 2-5. Other fabrication equipment: tile saw, left, and coring rig, right.....	10
Figure 3-1. Brookfield DV3T digital rotational viscometer at MAPIL.....	12
Figure 3-2. Anton Paar dynamic shear rheometer at MAPIL.....	13
Figure 3-3. Bending beam rheometer at MAPIL	14
Figure 3-4. MSCR test details and calculations.....	15
Figure 3-5. Testquip DC(T) apparatus.....	16
Figure 3-6. Typical load-CMOD curve from DC(T) testing	17
Figure 3-7. The Testquip IDEAL-CT apparatus at MAPIL	20
Figure 3-8. Typical load-displacement curve from Testquip software.....	21
Figure 3-9. Hamburg wheel tracking device: test device, left, and mixtures after test, right.....	22
Figure 3-10. Cooper 100 kN UTM machine at MAPIL	24
Figure 3-11. Attached gauge points on the samples using the pattern.....	25
Figure 5-1. DC(T) fracture energy test results of field cores.....	33
Figure 5-2. DC(T) fracture energy test results of plant mixtures	35
Figure 5-3. Comparing DC(T) results of field cores and plant mixtures.....	36
Figure 5-4. Comparing DC(T) results of field cores, plant mixtures, and lab mixtures	37
Figure 5-5. Typical I-FIT data analysis from Testquip SCB and ICT software.....	38
Figure 5-6. I-FIT test results for field cores.....	38
Figure 5-7. An example of very brittle behavior (US54_4-4ay tested sample).....	39
Figure 5-8. Comparing I-FIT results of field cores and plant mixtures.....	40
Figure 5-9. Comparing I-FIT results of field cores, plant mixtures, and lab mixtures.....	41
Figure 5-10. Comparison of DC(T) FE & SCB FI test results of field cores	41
Figure 5-11. Example of 95 mm thickness specimen, left, and 62 mm thickness specimen, right.....	43
Figure 5-12. Typical force vs. displacement curves obtained from IDEAL-CT test.....	44
Figure 5-13. IDEAL CT-index of the mixtures using compacted-to-62-mm samples (HPs).....	45
Figure 5-14. Comparing IDEAL-CT index of lab mix and plant mix	46
Figure 5-15. Load vs. displacement curves obtained from IDT strength test, (a) MO13_1, (b) US63_1, (c) US54_6, and (d) US54_1.....	47
Figure 5-16. IDT strength of the plant mixes	48
Figure 5-17. Hamburg wheel test results of field cores (at 20,000 passes)	49
Figure 5-18. Sample Hamburg test output from Cooper software.....	50
Figure 5-19. Stripping point analysis (a) Section US631, (b) Section US54_7, (c) Section SPS10-1, (d) Section MO13_1	51
Figure 5-20. Hamburg wheel track test results: plant mix vs. field cores	53
Figure 5-21. Hamburg wheel track test results: plant mix vs. field cores vs. lab mix.....	54
Figure 5-22. Hamburg-C(T) plot for Missouri field cores.....	55
Figure 5-23. Moisture sensitivity in Hamburg test for SPS10_1 (Sample 2).....	57

Figure 5-24. Hamburg-DC(T) plot for 10,000 Hamburg wheel passes	58
Figure 5-25. Generated DC(T) master curves for field cores	59
Figure 5-26. Generated DC(T) master curve for plant mixtures	60
Figure 5-27. IDT creep compliance master curve for plant mixtures (Ref. Temp: -24°C)	61
Figure 5-28. IDT and DC(T) creep m-values	62
Figure 5-29. Poisson's ratio from IDT creep testing	62
Figure 5-30. IlliTC stress and temperature outputs, (a) MO13_1, (b) US63_1, (c) US54_6, and (d) US54_1	66
Figure 6-1. Summary of binder grading using DSR and BBR	69
Figure 6-2. View inside ECR feeder unit showing pugmill-style agitation system.....	71
Figure 6-3. Connection of fiber and ECR-GTR hoses at similar location near bottom of drier drum.....	71
Figure 6-4. ECR SMA night paving on I-35 mainline in spring 2018	72
Figure 6-5. DC(T) fracture energy of SMA mixtures at -12°C for plant mixes	72
Figure 6-6. SCB cracking test results for SMA mixture at 25°C	73
Figure 6-7. IDEAL cracking test results for SMA mixtures at 25°C	74
Figure 6-8. Hamburg wheel track test results for SMA mixtures at 50°C.....	75
Figure 7-1. Series of ARAN photos for MO52_1.....	78
Figure 7-2. Series of ARAN photos for MO54_8.....	79
Figure 7-3. Series of ARAN photos for MO50_1.....	80
Figure 7-4. Series of ARAN photos for MO63_2.....	81
Figure 7-5. Series of ARAN photos for MO54_7.....	82
Figure 7-6. PASER rating vs. years in service.....	83
Figure 7-7. IRI vs. years in service.....	84

LIST OF TABLES

Table 2-1. Summary of SPS-10 project	3
Table 2-2. Summary of Level 1 projects selected.....	4
Table 2-3. Summary of Level 2 projects selected.....	4
Table 2-4. Finalized project sample labels	7
Table 3-1. MSCR thresholds.....	15
Table 3-2. DC(T) fracture energy thresholds.....	18
Table 3-3. Loading parameters used at different testing temperatures	24
Table 4-1. Viscosity of binders obtained from the RV device	27
Table 4-2. Summary of virgin binder testing results	28
Table 4-3. Summary of MSCR testing results	29
Table 5-1. Summary of field sections investigated.....	31
Table 5-2. Summary of plant mixtures	34
Table 5-3. COV of DC(T) and I-FIT measurements on field cores for Missouri Superpave mixes	42
Table 5-4. IDEAL-CT index of mixtures using different sample geometries (compacted to 95 mm thickness, compacted to 62 mm [HP] and cut to 62 mm [DP] thicknesses).....	44
Table 5-5. Stripping inflection point.....	52
Table 5-6. ANOVA test and Tukey-Kramer grouping for performance tests	63
Table 5-7. Summary of the inputs to IlliTC software	64
Table 6-1. Summary of mix design performance test results	68
Table 6-2. Summary of performance testing of fall 2017 test strip mixes	69
Table 6-3. Summary of BBR results on binders	70
Table 7-1. Field sections with significant time in service	77
Table 7-2. Performance measures in 2017 for field sections.....	77
Table 7-3. Field section details vs. average deterioration rate.....	83
Table 7-4. Field performance vs. lab cracking tests	84
Table 7-5. Test averages and coefficient of variability for field sections.....	85

ACKNOWLEDGMENTS

The authors would like to thank the Missouri Department of Transportation (MoDOT), the Midwest Transportation Center, and the U.S. Department of Transportation Office of the Assistant Secretary for Research and Technology for sponsoring this research. We would especially like to thank Jen Neely and Dan Oesch from MoDOT for their technical support during the conduct of this research. We would also like to thank Dave Ahlvers and Bill Stone for their guidance during this study, along with Dale Williams of the Missouri Asphalt Pavement Association (MAPA) for help in identifying field sections for study. The help provided by Richard Stegar and Vicki Woods of Ingevity is greatly appreciated, as is the assistance of the MoDOT contractors involved in the study, including Magruder Paving, LLC; Capital Paving & Construction; Ideker, Inc.; Asphalt Plus, LLC; and Apac-Missouri, Inc.

Special Note: MoDOT is publishing their version of this report, which includes more than 100 pages in appendices.

EXECUTIVE SUMMARY

A comprehensive laboratory and field investigation was carried out to evaluate the performance of recycled asphalt mixtures in Missouri by researchers at the University of Missouri-Columbia, in collaboration with the Missouri Department of Transportation (MoDOT). Eighteen field sections were evaluated, including a number of sections from the recent Long-Term Pavement Performance (LTPP), Special Pavement Sections (SPS-10) project in Osage, Beach, Missouri, which was constructed in 2016. Good and poor performing sections dating back as far as 2003 construction were sampled and tested. Binder testing and mix performance tests were carried out on field cores and laboratory compacted specimens. The study focused on medium traffic volume Superpave mixes. Additional funding was also provided by the Midwest Transportation Center (MTC), which is headquartered at Iowa State University. This allowed additional advanced laboratory tests to be carried on mixtures having three distinct preparation methods, including field produced - laboratory compacted (reheated plant mix), field cores, and field sampled mixture components – laboratory prepared. In addition to a full suite of Superpave binder testing, including continuous grading and multiple stress creep and recovery, an extensive suite of asphalt mixture performance tests were carried out. This suite included Hamburg wheel track testing (HWTT) (submerged), disk-shaped compact tension, or DC(T), fracture testing, semi-circular bend (SCB) crack testing using the Illinois flexibility index test (I-FIT) procedure, the IDEAL cracking test, indirect tension creep, and DC(T) creep. A total of 18 sections were sampled and tested, including 4 heavily sampled projects (Level 1 sampling). Field performance data for the five oldest sections were collected from MoDOT's online Pavement Surface Evaluation and Rating (PASER) system, including Automatic Road Analyzer (ARAN) video logs, which were used to delineate thermal cracks from block cracks.

Based on the findings of the study, the following conclusions were drawn:

1. Missouri's practices for the responsible and effective use of recycled materials is sound, and continues to improve over time; recent mix designs demonstrate more appropriate balancing between recycled material levels and virgin binder selection, resulting in better performance tests results when compared to older recycled mix designs.
2. Opportunities exist for further improving recycled mix design methods and recycling optimization in Missouri, including
 - a. Moving to higher ABR levels, by implementing mixture performance tests (balanced mix design)
 - b. Increasing the use of recycled ground tire rubber (GTR) in Missouri mixes, by using balanced mix design to certify mixes using new, more economical GTR recycling methods
 - c. Researching the use of recycled materials in stone mastic-asphalt (SMA) designs
3. The Hamburg-DC(T) plot can be used to quickly and effectively design and adjust recycled mixtures to meet rutting and cracking performance requirements.
4. A very good performing field section was identified and tested in this study (US54_7). This section has performed very well after 15 years in service, and still has low roughness (International Roughness Index [IRI]=53), low rutting (3 mm), and a high PASER rating (7/10). This, along with performance of the other four test sections, tended to validate the recommended long-term aged DC(T) minimum threshold of 400 J/m², while the I-FIT results

appear to suggest a threshold of around 1.0 for long-term flexibility index.

5. Most mixes exhibit sufficient “total” energy to pass Hamburg and DC(T) recommended criteria without major changes in the aggregate structure, recycling level, or binder cost; the use of a softer virgin binder grade will likely suffice.

Based on the conclusions, the following recommendations are suggested:

1. More work is needed to further evaluate and fine-tune mix performance tests for use in balanced mix design, which is particularly important for modern, heterogeneous recycled mixes. This should include:
 - a. Sampling and testing of additional field sections
 - b. Developing a reliability-based approach for setting performance test thresholds
 - c. Considering adjustments to the Hamburg test to make it more performance-based and climate-based
 - d. Working to improve the streamlining of and repeatability of mixture performance tests, and determining which tests are most appropriate for design, quality control, and quality assurance
 - e. Working toward a performance design approach for balanced mix design, where performance testing is given priority over mix volumetrics
2. More work is needed to evaluate GTR recycling, especially some of the new dry process techniques that are more economical, and more contractor friendly.
3. A better physical understanding of recycling physics (including micromechanics) and chemistry is needed in order to arrive at even higher recycling amounts in a confident manner.

1. INTRODUCTION

1.1. Overview

Asphalt concrete is the most recycled material on the planet. Yet, after several decades of increased usage, the procedures for incorporating reclaimed asphalt pavement (RAP) into asphalt mix designs is not completely performance-based. Hundreds of millions of scrap tires can be found in stockpiles in the United States, leading to an ample supply of potentially recyclable ground tire rubber (GTR). Over 10 million tons of tear-off roofing shingles are currently stockpiled, creating the potential for large-scale recycling of recycled asphalt shingles (RAS). Recycling these materials in asphalt pavements is a potentially sustainable solution and can often yield performance benefits if used correctly. However, a lack of scientific test results and effective tests, especially to evaluate new products and manufacturing processes, and a lack of clear quantification of costs versus benefits impedes implementation by state transportation agencies and industry. There is a particular lack of literature and research experience with regard to newer GTR asphalt products and their use in the Midwest. Adjustments to mix design procedures, particularly for those containing RAS, also need to be studied. The role of rejuvenators in adding resiliency to recycled materials as blending components, and to the restoration of pavement surfaces, is also an open research topic.

This project involved a research collaboration between the University of Missouri-Columbia, the Missouri Department of Transportation (MoDOT), and the Missouri Asphalt Paving Association (MAPA). A laboratory and field investigation of modern asphalt rubber products, RAP, RAS, and rejuvenators available in the Midwest was conducted. Investigations included both asphalt binder and mixture performance characterization, including materials sampled from the field projects.

This project also served as a matching project for a research investigation conducted under the Midwest Transportation Center (MTC). The delineation of work conducted under the two projects was dictated to a large extent by the start-up sequence in establishing the new University of Missouri-Columbia (Mizzou) Asphalt Pavement and Innovation Laboratory (MAPIL). A separate, but related, report will be generated for the MTC project, which is planned for completion in September 2018. Due to the time required to manufacture and install the large universal test frame, the following division of research tasks was established between the two projects:

- MoDOT sponsored project
 - Experimental design planning with MoDOT, and inputs from MAPA
 - Coring, plant sampling, and specimen labeling and storage
 - Superpave binder characterization, continuous grade and delta-T_c
 - Mainstream asphalt mixture performance testing and analysis
 - Disk-shaped compact tension testing
 - Illinois flexibility index test (I-FIT) testing
 - Hamburg wheel track testing (HWTT)
 - Creep compliance testing in DC(T), including test development

- Performance space diagram analysis
- Field performance data collection and analysis with respect to performance tests
- Advanced block cracking analysis
- Evaluation of current recycled material usage and recommendations for improved practices
- Evaluation of mixture performance tests and use for promoting and controlling mix performance for recycled mixes
- MTC-sponsored project:
 - Tests conducted on universal test machine and new indirect tensile asphalt (IDEAL)/I-FIT apparatus
 - Dynamic modulus (E^*) master curve
 - Creep compliance testing in indirect tensile test (IDT), IlliTC model simulations
 - IDEAL test
 - Acoustic emissions testing (subcontract to University of Illinois)

1.2. Literature Review

A wealth of information regarding RAP exists in the literature, along with a more modest amount of information on RAS, GTR, and rejuvenators. A detailed literature review was completed in the first quarter of this project, and delivered as a report in December 2016. This report appears in its entirety in MoDOT's version of this report.

1.3. Organization of Report

This remainder of this report is organized as follows:

- Chapter 2: Material Sampling and Processing
- Chapter 3: Test Methods
- Chapter 4: Binder Test Results
- Chapter 5: Mixture Test Results
- Chapter 6: Robber Demonstration Projects in Missouri
- Chapter 7: Performance Analysis
- Chapter 8: Summary, Conclusions, and Recommendations

2. MATERIAL SAMPLING AND PROCESSING

2.1. Project Selection

Based on the project proposal and further consultation with MoDOT, a total of 18 projects were selected for sampling and testing in this study. An effort was made to encompass the following factors:

- New vs. older projects
- Good and poor performers
- Range of recycled materials and additives, i.e., RAP, RAS, GTR, Rejuvenator, Polymer
- Geographic distribution across Missouri, balanced against a concentration of a majority of projects around the center of the state to reduce sample transportation costs
- Heavy sampling (coring plus plant and paver sampling), to enable future testing and testing of reconstituted lab mixes, versus light sampling for economy (coring only)

As a result, two levels of sampling were performed: Level 1 (Heavy Sampling) and Level 2 (Light Sampling). A total of 4 Level 1 projects were selected, along with 16 Level 2 projects, for a total of 18 projects. Fortunately, a Long Term Pavement Performance (LTPP) Special Pavement Section (SPS-10) was being constructed during the period of sampling for this project. The project was located on southbound driving lanes of US54 just north of Osage Beach, Missouri, which is near the dam that forms the Lake of the Ozarks. The asphalt contractor for the job was Magruder Paving, LLC, utilizing a drum-mix plant located near the intersection of Lakeside Road and US54, near Lakeland, Missouri, and incorporating aggregates from nearby quarries, including onsite. While the focus of the SPS-10 project was on warm-mix techniques, the project contained a robust collection of RAP, RAS, and rejuvenator combinations, as shown in Table 2-1.

Table 2-1. Summary of SPS-10 project

Test section	Approx. tons	Mix design	AC	ADD1	ADD2
291001	500	SP125 16-83	PG64-22H		
291003	500	SP125 16-100	PG64-22H		
291002	500	SP125 16-93	PG64-22H	EVO M1	
291004	460	SP125 16-84	PG64-22H		
291008	480	SP125 16-99	PG64-22H	FLEX	
291005	290	SP125 16-91	PG58-28		
291007	680	SP125 16-89	PG58-28		
291009	970	SP125 16-98	PG58-28		
291010	360	SP125 16-95	PG46-34		
291006	400	SP125 16-94	PG58-28	FLEX	IPC70

Several project planning meetings were held at the MoDOT materials laboratory, in Jefferson City, Missouri, to finalize the list of Level 1 and 2 projects. It was decided to focus all 18 projects on medium traffic volume facilities, which are comprised of asphalt mixes designed

following Superpave. It was determined that low-volume roads, comprised of MoDOT bituminous pavement (BP) mixes, and high-volume roads, comprised of stone mastic asphalt (SMA), would be reserved for study in future investigations. With consideration to the factors presented earlier in this chapter, the Superpave projects summarized in Table 2-2 and Table 2-3 were selected for sampling.

Table 2-2. Summary of Level 1 projects selected

Section short label	Job no.	County	Route /Dir	Location	Total %ABR	%ABR by RAP	%ABR by RAS	Misc.
MO13_1	J7P3010	Henry	MO 13 NB	S. of Clinton	16.6	16.6	0	1.5% Bag House Fines + 0.5% Mlife* T280
US54_6	J5P3131 mainline	Miller	US 54 NB	N. of Osage Beach	30.7	30.7	0	1% Mlife T280
US54_1	J5P3131 sect 10	Miller	US 54 SB	N. of Osage Beach	33	0	33	2.5% IPC-70 +3.5% PC 2106 + 1.5% Mlife T280
US63_1	J2P2213	Randolph	US 63 SB	S. of Moberly	35.2	35.2	0	2.5% IPC-70 +3.5% PC 2106 + 1.5% Mlife T280

*MORLIFE

Table 2-3. Summary of Level 2 projects selected

Section short label	Job no.	County	Route /Dir	Location	Total %ABR	%ABR by RAP	%ABR by RAS	Misc.
US63_2	J2P0773 SBL	Macon	US 63 SB	N of Macon, near LaPlata	29.9	19.9	10	1.5% Bag House Fines + 0.5% AD-here HP PLUS
US54_3	J5P3131 sect7	Miller	US 54	Osage Beach	33.1	17.9	15.2	1% Mlife* T280
US54_5	J5P3131 sect4	Miller	US 54	Osage Beach	0	0	0	1% Mlife T280
US54_4	J5P3131 sect5	Miller	US 54	Osage Beach	34.7	34.7	0	3% PC 2106, 1% MORLIFE T280
US54_2	J5P3131 sect8	Miller	US 54	Osage Beach	33.2	33.2	0	1% Mlife T280
US50_1	J5P0961	Moniteau/Morgan	US 50	Tipton	24.6	24.6	0	1% Lime
SPS10_1	J5P3131 Sect1	Miller	US 54 SB	N. of Osage Beach	23.6	23.6	0	1% Mlife T280
SPS10_2	J5P3131 Sect2	Miller	US 54 SB	N. of Osage Beach	24.5	24.5	0	1% Mlife T280
MO52_1	J5P0925	Morgan	MO 52	Versailles	33.5	0	33.5	1.5% BHF, 0.8% Adhere HP+
US54_7	J5P0769	Cole	US 54 WB	Brazito	0	0	0	0.25% LOF 65-00LS1
US54_8	J5D0600A	Cole	US 54	S of Jeff City	8.6	8.6	0	0.5% AD-here HP PLUS
SPS10_9	J5P3131 Sect9	Miller	US 54 SB	N. of Osage Beach	45.6	15.7	29.9	2% Mlife T280

*MORLIFE

Two of the four Level 1 projects were part of the SPS-10 project in Osage Beach, while the other two were located on US 63 near Moberly, Missouri, and US 13 near Clinton, Missouri. The main variable missing from the projects selected was GTR, resulting from the fact that very few Superpave sections were constructed in the desired time frame (probably due to the relatively low cost of binder and modest modification requirements for Superpave mixes in Missouri). Due to a lack of availability, it was decided that GTR would be investigated in demonstration projects, which are currently still in progress and will be included in the companion report to the Midwest Transportation Center.

Additional details regarding project location and core locations can be found in Appendix A of MoDOT's version of this report. A sample project location and sampling schematic is shown in Figure 2-1.

J5D0600A
US 54 both directions
south of Jeff City
Planned 2005

- Section 1 is north of Jeff City and is repaved in 2009 in project J5P2175
- Section 2 and 3 are in Jeff City
- Section 4 are WBL and section 5 are EBL of this project runs from roughly Stadium Blvd overpass to Moreau River bridge
- Best straight length between Cody Dr and Monticello Rd. - roughly 1.6 miles
- WBL 1.75" SP125C, 2.0" SP190C
- EBL mostly only 1.75" SP125C
 - PG grade not specified

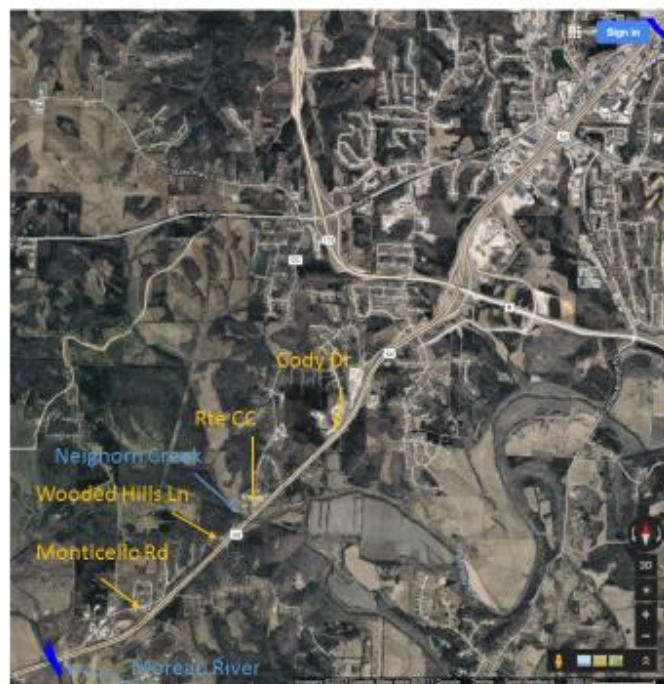


Figure 2-1. Example of project sampling schematic used to select coring locations: US 54

2.2. Material Sampling

Level 1 sampling consisted of sampling virgin aggregate stockpiles, recycled material stockpiles, mineral filler or baghouse fines (when available), asphalt binder, additives (liquid antistriper, rejuvenator), and adjusted job-mix formula information. Typical quantities of sampling and containers were:

- Binder: 2, 5-gallon steel pails per performance grade (PG) grade
- Aggregates: 120, 5-gallon polyvinyl chloride (PVC) buckets, proportioned according to mix design (Figure 2-2)



Figure 2-2. Example of project sampling: Magruder Paving, LLC, US 54 near Osage Beach

For both Level 1 and Level 2 sampling, 150 mm diameter cores were obtained, normally using a 150 mm inner diameter coring barrel, or slightly larger. In cases where surface asphalt mixture layers were difficult to snap off using the coring barrel, full-depth coring was performed. An example of a full-depth field core taken from US 63 near Moberly, Missouri, is shown in Figure 2-3 on the left, while a snapped-off core sample is shown in Figure 2-3 on the right.



Figure 2-3. Example of project coring with full-depth core, left, and asphalt layers only, right

Although full-depth cores are more time consuming to obtain and difficult to handle and transport, they are sometimes necessary to avoid damage to cores resulting from the application of a lateral prying pressure to the top of cores, often resulting in localized damage to the surface of the core. A better technique for applying lateral pressure in an attempt to snap off surface

layers from underlying layers during coring is to use an old core barrel, cut in half on the long axis, creating a half-circumference (semi-circular cross-section) prying device. The half barrel can be inserted and used to apply a more uniform lateral pressure, concentrated lower in the core hole and creating a more desirable, localized shear force near the interface to be separated.

2.3. Material Storage and Labeling

Materials were brought to and stored at Mizzou’s Remote Testing Facility (RTF), located on S. Lenoire St. at the Discovery Park in Columbia, MO. A detailed labeling scheme was used, as summarized in Table 2-4.

Table 2-4. Finalized project sample labels

Short label	Field core	Plant mix	Lab mix	DC(T)	I-FIT	HW TT	Example of specimen name	Note
US54_2	X						US54_2-4	4th core taken from US54_2
US63_1		X		X			US63_1 PD7B	140 mm, 7th gyro, bottom slice
US63_1		X			X		US63_1 PD8Bx	140 mm, 8th gyro, bottom left
US63_2	X						US63_2-8	8th gyro taken from US 63_2
MO13_1			X			X	MO13_1 LH2	63 mm, 2nd gyro
MO13_1			X			X	MO13_1 LH3	next 62 mm gyro compacted
MO13_1	X						MO13_1-3	3rd core taken from MO 13
MO13_1		X			X		MO13_1 PD9Ay	140 mm, 9th gyro, top slice, right
US54_7		X				X	US54_7 PH13	62 mm, 13th gyro
US50_1	X						US50_1-1	1st core taken from US 50

All sample names start with the short label of the sections as given in Table 2-2 and Table 2-3. The following codec was used to develop the labeling codes:

- Field cores were labeled with the core number from the order in which it was extracted from the pavement. Plant mixed, lab compacted specimens were labeled with the letter “P.” Lab mixed, lab compacted specimens were labeled with the letter “L.”
- Next, Hamburg samples were labeled with an “H.” Since DC(T) and I-FIT tests were cut from the same size geometry they were both initially labeled with a “D.” DC(T) and I-FIT gyratories were compacted at 140 mm. Then, two 50 mm slices were cut from the middle of the gyratory. These slices were arbitrarily labeled “A” and “B.” I-FITs were then further labeled with an x or y once the slices were cut into the half discs.

- Finally, the name was finished with the sequential number indicating the order in which the gyratory was compacted, starting from 1 for the first and incrementing up for each compaction of the same height.

2.4. Material Processing

For binder testing, it was desired to obtain small samples from the 5-gallon binder samples. In order to minimize the number of times the 5-gallon samples were fully reheated (and thereby slightly aged in the process), two main sample reduction strategies were employed: (1) for small sampling quantities, a heated spoon was used to obtain small samples from the top of the bucket sample; and: (2) for larger sampling (such as when asphalt mixture samples were made), the 5-gallon bucket was fully heated and poured into smaller gallon and quart cans to minimize future reheating.

For mixture testing, a majority of tests conducted in this study were performed on 150-mm diameter by 50 mm thick specimens. This includes disk-shaped compact tension testing, semi-circular bend tests, and indirect tension creep and strength tests. In addition, further sample fabrication cuts and coring operations were required, depending on the test requirements. A block saw was used to cut cores and gyratory specimens (Figure 2-4), while a tile saw and small coring rig were used to meet additional fabrication requirements for mixture mechanical tests.



Figure 2-4. Block saw

The fabrication equipment used was obtained from Testquip LLC and featured a 16 in. diameter block saw blade (stiffer than the more common 20 in. diameter blade), and purpose-built masonry (tile) saw and coring rig (Figure 2-5), which are equipped with adjustable fixtures to facilitate proper sample dimensioning.

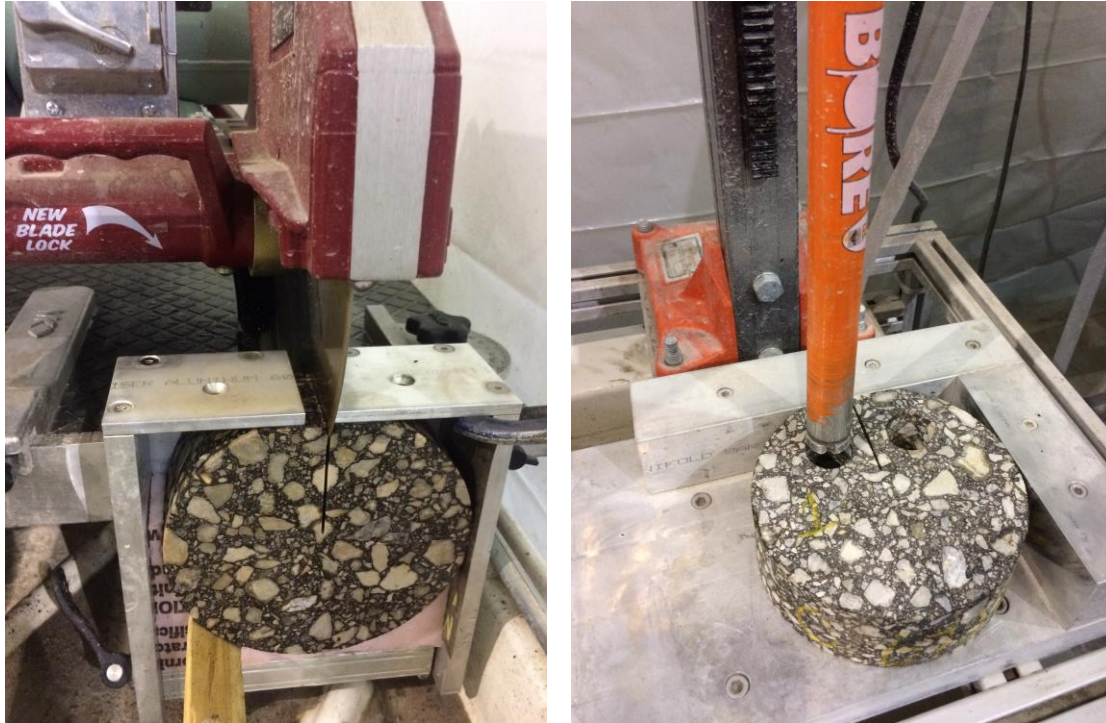


Figure 2-5. Other fabrication equipment: tile saw, left, and coring rig, right

All devices were water cooled to avoid overheating of samples.

The experimental design called for testing both field cores and gyratory compacted specimens. To create gyratory compacted specimens, two options were possible: for Level 1 projects, asphalt mix sampled from behind the paver was reheated and compacted in a Pine GB1 Superpave gyratory compactor. New asphalt mixture samples were created following the mix design and then gyratory compacted in the same GB1 Superpave compactor.

Plant-mixed samples were brought back to the lab in 5-gallon steel pails. The plastic handles were removed, and then the pails were placed in a forced draft oven to heat the asphalt mixture to a workable consistency. The heated mixture was then reduced to the gyratory sample mass following the quartering method in AASHTO R 47. After splitting to sample mass, the asphalt mixture was heated to compaction temperature as set by the (job mix formula) JMF. All samples were compacted to 7% air voids (AV). The 7% AV was measured on the 50 mm slices before notching and coring for the DC(T) specimens, or before cutting the slice in half and notching for the I-FIT specimens. For the Hamburg specimens, the original gyratory specimen (62 mm in height) was used for G_{mb} testing prior to cutting the flat face on one side.

Lab mixed samples were created from the aggregates and the binders collected from the asphalt plants. These materials were proportioned according to the job mix formula used for paving the field sections. A bucket of an aggregate was dumped on a table and aggregate samples were reduced by the quartering method according to ASTM C702. Aggregates were dried at 110°C overnight and then batched according to the JMF. Batched aggregates were then preheated with

binder to the appropriate mixing temperature and mixed in a bucket-style lab mixer. All lab mixes were short-term aged in a forced draft oven for 2 hours according to AASHTO R 30. Similar to the plant mix gyratories, 7% air voids were measured on the slices rather than targeting 7% on the full gyratory. There is generally a 0.5% to 1.0% reduction in air voids from the full gyratory to the sliced specimen. This is a technique often employed in research studies, but it is admittedly rather cumbersome. As balanced mix design and associated performance testing gain traction nationwide and in Missouri, a standard, practical method will need to be established to set void levels and void determination technique for asphalt mixture performance tests.

3. TESTING AND ANALYSIS METHODS

3.1. Overview

This chapter provides information regarding the test methods applied to materials sampled (as described in Chapter 2). Sample splitting and fabrication details were provided in Chapter 2.

3.2. Binder Testing

Binder tests were focused on the suite of mechanical tests specified in the Superpave Performance Grade (PG) binder grading system, along with continuous PG grade determination.

3.2.1. Rotary Viscometer Testing

To measure the viscosity of the virgin binders sampled in this study, rotational viscometer (RV) tests were performed at two different temperatures (135°C and 155°C). A Brookfield DV3T digital RV, Thermosel environmental chamber, and #21 spindle was used (Figure 3-1).

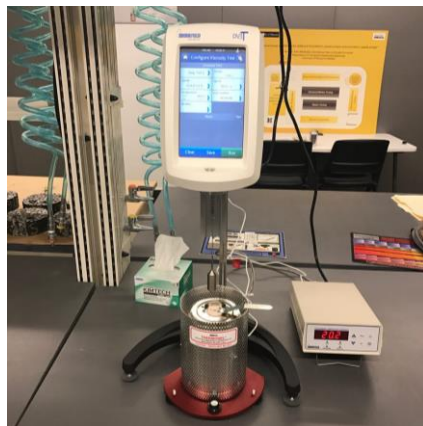


Figure 3-1. Brookfield DV3T digital rotational viscometer at MAPIL

For each sample, approximately 9 g of binder was poured into the sample chamber and allowed to equilibrate for 20 min. RV testing was carried out according to ASTM D4402-15.

3.2.2. Dynamic Shear Rheometer Testing

Superpave performance grading of binders requires viscoelastic characterization tests to be performed across a wide range of temperatures. To this end, one of the key devices required for rutting and fatigue crack mitigation is the dynamic shear rheometer (DSR) test, which was run on the five different neat binders sampled in this study. An Anton Paar MCR-102 SmartPave DSR, located at MAPIL was used (Figure 3-2).



Figure 3-2. Anton Paar dynamic shear rheometer at MAPIL

Dynamic shear modulus and phase angle are outputs from the DSR test, and they are used to characterize the rheological properties of binders. First, testing in the high pavement summer temperature range is conducted to obtain the rutting parameter, or $G^*/\sin \delta$. Testing is conducted across a range of Superpave PG high temperature grades, such as 58°C, 64°C, 70°C, and 76°C. Samples having 25 mm diameter are prepared using silicone molds, then loaded in the DSR, trimmed, conditioned, and tested according to ASTM D7175-15. Testing of both tank and rolling thin-film oven (RTFO)-aged (short-term aged) binder is then conducted. The critical high temperature grade is mathematically determined as either the temperature at which the tank binder rutting parameter reaches a threshold of 1 kPa, or the temperature at which the RTFO-aged binder rutting parameter reaches a threshold of 2.2 kPa—whichever temperature is lower.

Next, testing in the intermediate temperature range on long-term aged binder is conducted to obtain the fatigue parameter, or $G^*(\sin \delta)$. The pressure aging vessel (PAV) was used to age the binders to the long-term age condition. Testing was conducted at the Superpave intermediate temperature for the reported grade of the binder, which is generally either 22°C, 25°C, or 28°C. Samples having 8 mm diameter were prepared using silicone molds, then loaded in the DSR, trimmed, conditioned, and tested according to ASTM D7175-15. The fatigue parameter was then compared against an upper threshold value of 5,000 kPa.

3.2.3. Bending Beam Rheometer Testing

The bending beam rheometer (BBR) test (Figure 3-3) provides a measure of low temperature stiffness and relaxation properties of asphalt binders.

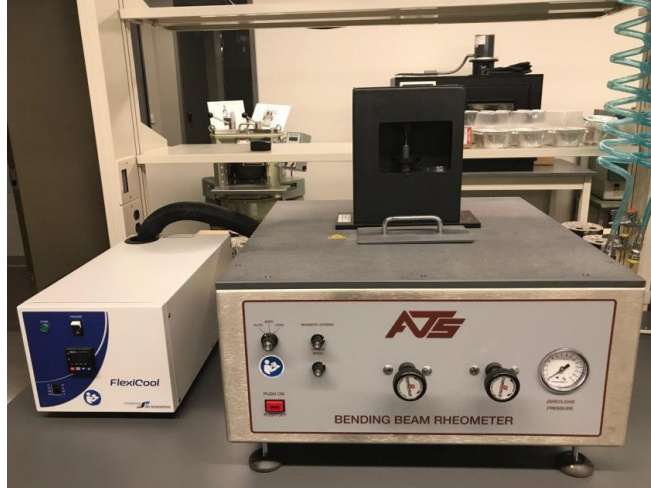


Figure 3-3. Bending beam rheometer at MAPIL

These parameters give an indication of an asphalt binder's ability to resist low temperature cracking. The BBR device is used to determine an asphalt binder's low temperature PG grade in accordance with AASHTO PP 42. BBR tests are conducted on PAV-aged asphalt binder samples. The continuous low temperature grade of the binder is determined as the higher of the two temperatures associated with a threshold creep stiffness of 300 MPa, or m-value of 0.3. The m-value is automatically computed in the BBR software, and represents the absolute value of the slope of the log creep stiffness-log time curve, evaluated at a loading time of 60 s. For Missouri binders, the continuous low temperature grade is expected to be in the range of -22°C to slightly below -34°C , depending on the binder grade being tested. PG XX-22 binders are generally required for the Missouri climate; however, binders as soft as PG XX-34 are sometimes used to counterbalance the binder stiffness arising from the use of recycled materials, such as reclaimed asphalt pavement (RAP) or recycled asphalt shingles (RAS).

3.2.4. Multiple Stress Creep Recovery Test

The multiple stress creep and recovery (MSCR) test method determines the percent viscoelastic strain recovery and accumulated viscoplastic strain in a binder under a predefined cyclic loading. The properties measured in the aforementioned Superpave testing are within the linear viscoelastic region and may not fully capture the nonlinear and irrecoverable responses. The MSCR test measures parameters at higher strains, therefore delineating binder modification strategies (e.g., polymer modification), i.e., having better potential to capture the difference between neat and modified binders in terms of rutting resistance. The test is performed in accordance to ASTM D7405-15 and measures the non-recoverable creep compliance (J_{nr}) of asphalt binders. The MSCR test is conducted using the dynamic shear rheometer (DSR) normally at the binder PG high temperature. The 25-mm parallel plate geometry with a 1-mm gap is used to conduct the test. In total, 30 cycles of 1 s loading and 9 s recovery were applied on the binder. The stress level in the first 20 cycles was 0.1 kPa. The first 10 cycles of 0.1 kPa loading were considered as conditioning and the measured data in the next 10 cycles followed by another 10 cycles of 3.2 kPa stress level testing were used for J_{nr} and $\%J_{nr,diff}$ parameter determination, as illustrated in Figure 3-4.

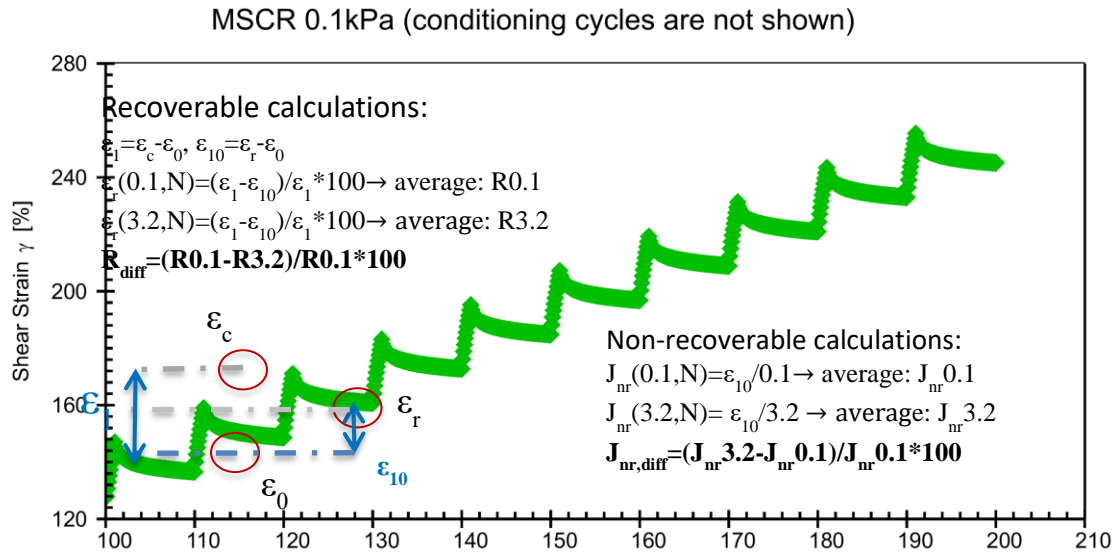


Figure 3-4. MSCR test details and calculations

Details including formulas for strain calculation are provided in ASTM D7405-15. The J_{nr} parameter is used to evaluate the rutting potential of the binder while $\%J_{nr,diff}$ determines the stress sensitivity of the tested binder.

Following the AASHTO M 332-14, four different traffic levels are defined as S, H, V, and E, which stand for standard, heavy, very heavy, and extremely heavy. According to the test results, the appropriate letter is added to the PG grade of the binder. Table 3-1 presents the J_{nr} and $\%J_{nr,diff}$ requirements for distinguishing different binders.

Table 3-1. MSCR thresholds

Parameter	S	H	V	E
Max J_{nr} , 3.2 kPa ⁻¹	4.5	2	1	0.5
Max $J_{nr,diff}$ %	75	75	75	75

For example, PG 64-22 H indicates a binder suitable for heavy traffic, passing MSCR test “H” requirements at 64°C as specified in Table 3-1.

3.3. Mixture Testing

3.3.1. Disk-shaped Compact Tension Testing

The DC(T) test was developed to characterize the fracture behavior of asphalt concrete mixtures at low temperatures. The testing temperature is 10°C warmer than the PG low temperature grade of the mixture, per ASTM D7313-13. Thermal cracking in asphalt pavements can be considered as occurring in pure tensile opening or fracture Mode I, as the cracks propagate perpendicular to the direction of the thermal-induced stresses in the pavement, i.e., transverse to the direction of

traffic. Block cracking develops in a similar manner; however, it is generally confined to the upper crust of the surface layer, and manifests itself as large, hexagonal or rectangular cracks. It is believed that the low-temperature DC(T) test controls both of these two cracking modes, and assists in slowing down reflective and fatigue cracking rates as well. For more direct control of reflective and fatigue cracking, the DC(T) is generally run across a range of temperatures. However, this was considered to be beyond the scope of the current study.

The DC(T) test procedure includes conditioning of the fabricated specimen at the selected test temperature in a temperature-controlled chamber for a minimum of two hours. After the conditioning, the specimens are suspended on loading pins in DC(T) machine, shown in Figure 3-5.



Figure 3-5. Testquip DC(T) apparatus

A portable Testquip DC(T) device was used, which is housed at the MAPIL laboratory. The test is performed at a constant crack mouth opening displacement (CMOD) rate, which is controlled by a CMOD clip-on gage mounted at the crack mouth. The CMOD rate specified in ASTM D7313-13 is 0.017 mm/s (1 mm/min). To begin the testing sequence, a seating load no greater than 0.2 kN (typically about 0.1 kN) is applied to seat the specimen. The test is completed when a crack has propagated and the post-peak load level is reduced to 0.1 kN. The fracture energy can be obtained by measuring the area under the load-CMOD curve and dividing it by the fractured area (ligament length \times thickness). A typical load-CMOD curve is shown in Figure 3-6.

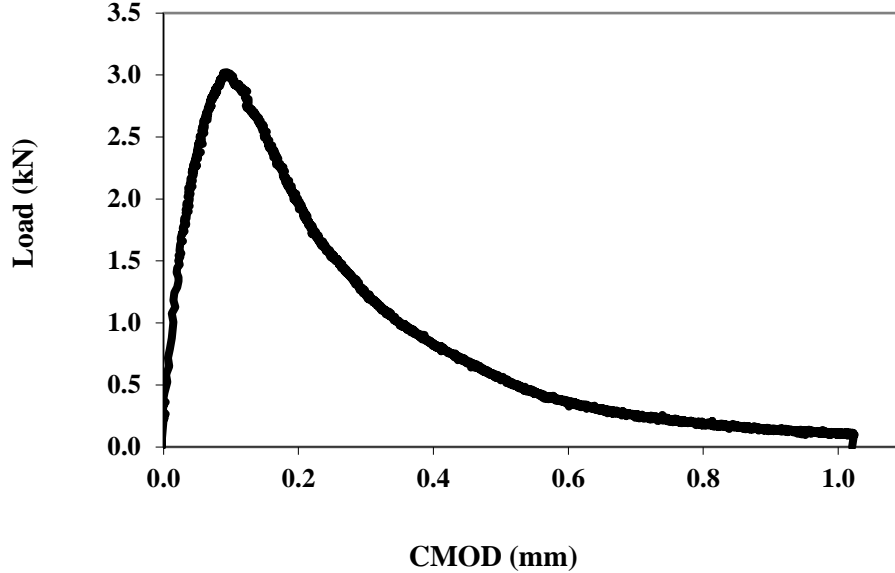


Figure 3-6. Typical load-CMOD curve from DC(T) testing

The fracture energy is computed as follows:

$$G_f = \frac{AREA}{B \cdot L} \quad (1)$$

where,

G_f = Fracture energy, in J/m^2

AREA = Area under Load-CMOD_{FIT} curve, until the terminal load of 0.1 kN is reached

B = Specimen thickness, in m, generally 0.050 m (except for field cores)

L = Ligament length, usually around 0.083 m.

The numerator of the equation represents the area under the Load-CMOD curve, which is the work required to create the fracture surface of size $b \cdot a$. The area is generally computed using the quadrangle rule for numerical integration. The CMOD curve is generally the fitted CMOD, where a straight line is fit through the CMOD vs. time curve to enable data smoothing (ASTM D7313-07). The denominator of Eq. 1 represents the fractured area, i.e., $B \cdot L$. Thus, fracture energy is computed as the work of fracture divided by the area fractured, which represents an average fracture energy density. Higher fracture energy values are associated with more crack resistant mixtures.

For specimen thicknesses other than 50 mm, a size effect correction factor should be applied. This may seem counterintuitive, since after all, the fracture energy equation itself is scaled for the specimen thickness. However, that alone is not enough to fully account for effects on total fracture energy caused by variations in the sample thickness. This is because the damage zone

ahead of the moving crack tip, called the fracture process zone, is sensitive to the three-dimensional stress state in that volume of material. The three-dimensional stress state approaches a plane stress condition (two-dimensional stress state, as the stress normal to the face will be zero) at the edges of the specimen (flat, circular faces of the specimen, i.e., the faces cut with the chop saw), which is less confined than the stress state along the crack front in the mid-thickness of the specimen (approaching plane strain). For thinner specimens, such as field cores with thin surface lifts, a larger proportion of the fracture process zone volume is affected by proximity to the free edge, and thus, the crack tends to propagate with less applied energy in those areas. As a result, when the total energy is summed up, there will be a lower experimentally determined fracture energy for thinner specimens. In order to arrive at the fracture energy that would have been measured had the specimen possessed a 50 mm thickness, a correction factor (multiplier) greater than 1.0 should be applied. Previous research has led to the following correction factor:

$$CF_t = 21.965(B)^{-0.788} \quad (2)$$

Where G_f from Eq. 1 is then multiplied by CF_t to arrive at the final, thickness-corrected G_f for instances where B is less than 50 mm. Practically speaking, this correction should be applied when the thickness is more than 1 mm away from the target 50 mm sample thickness. For example, the correction factor for a sample thickness of 48 mm is 1.035. Thus, ignoring the correction factor in this instance would lead to an error in the estimated fracture energy of 3.5%.

In terms of relation of DC(T) results to field performance, fracture energy thresholds to control thermal cracking with the DC(T) were first introduced in a Federal Highway Administration (FHWA) Transportation Pooled Fund study (Marasteanu et al. 2012), as shown in Table 3-2.

Table 3-2. DC(T) fracture energy thresholds

Contents	Project criticality/ Traffic level		
	High >30 M ESALs*	Moderate 10-30 M ESALs*	Low <10 M ESALs*
Fracture energy, min. (J/m ²)	690	460	400
Predicted thermal cracking using IlliTC (m/km)	< 4	<64	Not required

*ESALs = equivalent single axle loads

For the study conducted herein, which focused on Superpave mixtures, the moderate traffic level would be appropriate. This suggests a minimum fracture energy threshold for newly conducted pavements (thus, mixture in the short-term aged condition) of 460 J/m². When evaluating long-term field-aged mixtures (>7 years of field aging), a fracture energy threshold of 400 J/m² is generally used as a benchmark. This is because field aging reduces the mixture's ability to resist cracking, as the binder becomes more stiff and brittle, while the aggregates generally retain their original physical properties over time (although some degree of freeze-thaw and fatigue damage may accumulate in the aggregate over time). Although more accurate thermal cracking

assessment requires the addition of creep compliance testing at multiple temperatures, along with thermal cracking simulation using a model called IlliTC, as shown in Table 3-2, this practice is generally not followed except for detailed research investigations and/or very high project criticality in areas where thermal cracking is of primary concern. Thermal cracking simulations are reported in the companion report, describing research conducted for the Midwest Transportation Center (as described in Chapter 1).

Current field observations suggest that the DC(T) thresholds provided in Table 3-2 also serve to control block cracking. This is because some of the mechanisms behind thermal cracking and block cracking are thought to be closely related. A Ph.D. investigation is currently being devoted to testing this hypothesis at the University of Illinois at Urbana-Champaign. (A short summary of some of the completed research related to this project is provided in Appendix C of MoDOT's version of this report).

3.3.2. Illinois Flexibility Index Testing

In 2016, Ozer et al. introduced the Illinois semi-circular bending (IL-SCB) method for cracking resistance characterization in asphalt mixes (AASHTO TP 124-16). The goal of the research was to develop an inexpensive, rapid test as a means to limit general pavement cracking. It was decided to simplify the test procedure by testing at room temperature, or 25°C. It was observed that fracture energy obtained in this compact, arched bending mode at this temperature did not uniquely characterize mixture cracking properties. Rather than abandoning the test, the researchers observed that the post-peak slope of the load-displacement curve from semi-circular bending (SCB) test was sensitive to the changes in the asphalt mixture specimen composition and subsequently used this to develop the flexibility index (FI). The FI is an empirical index parameter that is computed as the total fracture energy divided by the absolute value of the slope of the post-peak softening curve. FI is proposed to provide a means to identify brittle mixtures that are prone to premature cracking and was specifically developed to be sensitive to recycled material content.

$$FI = \frac{G_f}{|m|} (0.01) \quad (3)$$

Where G_f is computed in a similar manner as to the DC(T) test, and m represents the slope of the post-peak softening curve. There are countless ways to estimate the slope of a curve resulting from a material test, and this became a challenge for test standardization early in the development of the I-FIT. At present, to address this source of variability, the slope parameter is usually determined using a sophisticated software program available from the Illinois Center for Transportation (SCB Testquip LLC. V2.0.0rc4).

To fabricate samples, a notch is cut along the axis of symmetry of a semi-circular bend specimen to a depth of 15 ± 1 mm. Test specimens are then conditioned in the environmental chamber at 25°C for 2 hr ± 10 min. After a contact load of 0.1 kN is reached, the test is carried out at a rate of 50 mm/min. The test is considered to be complete when the load drops below 0.1 kN, which is identical to the DC(T) test termination definition.

3.3.3. IDEAL-CT-Index Test

The indirect tensile asphalt cracking test (IDEAL-CT) is a recent mix performance test developed by the Texas Transportation Institute (TTI). The test is developed for routine quality control (QC) and quality assurance (QA). The test is still under evaluation (NCHRP IDEA 195). Additional mixes, field data, varied traffic load spectrum, and environmental conditions are required for further evaluation and validation (Zhou et al. 2017). The IDEAL-CT test was developed to characterize the potential of cracking in asphalt concrete mixes at room temperature. The test set-up is similar to the traditional indirect tensile strength test, but it is performed at 25°C at a constant loading rate of 50 mm/min until failure occurs (Figure 3-7).



Figure 3-7. The Testquip IDEAL-CT apparatus at MAPIL

The specimens are cylindrical with a diameter of 100 or 150 mm and a thickness of 38, 62, 75 mm, etc. The specimen does not require gluing, notching, drilling or additional cutting. For simplicity, in Missouri a current practice is to use a specimen with the same thickness as the Hamburg Wheel tracking test with a 7 ± 0.5 air voids. In this study, specimens were fabricated at both 62 mm and 95 mm thickness with a 150 mm diameter for comparison.

The test procedure includes conditioning the specimens in a temperature-controlled chamber for a minimum of 2 hours at a 25°C. After conditioning, the specimens are centered between loading platens. A seating load of 0.1 kN is applied in order to make appropriate contact between the loading platens and the sample. The sample is then loaded under a displacement control mode of 50 mm/min while the loading level is measured and recorded by the device. Figure 3-8 shows a sample of the software output, i.e., the load vs. displacement curve.

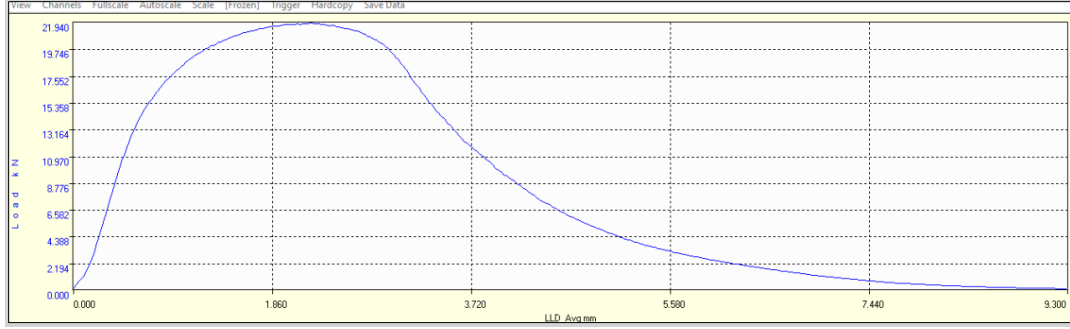


Figure 3-8. Typical load-displacement curve from Testquip software

The cracking parameter for the IDEAL-CT is derived from the load vs. displacement curve and is inspired by the Paris' law (Paris and Erdogan 1963) and by Bazant and Prat (1988), dealing with crack propagation. The CT index equation for a specimen of 62 mm thickness is as follows:

$$CT_{index} = \frac{G_f}{|m_{75}|} \times \left(\frac{l_{75}}{D} \right) \quad (4)$$

where,

G_f = Fracture energy (area under the curve normalized by the area fractured)

$AREA$ = Area under the load – displacement curve, until the terminal load of 0.1 kN is reached

m_{75} = Modulus parameter (absolute value of the slope at 75% of peak load)

$\frac{l_{75}}{D}$ = Strain tolerance parameter (when load is reduced to 75% of peak load)

l_{75} = Vertical displacement when the load is reduced to 75% of peak load

D = Diameter of the sample

t = Specimen thickness.

For samples other than 62 mm thickness, the following equation is used:

$$CT_{index} = \frac{G_f}{|m_{75}|} \times \left(\frac{l_{75}}{D} \right) \times \left(\frac{t}{62} \right) \quad (5)$$

where the thickness is in mm to be consistent with the ratio $\left(\frac{t}{62} \right)$. The larger the CT-index, the better cracking resistance of the mixture; however, no widely accepted thresholds or criteria have been established.

3.3.4. Hamburg Wheel Track Testing

Permanent deformation (rutting) in an asphalt pavement is a result of consolidation and shear flow caused by traffic loading in hot weather. This results in gradual accumulation of volumetric and shear strains in the hot mix asphalt (HMA layers). The measured deformation of different layers of flexible pavement revealed that the upper 100 mm serves the main portion of the pavement rut depth such that the asphalt layer accumulates up to 60% of total permanent

deformation. Lack of shear strength of the asphalt layer to resist the repeated heavy static and moving loads results in downward movement of the surface and provides the potential for upheaval and microcracks along the rut edges. In addition to the structural failure issues, safety concerns rise when the steering becomes difficult and also the surface water flows through the ruts and causes hydroplaning. Wheel load tracking (WLT) tests are the most common performance tests for measuring rutting potential of HMA mixes. The WLT methods simulate traffic by passing over standardized wheels simulating real-life traffic loads on HMA specimen at a given temperature. The two most common WLT test devices are Hamburg wheel tracking test (HWTT) and the asphalt pavement analyzer (APA) (formerly known as Georgia-loaded wheel tester). The HWTT is performed in accordance to AASHTO T 324 standard. A loaded steel wheel, weighing approximately 71.7 kg tracks over the samples placed in a water bath at 50°C. The vertical deformation of the specimen is recorded along with the number of wheel passes. The test is generally stopped when either the specimen deforms by 20 mm or the number of passes exceeds 20,000. A Cooper Hamburg device (Figure 3-9) was used in this study.



Figure 3-9. Hamburg wheel tracking device: test device, left, and mixtures after test, right

3.3.5. DC(T) Creep Testing

Due to the viscoelastic nature of asphalt binder, asphalt concrete under loading likewise exhibits time- and temperature-dependent response. This behavior can be characterized using various mixture testing modes such as the IDT, SCB or DC(T) (and is discussed further in Appendix B of MoDOT's version of this report). In this report, the DC(T) creep test has been carried out at three different temperatures: 0°C, -12°C, and -24°C. Similar to the IDT creep test, a constant creep load is applied for 1,000 s on the samples and crack mouth opening displacement (CMOD) response is measured. Prior to testing, samples are kept in the DC(T) chamber to be conditioned at the testing temperature for approximately 3 hours. After conditioning, the loading fixtures are inserted into the samples. The geometry of the sample (radius, thickness, and ligament), loading level and a correction factor are then introduced by the user to the software. First, a relatively low seating load is applied to fix the sample at the proper location and then the displacement response is measured and reported as a text file for every 0.3 s during the 1,000 s loading time.

(The procedure employed to calculate the creep compliance of the mixture is explained in detail in Appendix B of MoDOT's version of this report).

Creep compliance testing should be conducted in the linear viscoelastic range of the mixture being tested. Therefore, the level of creep loading should be chosen to stay in this range. This also served to minimize damage to the asphalt samples, since they can ideally be retained, allowed to relax, and subsequently tested to determine fracture energy. Considering the creep compliance at -24°C as the reference, shift factors are calculated to horizontally move the other two creep compliance curves at 0°C and -12°C to obtain a unique smooth curve and resulting master curve. Fitting a generalized Voigt-Kelvin model, consisting of an isolated spring, an isolated dashpot, and five Voight-Kelvin elements, a viscoelastic constitutive model is obtained. In addition, by subsequently fitting a power law function to the master curve, the m-value parameter can be obtained.

Similar in concept (but not in magnitude) to the BBR m-value, the mixture m-value is an indicator with the stress relaxation capability of the mixtures at low temperatures. The reason that the m-value for binder and mixture are not the same stems primarily from the fact that different models are used, different selected low temperatures, along with different methods to obtain the m-parameter from those models. The binder m-value is obtained at a loading time of exactly 60 s, while the mixture m-value represents the exponent parameter in the power law equation, and represents the linear asymptotic slope of the log compliance-log time master curve at very long loading times (much longer than 60 s). The BBR test is performed at the PG low temperature grade plus 10°C , while the mixture master curves obtained in this study were evaluated at a reference temperature of -24°C . Also, the BBR tests were performed on the virgin binders, while the mixture samples contained both virgin and recycled binders. Thus, while these parameters may in fact trend in the same direction, it is not advisable to directly correlate BBR m-values to mixture m-values. That notwithstanding, both parameters are of use in evaluating virgin binders and recycled mixtures, respectively.

3.3.6. Indirect Tension (IDT) Creep Compliance and Strength

The IDT creep and strength tests were carried out using a Cooper universal testing machine (UTM) at MAPIL with a capacity of 100 kN (Figure 3-10).



Figure 3-10. Cooper 100 kN UTM machine at MAPIL

The deflection measurements were made using horizontal and vertical extensometers. IDT creep and strength tests were performed following AASHTO T 322. To carry out the IDT creep test, three samples were conditioned at three different temperatures including 0°C, -12°C, and -24°C. Each sample was kept at the testing temperature for 2 hours. The conditioned sample was then put into the IDT fixture. In order to compensate for the temperature loss due to opening the chamber door and installing the extensometers, the sample was kept for another half-hour to reach the testing temperature. During this time, the response of extensometers was monitored to ensure that there was no temperature effect on the measured signal. Monitoring the response of the extensometer also helps identify poorly affixed sensors. Next, a seating load of 0.1 kN was applied on the sample. Shortly afterward, the load level was quickly ramped to the creep load, which is temperature dependent (higher loads used at lower temperatures). The creep load was reached in one second, which provided a reasonable approximation of a true step load (square wave). The creep load was then maintained for 1,000 s, and the displacements were recorded. The loading parameters are shown in Table 3-3.

Table 3-3. Loading parameters used at different testing temperatures

Testing temp. (°C)	Chamber temp. (°C)	Seating load (kN)	Ramp time (s)	Creep load (kN)	Creep time (s)
0	-1.5	0.1	1	4	1,000
-12	-14	0.1	1	8	1,000
-24	-26	0.1	1	20	1,000

In order to observe the viscoelastic behavior and accumulated damage of the asphalt mixtures, the creep test applies a static load to the specimen for 1,000 s. During the load application, the horizontal and vertical deformations are recorded. Three mixture parameters can be obtained from creep test: the creep compliance curve, the m-value and Poisson's ratio. The m-value can be obtained by applying power-law curve fit to the creep compliance curve. D1 in the power law describes the initial creep compliance. The m-value characterizes the long term slope of the creep compliance curve, and is related to mixture stress relaxation ability.

3.3.6.1. Sample Preparation

- Measuring thickness and diameter

To prepare the IDT testing samples, gyratory samples were compacted in the laboratory to 140 mm height and 7.5% air void using the plant produced materials. From each gyratory, two slices with 50 mm thickness were obtained with air void of $7\% \pm 0.5$. Three replicates for each of the four Level 1 section were prepared to be tested.

- Using the template to attach four gauge points on the surface

After cleaning the dust on the surface of each sample, gauge point locations were set using a marking template (as shown in Figure 3-11).

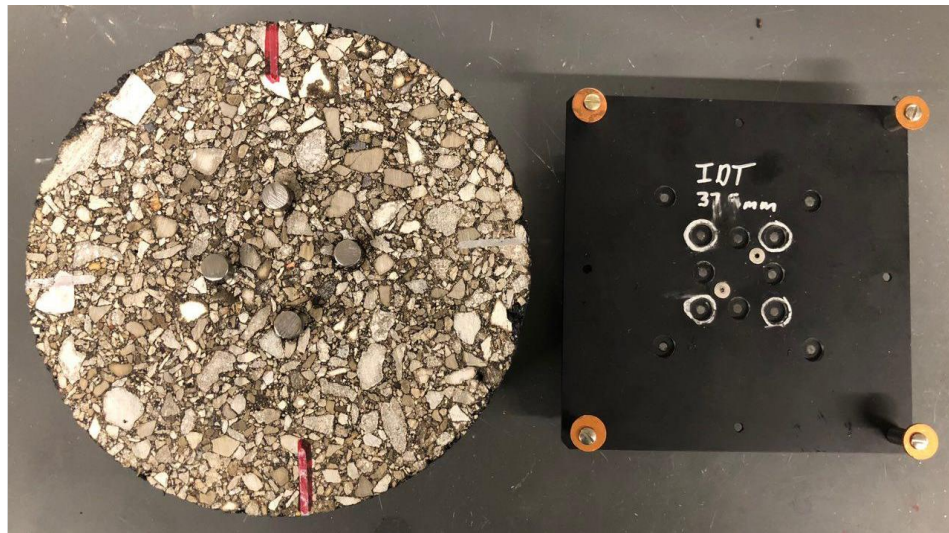


Figure 3-11. Attached gauge points on the samples using the pattern

Afterward, the perpendicular marks aligned with the gauge points were drawn on the sample in order to accurately align the sample in IDT fixture. The same procedure was followed on both sides of the specimen.

3.3.6.2. Data Analysis (per AASHTO T 322-07)

- Extract extensometer measurements
- Normalize the data using the load level and geometry, where:

$$\Delta X_{n,i,t} = \Delta X_{i,t} \times \frac{b_n}{b_{avg}} \times \frac{D_n}{D_{avg}} \times \frac{P_{avg}}{P_n} \quad (6)$$

- Using the normalized deflection at 500 s, discard the maximum and minimum measurements for both vertical and horizontal deflections (each direction has 3 samples \times 2 surfaces = 6 measurements)
- Average out the four remaining measurements for both vertical and horizontal directions
- Determine the correction factor, where:

$$C_{cmt} = 0.6354 \times \left(\frac{X}{Y} \right)^{-1} - 0.332 \quad (7)$$

- Calculate the creep compliance, where:

$$D(t) = \frac{\Delta X_{tm,t} \times D_{avg} \times b_{avg}}{P_{avg} \times GL} \times C_{cmt} \quad (8)$$

- Construct the creep compliance master curve using creep versus time data

The strength test was performed by applying an increasing load at a constant displacement rate until the failure occurs in the specimen. The tensile strength was then calculated as follows:

$$S_t = \frac{2P_{max}}{\pi * t * D} \quad (9)$$

where the P_{max} is the maximum load that the sample could tolerate in N, and t and D are the thickness and diameter of the sample, respectively, in mm.

4. BINDER RESULTS

4.1. Overview

Asphalt binder testing results including the RV, DSR, and BBR tests are discussed in this chapter. A detailed discussion regarding the test results is provided in the following sections.

4.2. Rotational Viscosity Test on Binders

After the temperature stabilization conditioning process is complete, rotational viscosity testing begins and data is collected at 1 min. intervals for a total of 3 min. The viscosity of the tested binder in mPa.s (miliPascal times second) is averaged over these measurements and can then be used to calculate appropriate mixing and compaction temperatures for the purposes of asphalt mixture production (Table 4-1).

Table 4-1. Viscosity of binders obtained from the RV device

Binder type	Viscosity (mPa.s)		Mixing temperature (°C)	Compaction temperature (°C)
	135°C	155°C		
MO13-64-22H	653.7	261.8	165.4	153.4
US54-64-22H	901.5	360.8	173.7	161.1
US63-58-28	217.2	96.4	140.7	129.3
US54-58-28	278.8	123.2	146.8	134.9
US54-46-34	181.0	83.6	136.5	124.9

Mixing and compaction temperatures correspond to 170 and 280 cP viscosity levels, respectively. The viscosity at 135°C can also be checked against the Superpave upper limit of 3,000 mPa.s, which was easily met in all cases.

4.3. Dynamic Shear Rheometer Test on Binders

The results of DSR testing of virgin binders are shown in Table 4-2.

Table 4-2. Summary of virgin binder testing results

Binder type	High temperature		Low temperature			UTI* (°C)
	Continuous PGHT	PGHT	Continuous PGLT	PGLT	ΔT_c	
MO13-64-22H	70.7	70.0	-21.2	-16.0	-8.6	91.9
US54-64-22H	73.1	70.0	-25.2	-22.0	-3.3	98.3
US63-58-28	56.1	52.0	-29.0	-28.0	-3.9	85.1
US54-58-28	60.6	58.0	-28.8	-28.0	-1.4	89.4
US54-46-34	52.7	52.0	-33.7	-28.0	-2.5	86.4

*Useful temperature interval

The continuous high temperature PG is calculated based on the critical high temperature PG, which is obtained based on RTFO and tank binder test results.

4.4. Bending Beam Rheometer

The results of the BBR test are used to evaluate the low temperature cracking resistance of the binder. Besides the low temperature PG, ΔT_c can be calculated. This parameter has been proposed to evaluate age-related cracking potential of the binder. It is defined as the numerical difference between the low continuous grade determined from the bending beam rheometer (BBR) by stiffness criteria (which is the temperature at which the stiffness, S [$t=60$ s], equals 300 MPa) and the low continuous grade temperature determined from the BBR m -value (which is the temperature at which the m -value equals 0.3). Higher ΔT_c values are associated with better aging and cracking resistance. According to the summary of binder results, which is provided in Table 4-2, US54-58-28 has the highest (least negative) ΔT_c value, while MO13-64-22H exhibited the lowest ΔT_c value.

Some of the study binders were not found to meet the reported performance grade (Table 4-2), which in theory would lead to an increased pavement deterioration risk. However, the deviations were less than 2°C in both cases. Quite a large difference existed between the two 64-22H binders evaluated in this study, where the MO13 binder had a useful temperature interval (UTI) of 91.9°C, while the US54 binder possessed a considerably better UTI value of 98.3°C.

4.5. Multiple Stress Creep Recovery

The MSCR test was conducted on the five different binder types sampled for this project. In addition to the labeled PG high temperature (PGHT) of each binder, the measured PGHT using DSR test was used to determine the binder final grade. Table 4-3 presents the average of the MSCR testing results.

Table 4-3. Summary of MSCR testing results

Binder	Testing temp.	Jnr, 3.2 kPa-1	Jnr, diff %	Traffic
MO13-64-22H	64	1.42	34.97	H
	70	3.49	38.36	S
US54-64-22H	64	0.78	72.06	V
	70	2.26	87.66	Failed
US63-58-28	52	2.30	14.38	S
	58	5.52	15.01	Failed
US54-58-28	58	2.84	13.12	S
	64	6.69	14.06	Failed
US54-46-34	46	1.37	14.78	H
	52	3.62	14.78	S

According to Table 4-3, the following conclusions can be made:

- MO13-64-XX H has been properly designated based on MSCR test. That notwithstanding, this binder could be labeled as PG70-XX S as it passed the high PG required a temperature of 70°C. The MSCR test determined the standard traffic level at 70°C for this binder.
- US54-64-XX H could be designated as PG64-XX V, which is more resistant to permanent deformation based on MSCR test. Although this binder passed the PGHT requirements at 70°C, this binder could not be labeled as PG70-XX due to the failure in MSCR test at this temperature.
- Similar to the PGHT test, the US63-58-XX binder could not meet MSCR test requirements at 58°C. Therefore, this binder is softer than its stated grade and should be designated as PG52-XX S.
- While it failed the MSCR test at 64°C, US54-58-28 could meet the requirements of this test at 58°C. Taking into account the PGHT test results in Table 4-2, this binder was properly labeled as PG58-XX.
- The US54-46-34 binder, which could be designated as PG50-XX, could also pass the MSCR test at 52°C and can be labeled as PG52-XX considering both PGHT and MSCR test.

5 .MIXTURE RESULTS

5.1. Overview

In this portion of the study, field cores and lab-produced samples obtained from the study field sections were characterized by mixture mechanical tests (mix performance tests). This included the DC(T), I-FIT and Hamburg tests. Table 5-1 provides details of the mixtures associated with each field section.

Table 5-1. Summary of field sections investigated

No.	Cons. year	Section	ABR ⁹ %		Total Pb ¹⁰ %	Virgin binder	Additive	NMA S (mm)
			%RAP	%RAS				
1	2016	MO13_1 (17-17-0)	17	0	5.7	PG64-22 H ¹¹	Type 1 ¹ :0.5%	9.5
2	2016	US63_1 (35-35-0)	35	0	5.1	PG58-28	Type 2 ² :0.5% + Type 3 ³ :1.75%	12.5
3	2016	US54_6 (31-31-0)	31	0	5.1	PG58-28	Type 1:1%	12.5
4	2016	US54_1 (33-0-33)	0	33	5.2	PG58-28	Type 4 ⁴ :2.5% + Type 5 ⁵ :3.5% + Type 1:1.5%	12.5
5	2011	US50_1 (25-25-0)	25	0	4.5	PG64-22	Type 6 ⁶ :1.5% + Type 7 ⁷ :1%	12.5
6	2010	MO52_1 (34-0-34)	0	34	4.8	PG64-22	Type 6: 1.5%, Type 7:0.8%	12.5
7	2008	US63_2 (30-20-10)	20	10	5.6	PG64-22	Type 6: 1.5% + Type 7: 0.5%	12.5
8	2016	US54_2 (33-33-0)	33	0	5.3	PG58-28	Type 1: 1%	12.5
9	2016	US54_3 (33-18-15)	18	15	5.2	PG58-28	Type 1: 1%	12.5
10	2016	US54_4 (35-35-0)	35	0	4.8	PG64-22 H	Type 5:3% + Type 1:1%	12.5
11	2016	US54_5 (0-0-0)	0	0	5.4	PG64-22 H	Type 1: 1%	12.5
12	2003	US54_7 (0-0-0)	0	0	6.2	PG64-22	Type 8 ⁸ : 0.25%	12.5
13	2006	US54_8 (9-9-0)	9	0	5.6	PG70-22	Type 7: 0.5%	12.5
14	2016	SPS10-1 (24-24-0)	24	0	5.2	PG64-22 H	Type 1:1%	12.5
15	2016	SPS10-2 (25-25-0)	25	0	5	PG64-22 H	Type 1:1%	12.5
16	2016	SPS10-3 (25-25-0)	25	0	5	PG64-22H	Type 1:1% + Type 2: 0.5%	9.5
17	2016	SPS10-6 (17-0-17)	0	17	5.4	PG58-28	Type 1: 1%	9.5
18	2016	SPS10-9 (46-16-30)	16	30	5.3	PG46-34	Type 1: 2%	12.5

¹Type 1. Anti-stripping agent (Morelife T280)

²Type 2. Warm-mix additive (Evotherm)

³Type 3. Rejuvenator additive (EvoFlex CA)

⁴Type 4. Anti-stripping agent (IPC-70)

⁵Type 5. Warm-mix additive (PC 2106)

⁶Type 6. Bag house fines

⁷Type 7. Anti-stripping agent (AD-here HP Plus)

⁸Type 8. Anti-stripping agent (LOF 65-00LS1)

⁹ABR = Asphalt binder replacement

¹⁰By total mass of binder, including neat and recycled

¹¹Heavy traffic designation (from MSCR test)

Most of the sections (13 out of 18 sections) were constructed in 2016 and cored soon thereafter (within two weeks after construction), which represents the short-term aging condition. The other five sections are highlighted in different colors to easily distinguish between the recently constructed and aged sections. The oldest section investigated was US54_7, which was constructed in 2003 and did not contain any RAP and RAS. Asphalt binder replacement (ABR) by RAP and RAS, the total percentage of asphalt content by mixture mass (Pb), PG of the virgin binder, the type and dosage of additives, and nominal maximum aggregate size (NMAS) are summarized in Table 5-1. For convenience, the percentage of ABR and RAP/RAS contents have been included in the section labels. As an example, MO13_1 (17-17-0) has an ABR of 17%, resulting from 17% replacement by RAP and 0% by RAS. As shown, 11 out of 18 sections had a Superpave Performance Grade low temperature (PGLT) grade of -22°C, which is the low temperature binder grade currently specified in Missouri.

5.2. Thermal Cracking Performance Based on DC(T) Fracture Energy

5.2.1. Field Core Fracture Energy Results

This section presents DC(T) fracture energy testing results obtained from field cores. Testing of at least three, and usually four, sample replicates were performed. A testing temperature of -12°C was used in all cases, which is 10 degrees warmer than the plan low temperature Superpave PG grade for binders specified in Missouri. Note that for convenience, the percentage of ABR and RAP/RAS contents have been included in the section labels. As an example, MO13_1 (24-24-0) has an ABR of 24%, resulting from 24% replacement by RAP and 0% by RAS. Figure 5-1 presents the fracture energy results obtained for all 18 study mixtures. The PG low temperature grade (PGLT) of the virgin asphalt binder is also shown on the plot, as indicated by the red line.

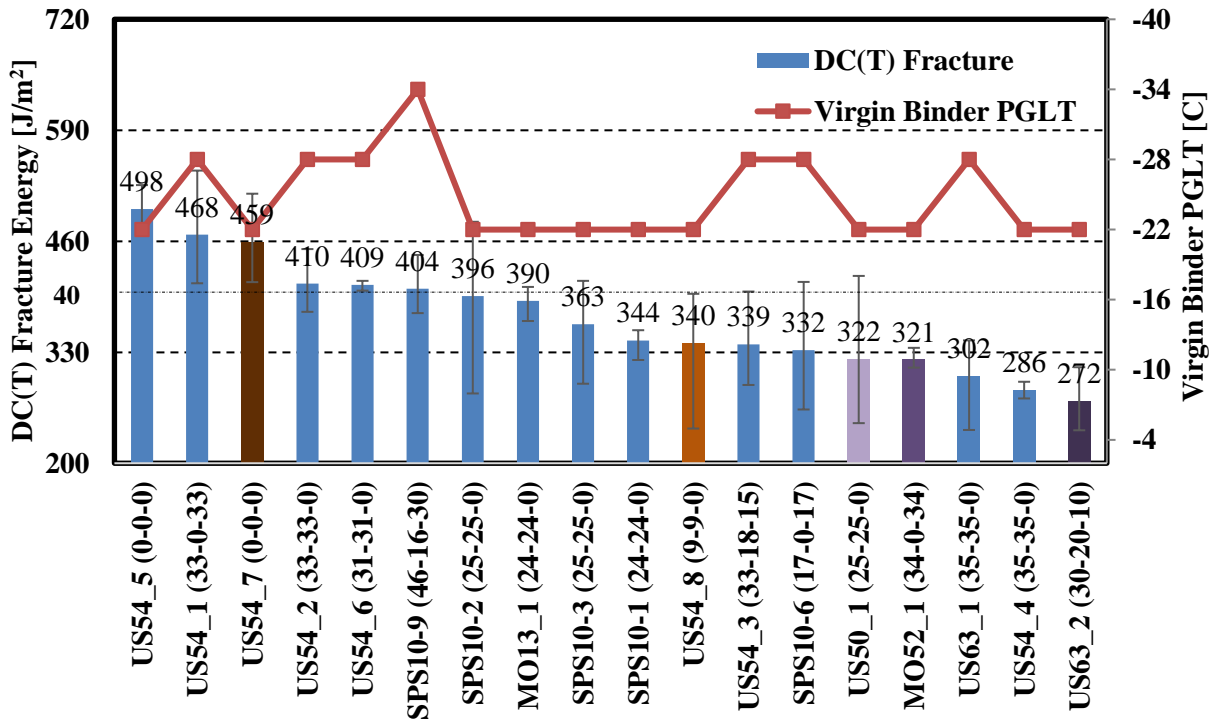


Figure 5-1. DC(T) fracture energy test results of field cores

Some general observations regarding DC(T) fracture energy from cores are:

- All aged mixtures fall below the desirable 400 J/m² minimum threshold for the long-term aging criteria except US54_7 (14 years aging), which is a virgin mixture with 6.2% binder content. MO52_1 (6 years aging), US54_8 (11 years in service), US50_1 (6 years aging) and US63_2 (9 years aging) possessed fracture energy levels of 321, 340, 322, and 272 J/m², respectively. This indicates a sensitivity to thermal and block cracking in these sections, particularly US63_2.
- Among the highest fracture energy results obtained, a combination of virgin mixes and those containing RAP and/or RAS fell in this top grouping with fracture energy values above the recommended 460 J/m² threshold for short-term aged mixes. These particular recycled mixes appeared to benefit from the use of a softer base binder. For example:
 - US54_1 had 33% ABR by RAP with a PG 58-28 binder (468 J/m²), and;
 - SPS10_9 had 46% ABR (16% by RAP and 30% by RAS), along with a PG 46-34 binder (467 J/m²).
 - By comparison, US54_5 is a virgin mix with a PG 64-22H binder (497 J/m²).
- Only two of the newer mixes investigated (i.e., those sampled in the short-term aged condition in 2016), had noticeably low fracture energy. These were:
 - US63_1, which had 35% ABR by RAP and a single grade bump to PG 58-28 (302 J/m²). This may indicate that a second grade bump or lower RAP level was needed in the design. The research team also found the aggregate or RAP source used appears to have a moisture sensitivity issue as well, which is discussed further later in this chapter.
 - US54_4, which also had 35% ABR by RAP, but which used a modified but stiff PG 64-

22 H binder (286 J/m²). This may indicate that a better choice for binder would have been a PG XX-28 or even a PG XX-34, rather than investing in the polymer modified PG 64-22 H. The team also found that this section had a very low Hamburg rut depth, supporting the notion for binder bumping to a softer low temperature grade, which is discussed further later in this chapter.

- A number of the other newer mixes would have also benefitted from minor adjustments to a softer low temperature grade, in order to reach the 460 J/m² fracture energy level.

5.2.2. Plant Mixture Fracture Energy Values Obtained with the DC(T)

This section presents DC(T) fracture energy testing results obtained from field cores. In all cases, four sample replicates tests were performed. Table 5-2 summarizes the results from these four sections, which were in the Level 1 sampling category.

Table 5-2. Summary of plant mixtures

Sample	Const . year	Virgin binder grade	NMAS (in.)	AC content	ABR (%)	%ABR by RAP	%ABR by RAS
MO13_1 (17-17-0)	2016	PG64-22 H	3/8	5.70%	16.6	16.6	0
US63_1 (35-35-0)	2016	PG58-28	1/2	5.10%	35.2	35.2	0
US54_6 (31-31-0)	2016	PG58-28	1/2	5.10%	30.7	30.7	0
US54_1 (33-0-33)	2016	PG58-28*	1/2	5.20%	33.0	0	33.0

*Contained 3.5% rejuvenator by weight of binder.

Figure 5-2 summarizes the fracture energy results obtained with the DC(T) on the four plant mixes sampled.

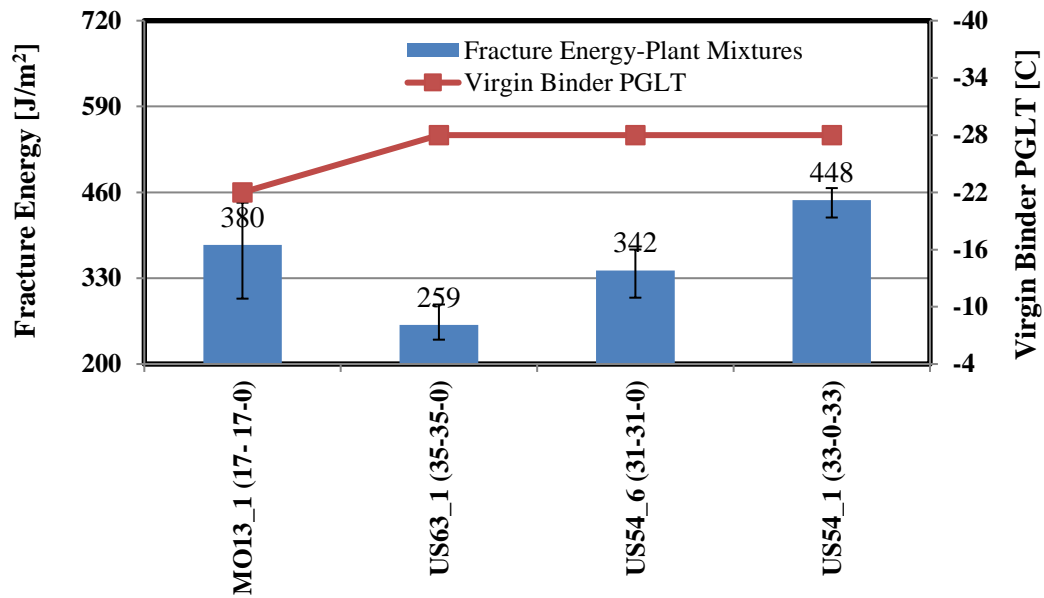


Figure 5-2. DC(T) fracture energy test results of plant mixtures

The following observation was made from this figure:

Comparing US54_6 (31% ABR by RAP) and US54_1 (33% ABR by RAS), the higher fracture energy in the mix containing RAS might be explained by the fact that this mix used 3.5% of rejuvenator along with the PG58-28 binder. The statistical analysis in section 5-9 determined the ranking of the plant mixes in terms of fracture energy.

Figure 5-3 compares the average DC(T) fracture energy of Level 1 field cores and plant mixtures (sampled at the paver and compacted in the laboratory after storage and reheating of mix).

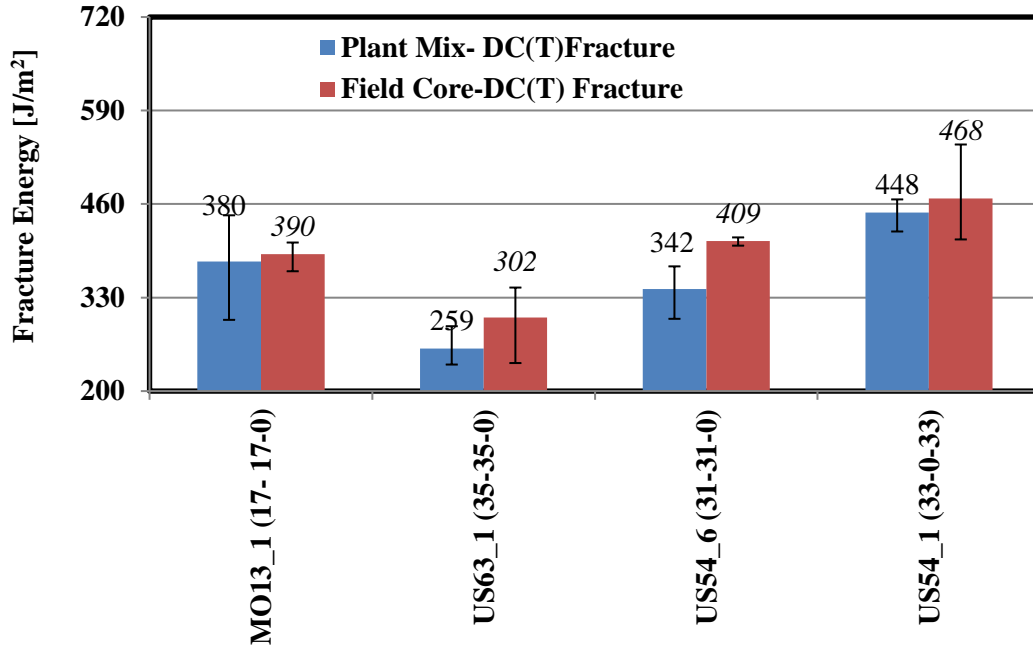


Figure 5-3. Comparing DC(T) results of field cores and plant mixtures

As shown, the fracture energy of field core and plant mixture of MO13_1 and US54_1 are very close to each other, with the field cores yielding slightly higher DC(T) fracture energy. However, the fracture energy of US63_1 and US54_6 field cores are about 50 J/m² higher than their corresponding plant mixtures. This can be attributed to the reheat that the buckets of plant mixtures experienced before compaction. The plant mixtures in buckets were reheated to 100±5°C to be warm enough to be split into pans. The pans were then kept in the oven to reach the compaction temperature. This process might induce additional aging to the binder and make the plant produced-laboratory compacted mixtures more brittle than field cores.

5.2.3. Laboratory Mixture Fracture Energy Values Obtained with the DC(T)

In addition to the field cores and plant mixtures, laboratory mixtures were fabricated using the job mix formula (JMF) of MO13_1 and US63_1 sections. As Figure 5-4 shows:

- A good comparison between field core, plant-produced mix, and laboratory mix (lab produced, lab compacted mix) was observed (within 20%).

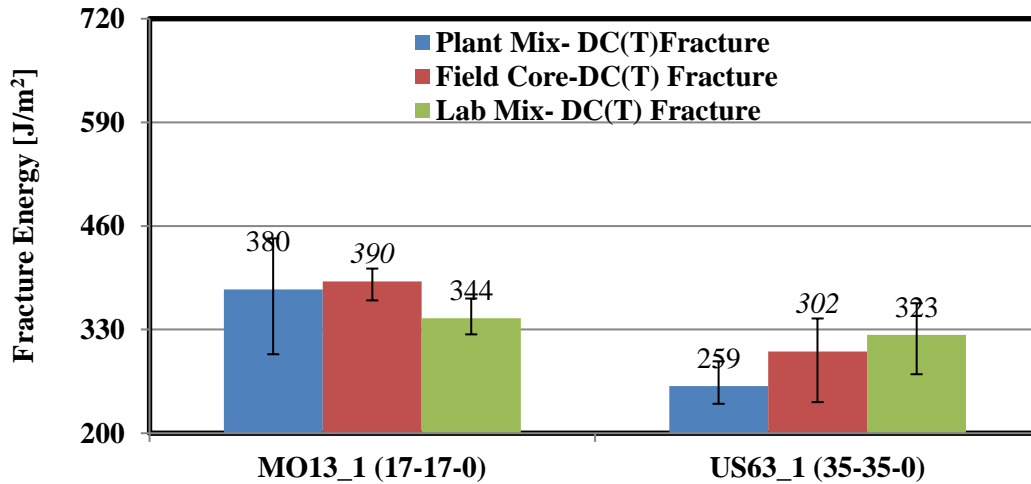


Figure 5-4. Comparing DC(T) results of field cores, plant mixtures, and lab mixtures

- A slight trend of lower fracture energy for the laboratory compacted mix was observed. As mentioned in Section 5.2.2, this might possibly be explained by the fact that these mixes were reheated, and by differences in field compaction versus laboratory compaction. The difference in fracture energy of field core, plant and laboratory mixes might be due to the differences in aggregate orientation, breakage, void levels, and gradients thereof.

5.3. Cracking Resistance Using SCB Flexibility Index

This section presents the results of testing conducted on mixture cores and plant samples using the I-FIT device at room temperature, which uses the semi-circular bend geometry. The test usually involves the computation of a flexibility index (FI), which combines fracture energy and the slope of the load-displacement curve after the peak. Figure 5-5 shows a typical output from the Testquip I-FIT device.

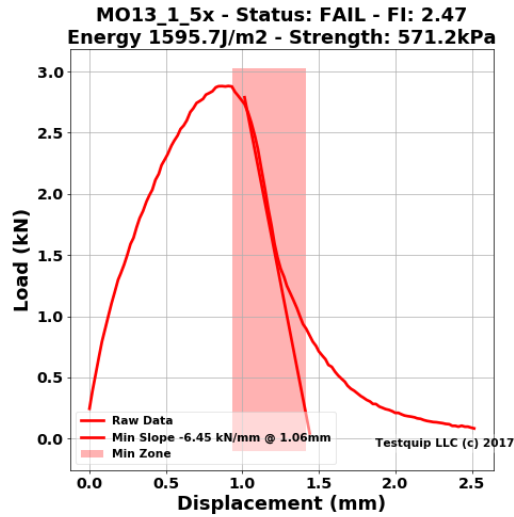


Figure 5-5. Typical I-FIT data analysis from Testquip SCB and ICT software

5.3.1. Field Core Flexibility Index Results

Figure 5-6 presents the results of I-FIT testing of Missouri mixes as sampled from field cores.

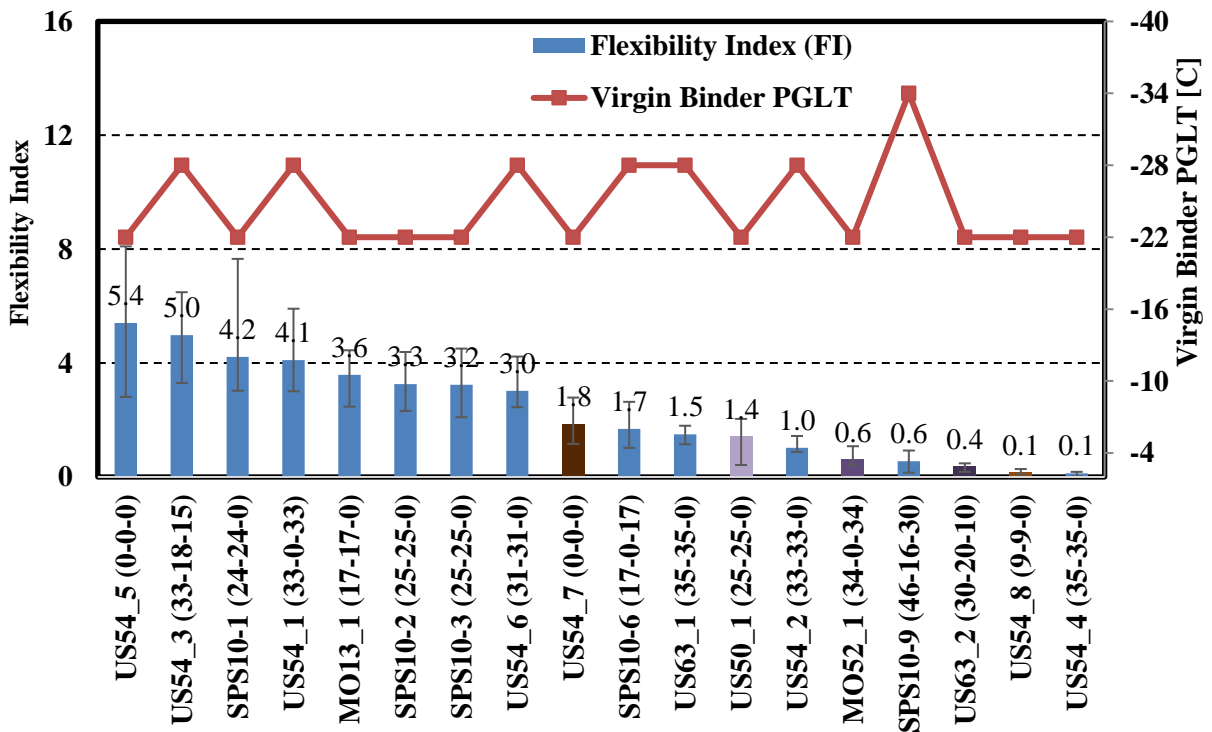


Figure 5-6. I-FIT test results for field cores

None of the mixtures tested possessed an FI value in excess of 8.0, and in fact, all samples were found to be below an FI value of 6.0. Recall from Table 5-1 that the 18 mixtures tested were comprised of 11 newer mixes, and 5 field-aged mixes. Some samples had very low FI values, less than 2.0, and in some cases, nearly zero. These specimens exhibited very brittle behavior in the I-FIT test, with snap-back type softening curves and very few data points following the peak load, indicating a very brittle failure. Analysis of data sets with very steep post-softening curves is not adequately described in the test specification, and requires analyst judgment. These mixes often possess the highest variability between test replicates, which is addressed in the following section. Considering the I-FIT testing results, some comparisons can be made as follows:

- The source of ABR was found to be very important. Considering US54_2 and US54_3, which have the same ABR but different combinations of RAP and RAS, US54_2 showed 400% higher FI than US54_3.
- US54_6 and US63_1 with different additives had a difference of 50% in FI. The significant effect of additive was also noticeable in DC(T) fracture energy.
- Comparing US54_2 and SPS10-1, one grade bump could not compensate for the presence of 9% ABR. The FI of SPS10-1 (24-24-0) is 320% higher than US54_2 (33-33-0).
- Comparing to US54_3, one grade bump and 1% more Mlife additive did not help SPS10-9 to compensate for 15% additional ABR by RAS.

It is also worth mentioning that four replicates were tested in I-FIT and the results were averaged out and reported in Figure 5-6. However, for two sections (SPS10-9 and US54_4), no FI could be calculated for one of the tested replicates due to the very brittle post-peak behavior, as shown in Figure 5-7 (quadrilateral and cut-back shape of load-displacement plot).

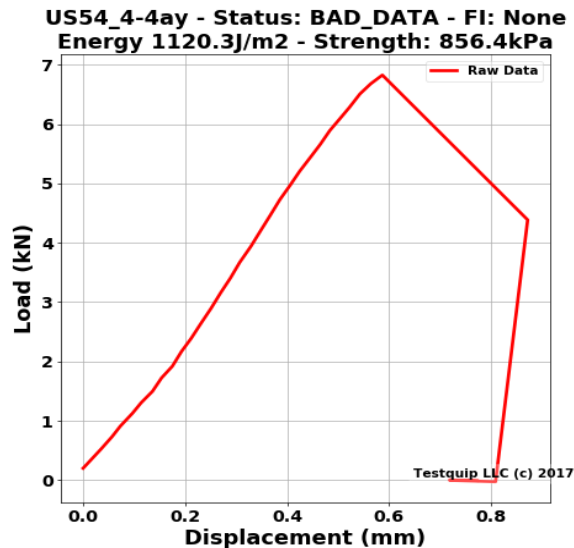


Figure 5-7. An example of very brittle behavior (US54_4-4ay tested sample)

In this case, the slope that is used to determine the FI could not be calculated. Therefore, no FI was considered for those two replicates in the average as it was reported as “None” by software.

5.3.2. Plant Mixtures Flexibility Index Results

Figure 5-8 presents the side-by-side comparison of the field core and plant mix flexibility index for four sections in Level 1.

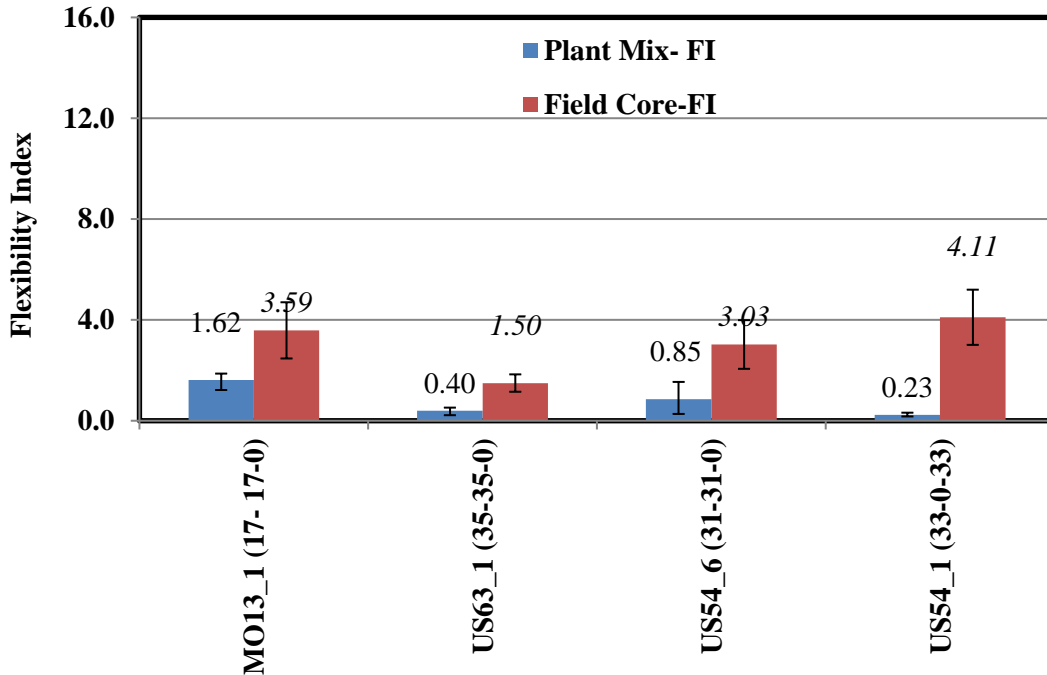


Figure 5-8. Comparing I-FIT results of field cores and plant mixtures

As shown, there is a significant difference in average FI between these two types of samples. Unlike DC(T) fracture energy, the field cores and plant mixtures of the sections do not follow the same trend. The US54_1 sample, which had been the best field core performer, exhibited the poorest performance in plant mixtures. The closest field core to plant mixture was recorded by MO13_1 in which the field core FI is 2.2 times the plant one. Given the more aging that the plant mixtures could experience in the fabrication process (discussed in section 5.2.2) and lower FI of the plant mixtures comparing to field cores, this parameter is believed to be heavily dependent on aging and fabrication process of the asphalt samples.

5.3.3. Lab Mixtures Flexibility Index Results

Comparing the FI obtained from field cores, plant and laboratory mixtures presented in Figure 5-9, it was observed that lab mixtures yielded similar FIs to field cores (within 10%).

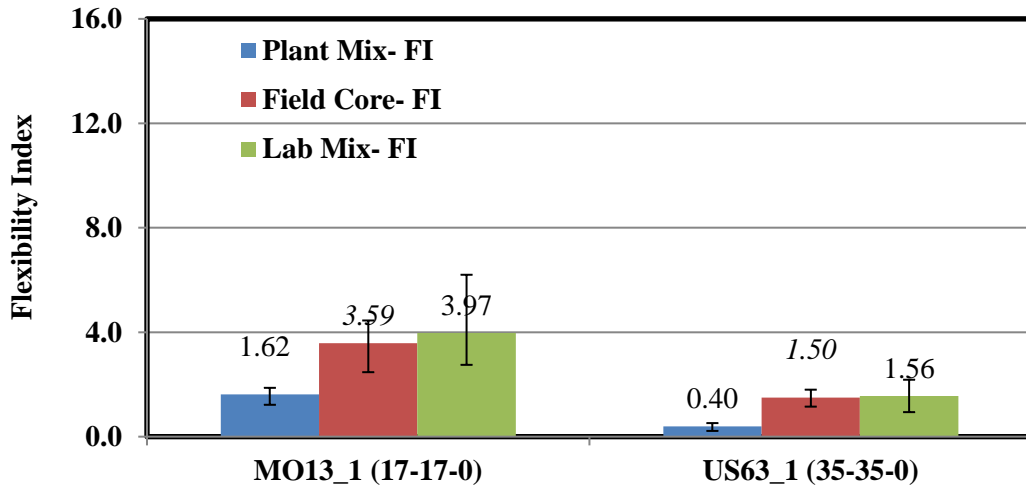


Figure 5-9. Comparing I-FIT results of field cores, plant mixtures, and lab mixtures

According to the sensitivity of I-FIT to aging, this similarity implies that the aging the two types of samples (field core and lab mix) experienced are comparable to each other.

5.3.4. Comparing DC(T) and I-FIT Test Results

Fracture energy (FE) and flexibility index for the various field core samples were normalized and plotted in Figure 5-10.

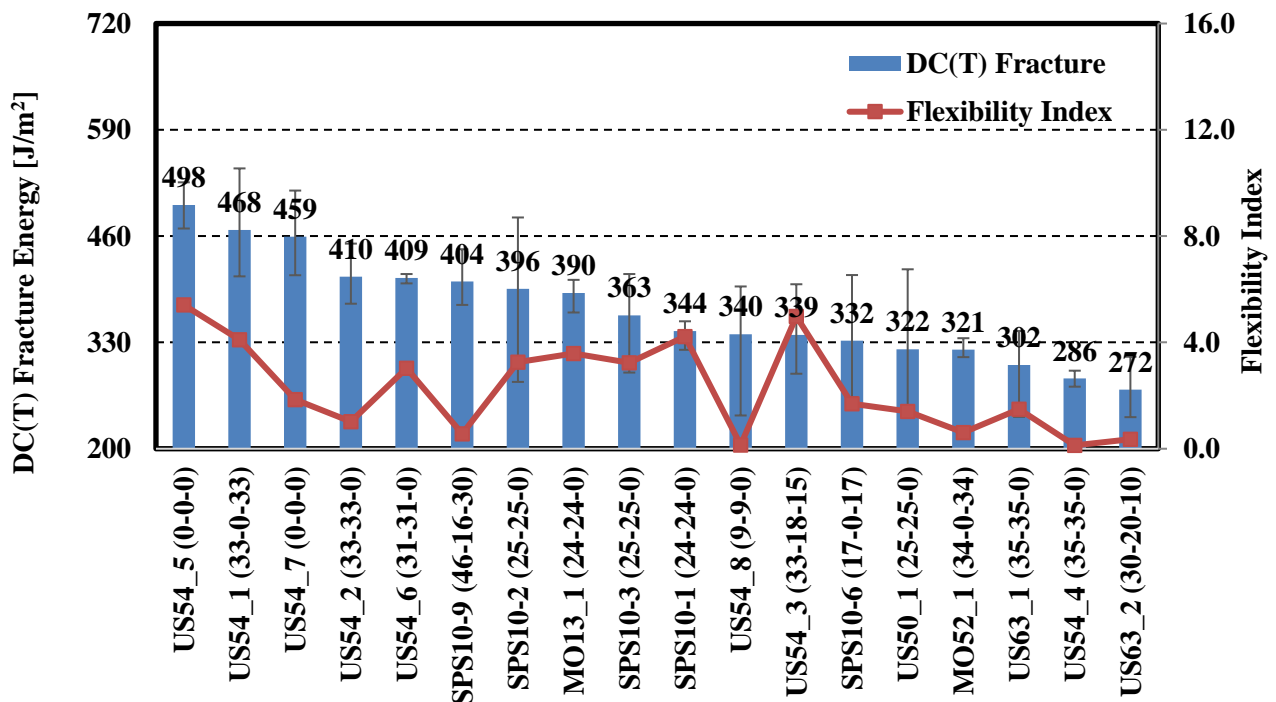


Figure 5-10. Comparison of DC(T) FE & SCB FI test results of field cores

Some similarity in trends were observed, but it is clear that the DC(T) and I-FIT tests provide different cracking measures overall. Thermal cracking resistance as measured in the DC(T) for various Missouri mixtures tends to vary by about 40% for Superpave mixtures (around 0.6 to 1.0 on the normalized plot). On the other hand, the I-FIT parameter varies from nearly zero to just over 5.0, and on the normalized FI plot, varies across the entire scale from zero to 1.0. This clearly results from the wide array of post-peak slope behavior observed in the test. Apparently, because of the stiff specimen geometry and very fast loading rate, the fracture process in some of the stiffer specimens becomes unstable, leading to an explosive failure (very fast crack propagation) once the peak load is reached and the stored strain energy from bending begins to transfer to the crack face.

Table 5-3 shows the coefficient of variability (COV) of the field cores tested for both the DC(T) test and the I-FIT test.

Table 5-3. COV of DC(T) and I-FIT measurements on field cores for Missouri Superpave mixes

Section	DC(T)		I-FIT					
	Avg. FE (J/m ²)	COV %	Avg. FE (J/m ²)	COV %	Avg. slope (kN/mm)	COV %	Avg. FI	COV %
MO13_1 (17-17-0)	390.3	5.4	1623.6	4.4	4.73	25.5	3.59	23.5
US63_1 (35-35-0)	302.4	18.4	1092.6	15.0	7.59	25.1	1.50	23.3
US54_6 (31-31-0)	408.8	1.4	1883.6	7.8	6.56	27.2	3.03	32.1
US54_1 (33-0-33)	467.6	14.5	1788.4	15.2	4.53	17.4	4.11	32.2
US54_2 (33-33-0)	410.4	9.1	1410.1	9.1	14.41	19.7	1.02	29.9
US54_3 (33-18-15)	339.2	16.5	2227.9	18.8	4.57	16.4	4.98	32.2
US54_4 (35-35-0)	285.8	3.4	1208.7	21.2	301.18	124.0	0.13	77.8
US54_5 (0-0-0)	497.9	5.7	2229.1	14.7	4.62	33.2	5.41	43.7
SPS10-1 (24-24-0)	343.9	5.8	2183.6	20.0	6.04	37.7	4.22	57.6
SPS10-2 (25-25-0)	395.6	26.1	1864.6	10.2	5.39	16.7	3.27	28.7
SPS10-3 (25-25-0)	363.0	17.2	2152.2	10.7	7.14	30.5	3.24	31.8
SPS10-6 (17-0-17)	332.3	22.7	1837.5	13.0	11.97	32.2	1.69	41.0
SPS10-9 (46-16-30)	404.4	8.8	1142.7	12.5	34.80	86.6	0.56	76.1
US50_1 (25-25-0)	321.5	27.6	759.4	7.6	7.68	81.7	1.41	51.6
MO52_1 (34-0-34)	321.2	3.8	546.2	13.1	10.67	43.3	0.61	51.4
US63_2 (30-20-10)	272.4	13.7	634.7	3.0	20.14	49.9	0.36	35.4
US54_8 (9-9-0)	340.2	25.5	1170.7	35.4	262.08	141.2	0.14	80.7
US54_7 (0-0-0)	459.3	11.4	1221.2	7.4	7.19	30.1	1.85	37.6
Ave COV%		13.2		13.3		46.6		43.7

DC(T) COVs ranged from 1.4% to 27.6%, with an average of 12.7%. I-FIT COVs ranged from 23.3% to 80.7%, with an average of 44.6%. In general, for mix testing, it is desirable to keep COV values under 15–20%.

5.4. IDEAL CT Index Test

5.4.1. Plant Mixture Ideal CT Test Results

In terms of specimen dimensions, all samples are 150 mm in diameter with a thickness of either 62 or 95 mm. For 62 mm thickness, two different gyratory specimens were fabricated. For the first type, gyratory samples were compacted to 62 mm and then were tested (DPs). The second type consists of 62 mm height slices (HPs), which were obtained from 140 mm height gyratory specimens after cutting. From each 140 mm gyratory specimen, two 62 mm height IDEAL samples were obtained. Also, 95 mm height samples were compacted in gyratory compactor to 95 mm height without any cutting (Figure 5-11).

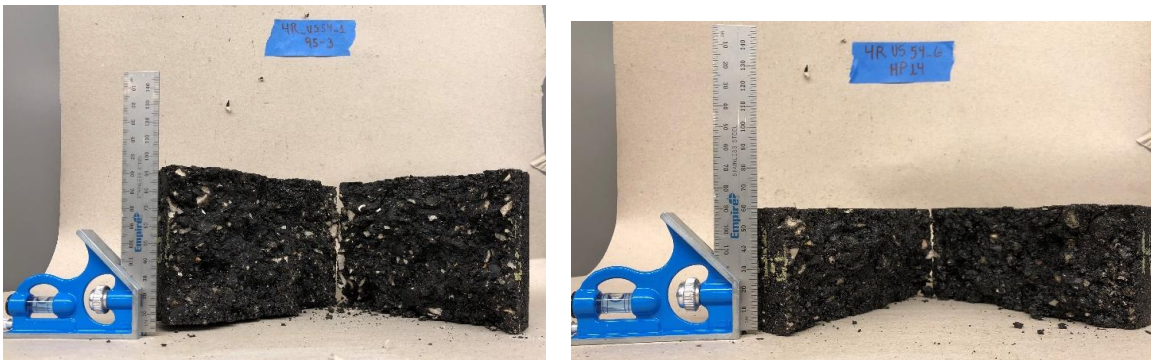


Figure 5-11. Example of 95 mm thickness specimen, left, and 62 mm thickness specimen, right

This approach provided a means to determine the effect of geometry surface cut on the IDEAL-CT index. Figure 5-12 shows an example of the IDEAL-CT force versus displacement curves.

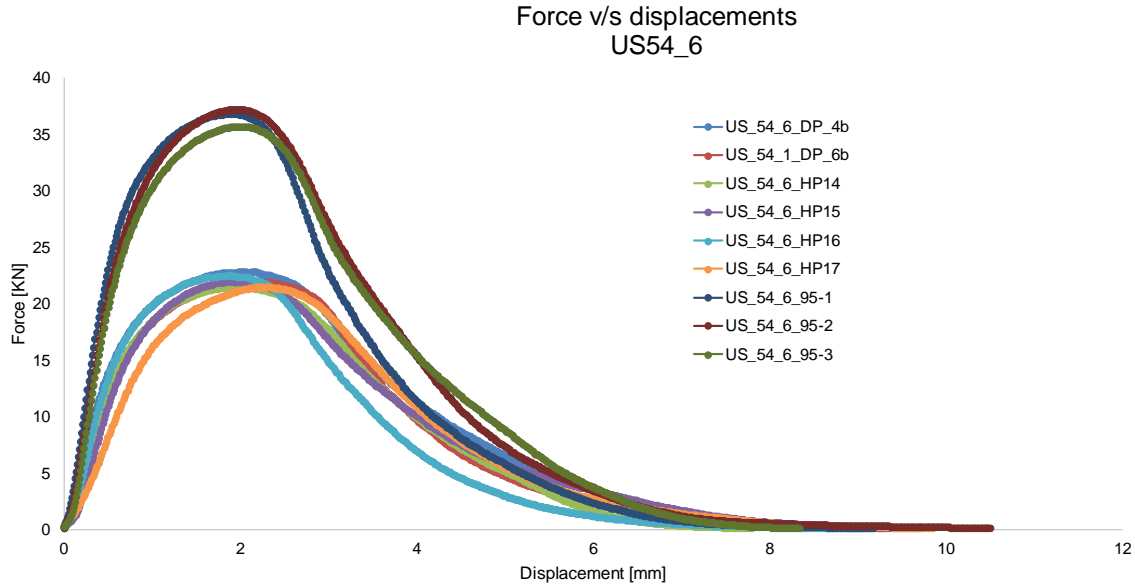


Figure 5-12. Typical force vs. displacement curves obtained from IDEAL-CT test

As Figure 5-12 shows, the 95-thickness specimens have higher peak load and post-peak slope than the 62-thickness specimens, however, not necessarily higher fracture energy. Section MO13_1_DP/HP has an average peak load of 17.8 kN while MO13_1_95 has an averaged peak load of 29.4 kN. Section US63_1_DP/HP has an averaged peak load of 19.6 kN while US63_1_95 has an averaged peak load of 37.0 kN. Section US54_6_DP/HP has an averaged peak load of 22.2 kN while US54_6_95 has an averaged peak load of 36.5 kN. Section US54_1_DP/HP has an averaged peak load of 22.2 while US54_1_95 has an averaged peak load of 39.7 kN.

Table 5-4 shows the CT index of different mixtures.

Table 5-4. IDEAL-CT index of mixtures using different sample geometries (compacted to 95 mm thickness, compacted to 62 mm [HP] and cut to 62 mm [DP] thicknesses)

Section	Sample	Averaged CT index	COV (%)
MO13_1	MO13_1_DP	61.2	33.7
	MO13_1_HP	40.0	34.5
	MO13_1_95	53.4	50.1
US63_1	4R63_1 DP	12.8	42.0
	4R63_1 HP	9.2	11.1
	4R63_1 -95	5.9	16.2
US54_6	4R54_6 DP	17.3	19.6
	4R54_6 HP	17.7	23.7
	4R54_6 -95	23.6	72.6
US54_1	4R54_1 DP	17.1	34.7
	4R54_1 HP	8.2	12.4
	4R54_1 95	9.7	45.7

Observations from the CT index by type of sample are:

- There is no consistent trend between the results of the CT index and their respective COV between a specimen of 62 mm (either DP or HP) and a 95 mm specimen.
- There is no clear trend between the results of the CT index and their respective COV between specimens of 62 mm either DP or HP.
- The highest CT index is for MO13_1_DP of 61.2.
- The highest COV by type of specimen is for US54_6_95 with a 72.6%.
- Only 4 out of the 12 COV results presented by type of sample are under 20% COV. Therefore, no clear conclusion about the specimen type effect can be drawn.
- Since the compacted-to-62-mm samples (HPs) had the relatively lower COVs among the three tested geometries, this geometry is chosen to compare the CT indexes in Figure 5-13.

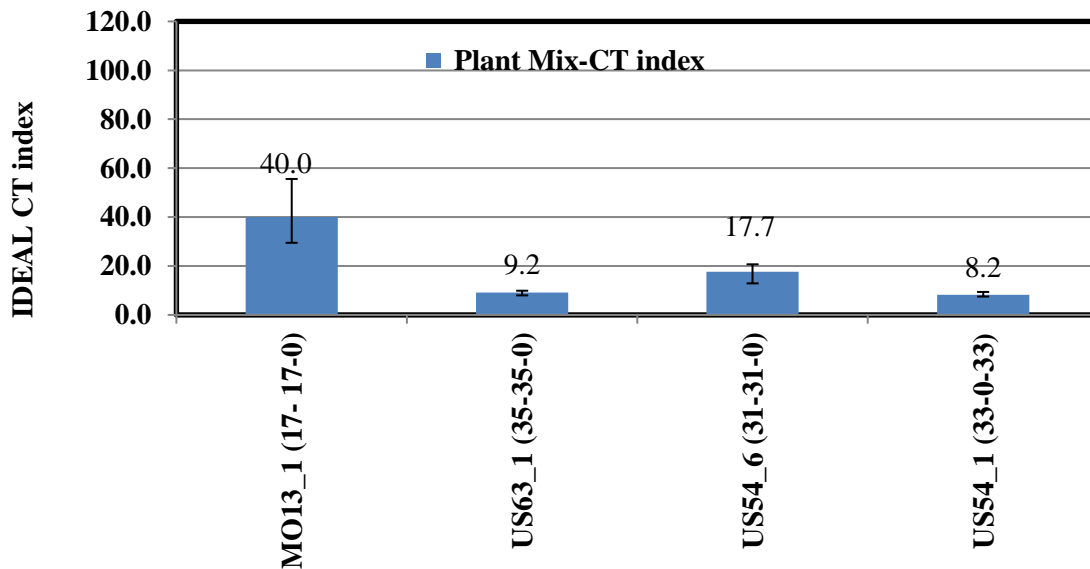


Figure 5-13. IDEAL CT-index of the mixtures using compacted-to-62-mm samples (HPs)

As Figure 5-13 shows, MO13_1 section had the highest CT index among the sections. Taking into account the ABR of the sections, it can be noticed that the higher the RAP content is, the lower the CT-index will be. Also, US54_1 with the 33% ABR by RAS yielded the lowest CT index.

5.4.2. Lab Mixture IDEAL-CT Test Results

As shown in Figure 5-14, the CT index obtained from lab mixtures are higher than those from plant mixtures.

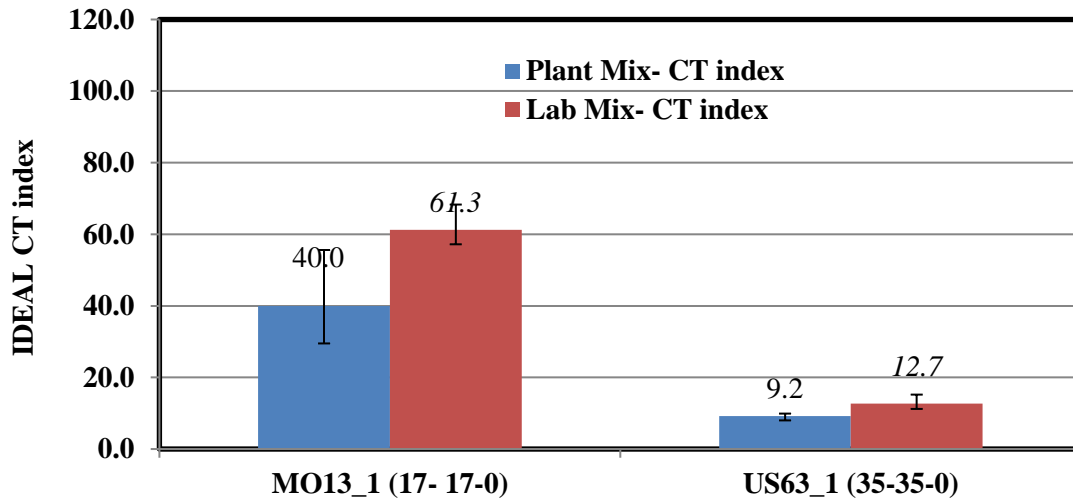
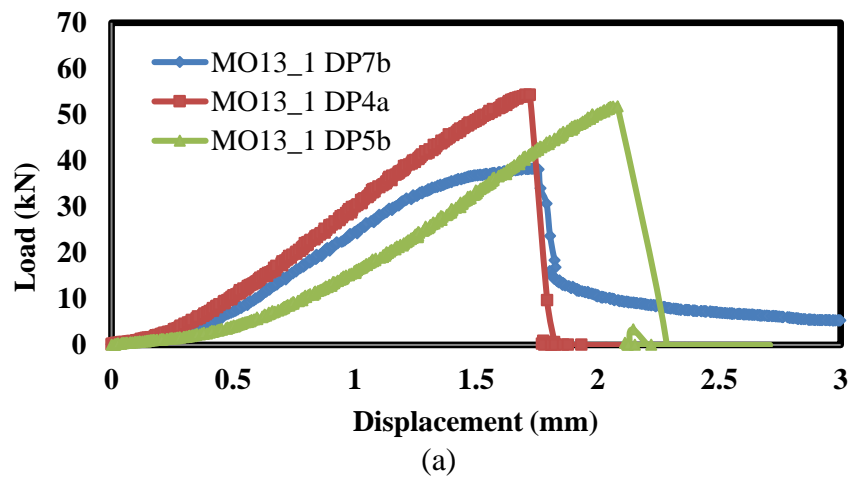


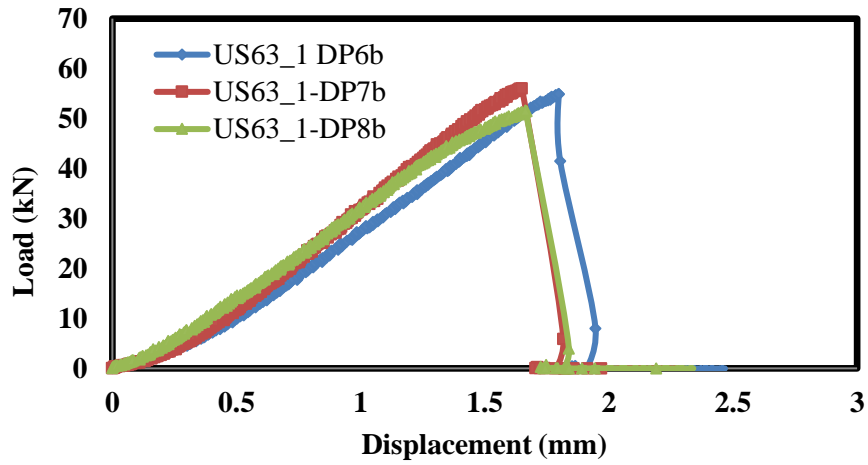
Figure 5-14. Comparing IDEAL-CT index of lab mix and plant mix

This might be attributed to the reheat that the plant mixtures experienced during the sample production. However, even the lab produced lap compacted mixtures did not show satisfactory performance in this cracking test. This observation is in accordance with the other cracking tests such as DC(T) and I-FIT.

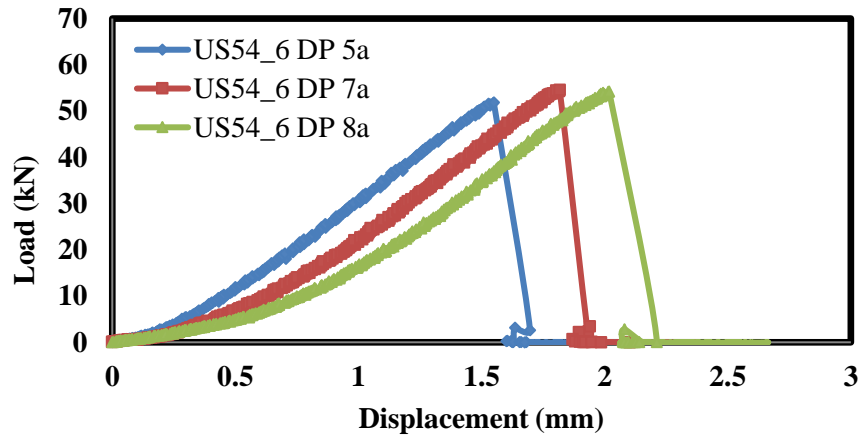
5.5. Indirect Tension Test Results

Figure 5-15 presents the load-displacement curves obtained from the IDT testing at -12°C.

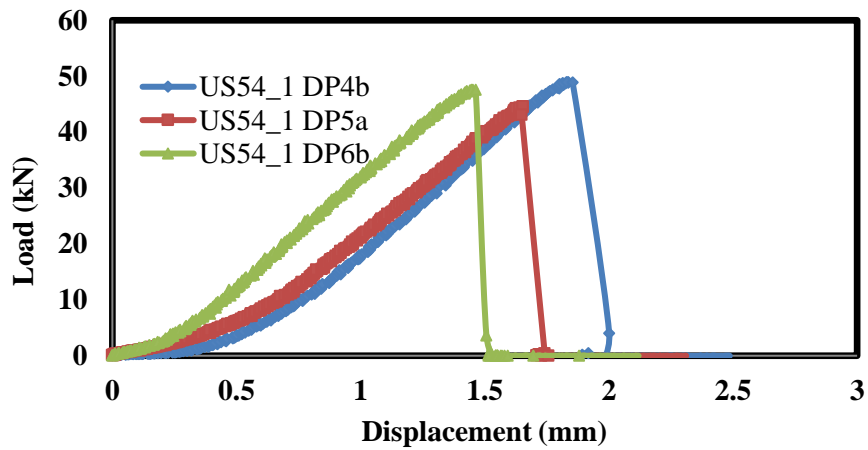




(b)



(c)



(d)

Figure 5-15. Load vs. displacement curves obtained from IDT strength test, (a) MO13_1, (b) US63_1, (c) US54_6, and (d) US54_1

As it can be seen, the three replicates of each section had reasonable repeatability such that the COV of this test was among the lowest COVs of the performed tests. However, the peak loads recorded by different mixtures were very similar to each other, which resulted in very close tensile strength values (Figure 5-16).

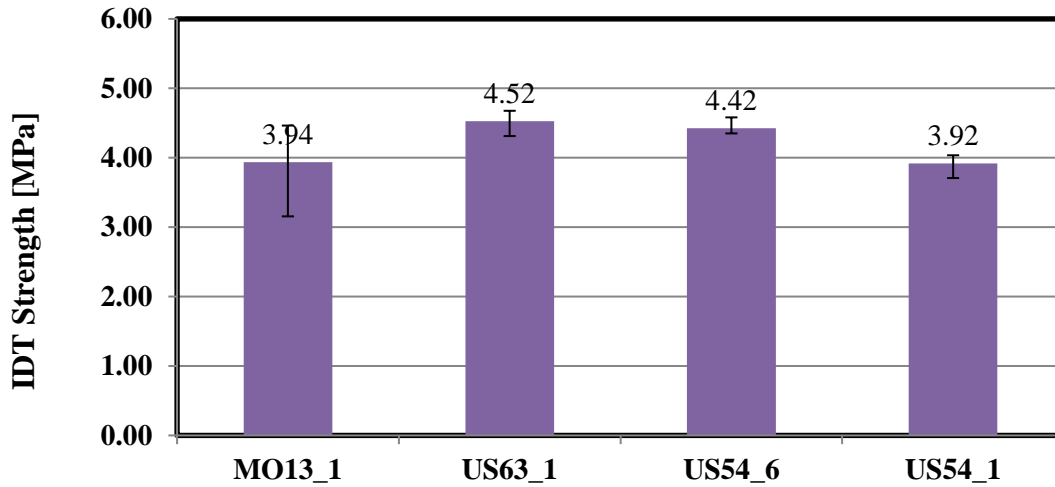


Figure 5-16. IDT strength of the plant mixes

From this observation, it can be concluded that the IDT strength might not be an appropriate test to differentiate different mixtures. Thus, performing other cracking tests such as DC(T), which is also performed at low temperature, can be a potential candidate to be used instead of IDT strength test.

5.6. Hamburg Wheel Track Test Results

5.6.1. Field Core Rutting Resistance

Figure 5-17 presents the results of Hamburg wheel tracking tests.

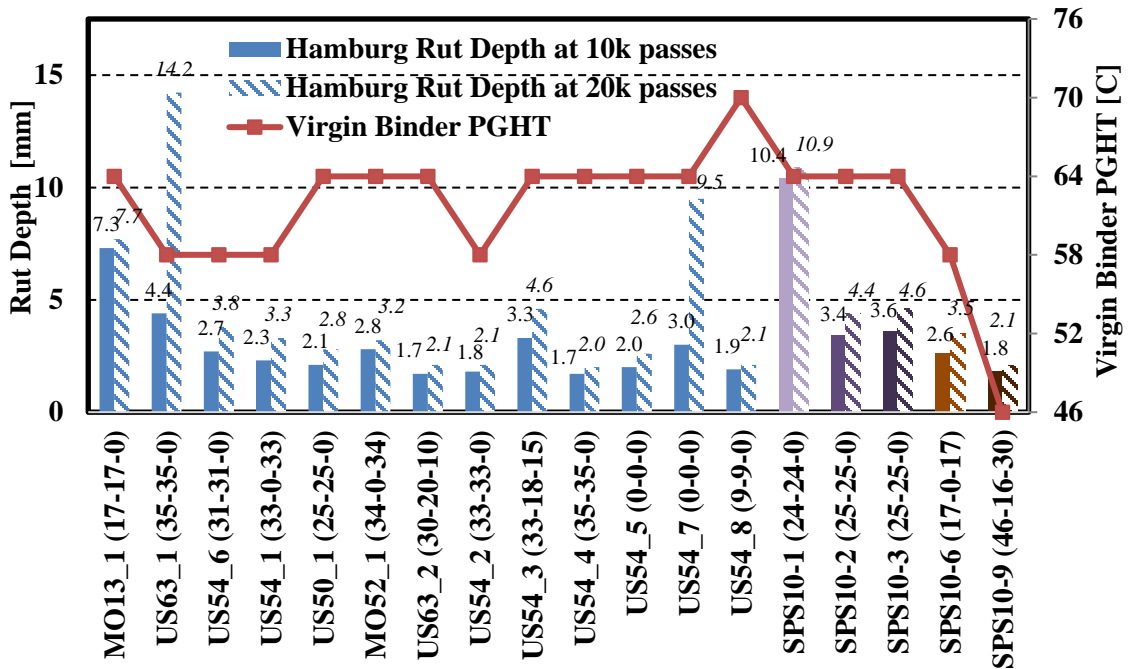


Figure 5-17. Hamburg wheel test results of field cores (at 20,000 passes)

All mixtures rutted less than 12.5 mm at 20,000 passes except US63_1, which is a section that contained a relatively high percentage of RAP. It should be noted that Superpave mixtures in Missouri are used on medium-volume facilities, and a rutting threshold of 12.5 mm at 10,000 passes is more appropriate. However, 20,000 pass tests were run in order to better delineate between mixes, and to identify any potential moisture sensitivity. Although RAP usually tends to lower Hamburg rut depths, sometimes moisture sensitivity will result. In these instances, Hamburg rut depths will often increase.

Figure 5-18 shows a sample output from the Hamburg test, where Sample 1 in this case is the US63_1 field core result.

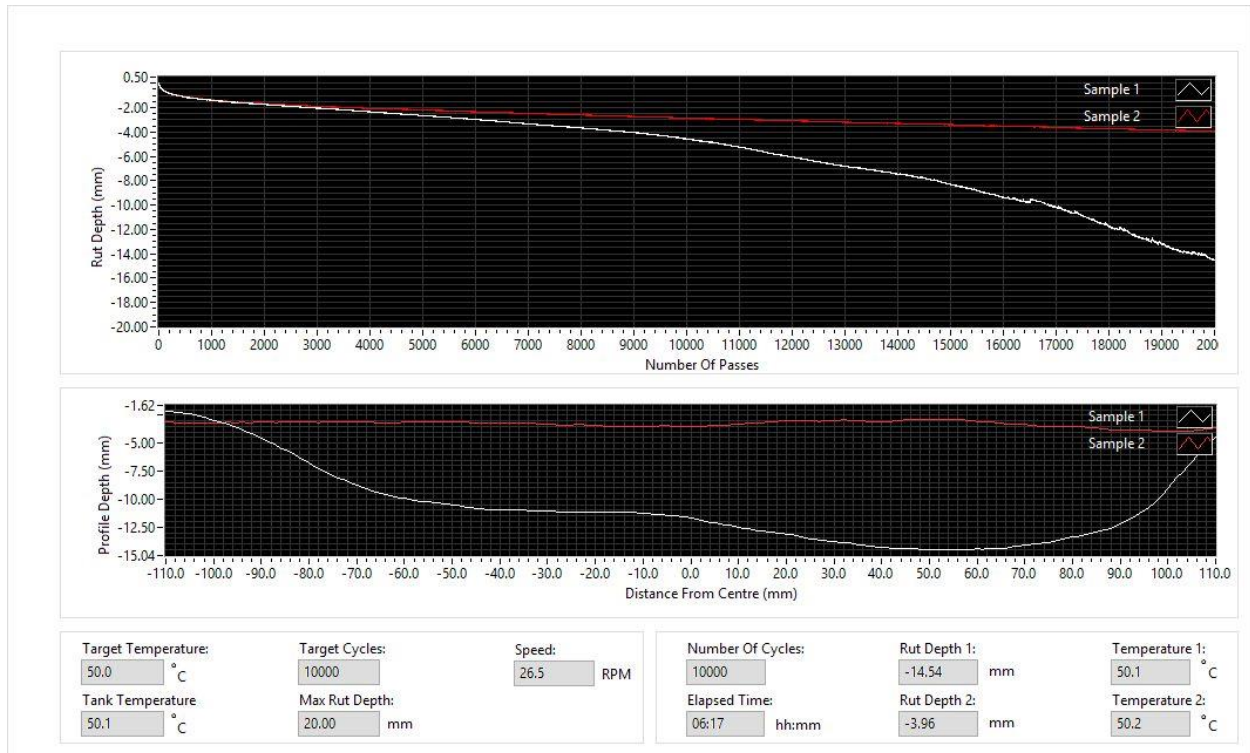


Figure 5-18. Sample Hamburg test output from Cooper software

The white data trace (curve) on the top plot shows the maximum rut depth plotted against the wheel pass number. The white trace on the bottom plot shows the rutting profile along the length of wheel travel. Because two cores are placed side-by-side to create a sufficiently long wheel track for testing (see Figure 3-9), it is clear from the bottom plot that although both replicates lying on the same wheel track had poor rutting resistance, the second specimen had a deeper rut depth than the first half. The final test result, however, represents the largest rut depth along the total wheel track.

Moreover, the white trace on the top plot shows an inflection in the curvature, starting at around 3,000 passes. The presence of a stripping inflection point is viewed as an indication of moisture susceptibility in the mix. There was only one other field core set that exhibited a distinct stripping inflection point. This was the US54_7 section (Brazito, Missouri). Unlike, US63_1, this mix did not contain any recycled materials. Both mixes contained a liquid anti-strip product; however, this did not seem to mitigate moisture sensitivity in either of these mixes. The virgin aggregates in these mixes could also underlie the cause of the moisture sensitivity measured.

5.6.2. Field Core Moisture Damage Performance

The Hamburg wheel tracking test has been implemented by many researchers and agencies to address the permanent deformation (rutting). In addition, conducting the test in a submerged condition provides the opportunity to measure stripping potential. To this end, the concept of stripping inflection point (SIP) is defined and currently used by agencies such as California,

Wisconsin, and Iowa departments of transportation (DOTs). SIP is reported in “number of passes” and represents the point at which the rutting versus wheel pass curve has a sudden increase in rut depth. This is believed to be the point where the asphalt binder starts to separate from aggregates (Mohammad et al. 2015). In this study, the research team implemented the Iowa method to calculate the SIP as follows.

- Fit a 6th degree polynomial curve on the rut depth versus wheel pass curve.
- Take the first derivative of the fitted curve.
- Determine the stripping line using the tangent at the point nearest the end of the test where the minimum of the first derivative of the fitted curve occurs.
- Determine the creep line using the tangent at the point where the second derivative of the fitted curve equals zero.
- Intersect the creep and stripping lines. The wheel pass at which these two lines intersect is determined as the SIP.

Figure 5-19 shows the rut depth at different passes of four critical sections (US63_1, US54_7, SPS10-1 and MO13_1), which had the highest permanent deformation in HWTT.

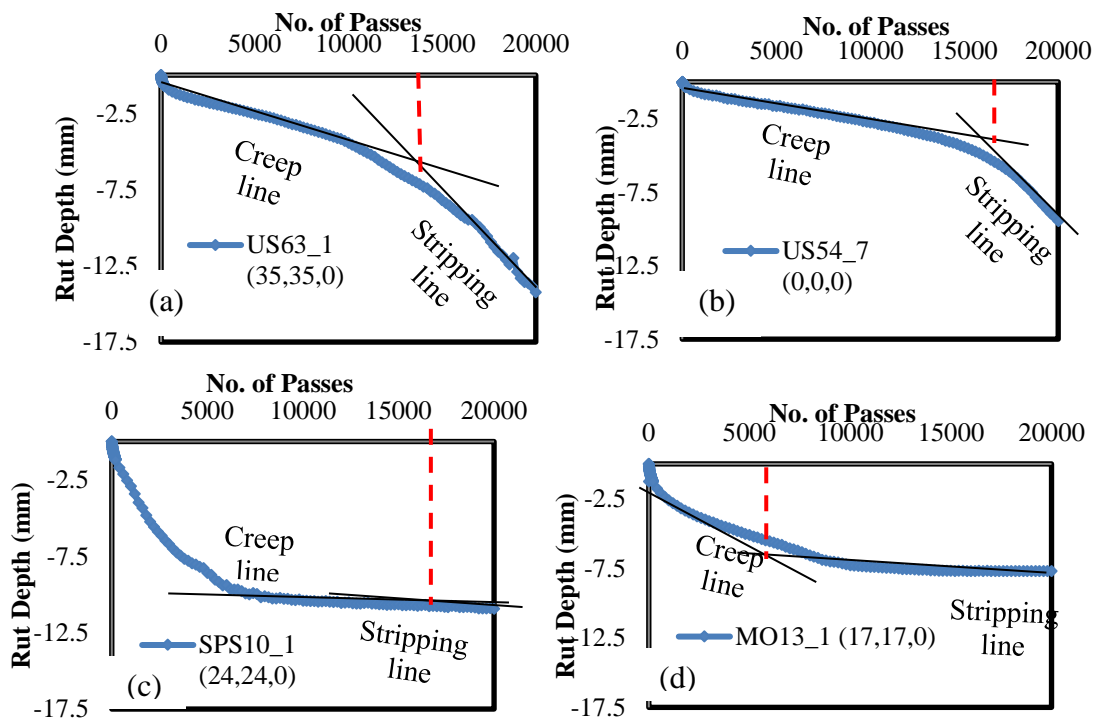


Figure 5-19. Stripping point analysis (a) Section US631, (b) Section US54_7, (c) Section SPS10-1, (d) Section MO13_1

For these sections, the creep and stripping lines, and their intersection as SIP are characterized and schematically shown in the figure. In addition, the details of the parameters are shown later in Table 5-5.

Table 5-5. Stripping inflection point

Section	Rut depth at 20k pass	Creep line	Creep intercept	Stripping line	Stripping intercept	SIP (IOWA method)
US63_1 (35,35,0)	14.2	$y=-0.00021x-1.4$	3818	$y=-0.00173x+19.8$	20000	13874
US54_7 (0,0,0)	9.5	$y=-0.00015x-0.8$	3742	$y=-0.00183x+26.2$	20000	16094
SPS10_1 (24,24,0)	10.9	$y=-0.00002x-10.3$	12827	$y=-0.00012x-8.7$	17544	Non-stripping (15415)
MO13_1 (17,17,0)	7.7	$y=-0.00040x-3.1$	4110	$y=-0.00026x-3.8$	17603	Non-stripping (5528)

As Figure 5-19 a and b depict, US63_1 and US54_7 mixes started to undergo a high rate of deformation around 15,000 passes. This was also clear when the rut depths at 10,000 and 20,000 were compared in Figure 5-17. Following the steps from the Iowa method, the SIPs for US63_1 and US54_7 were calculated as 13,874 and 16,094 passes, respectively. It suggests that after undergoing these numbers of passes, the bond between the binder and aggregates strips away due to moisture damage. Despite the fact that SIP was calculated for SPS10-1 and MO13_1, having ratios of stripping over creep lines were less than two. According to Iowa DOT specification, these mixtures are not considered as stripping. As shown in Figure 5-19 c and d, most of the deformation occurred at the phase stage of loading (<5,000 passes). This indicated that moisture damage did not contribute to rutting and the permanent deformation was due to the mixture densification and/or reorientation and displacement of the aggregates. To address the rutting distress of the stripping mixtures (US63_1 and US54_7), it is suggested to use anti-stripping agents and aggregates with higher quality.

5.6.3. Plant Mixture Rutting Resistance

Figure 5-20 shows plant-produced, laboratory compacted mix (sampled at the paver) Hamburg results.

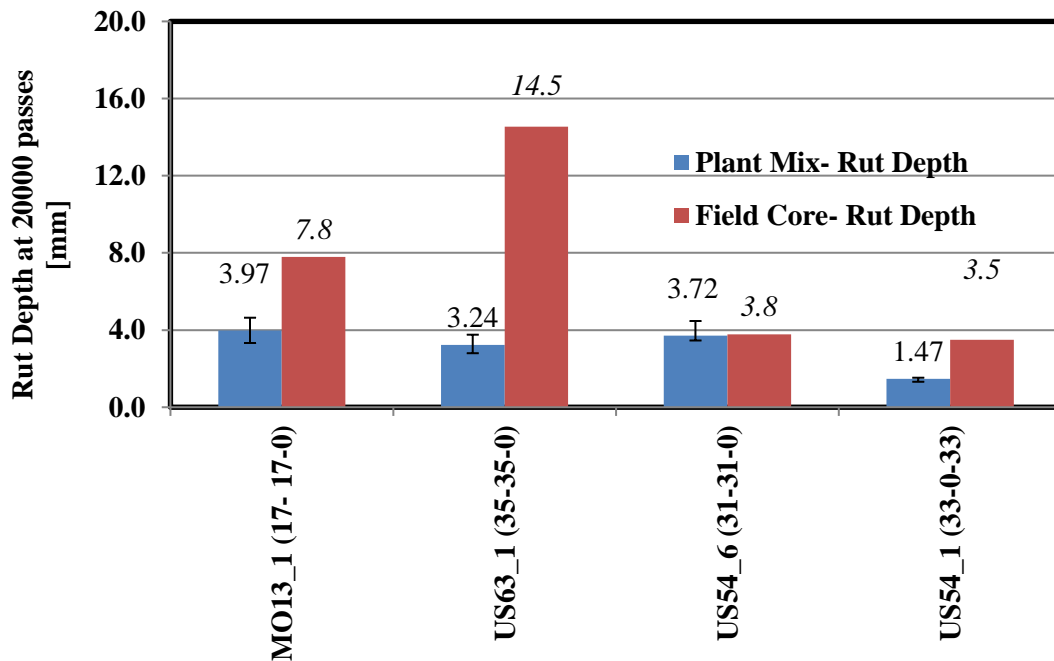


Figure 5-20. Hamburg wheel track test results: plant mix vs. field cores

Again, plant mix results are available only for the four, Level 1 sampled projects. In general, the field cores exhibited higher rut depths than the samples produced using plant mix sampled at the paver and gyratory compaction in the laboratory. The biggest difference was for US63_1, where the stripping inflection measured on cores as described in the previous section was not observed on the plant mix, and as a result, rut depths were much smaller at 20,000 passes. This discrepancy probably should be confirmed with the testing of additional field cores. One cause for the discrepancy could stem from the fact that the plant samples were stored, then reheated prior to compaction. However, it is not clear whether this can explain the large discrepancies for the MO13_1 and US63_1 sections. In these cases, a significant difference might have existed in the mix, i.e., the material in the core samples did not closely match the plant mix sampled.

It appears that the stripping inflection point might be a useful indicator of relative mix performance, but will require additional validation against field performance. It is recommended that this be done in future research. Future research could also test whether or not the AASHTO T 283 test could be replaced by the Hamburg stripping inflection point assessment.

5.6.4. Lab Mixture Rutting Resistance

Figure 5-21 compares the rut depth of three different mixture production processes (field core, plant produced-lab compacted, and lab produced-lab compacted).

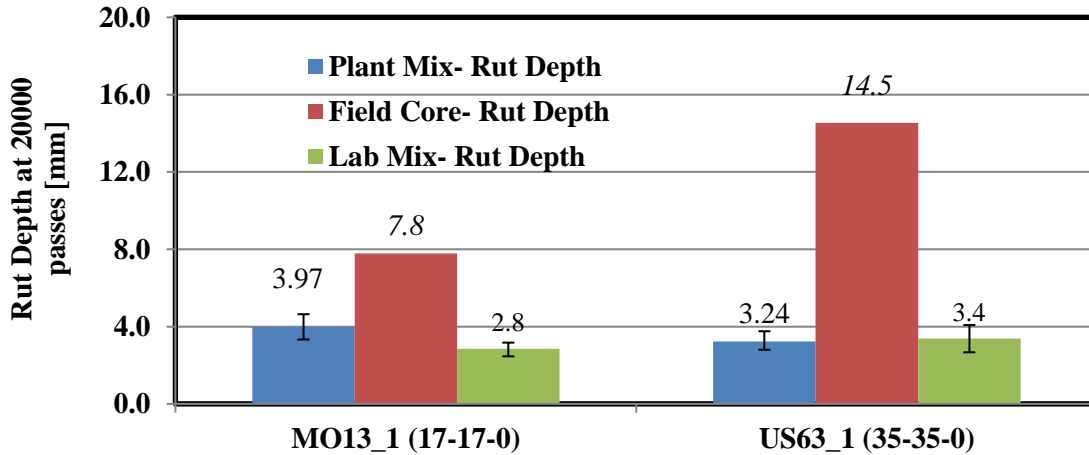


Figure 5-21. Hamburg wheel track test results: plant mix vs. field cores vs. lab mix

As shown, the lab mixtures accumulated the lowest rut depth for MO13_1 and US63_1 sections. However, the plant and lab rut depths are in an acceptable range and can be compared together very well.

5.7. Hamburg-DC(T) Performance Space Diagram Results

Figure 5-22 presents a useful x-y plotting form known as the performance space diagram, or more specifically in this case, the Hamburg-DC(T) plot.

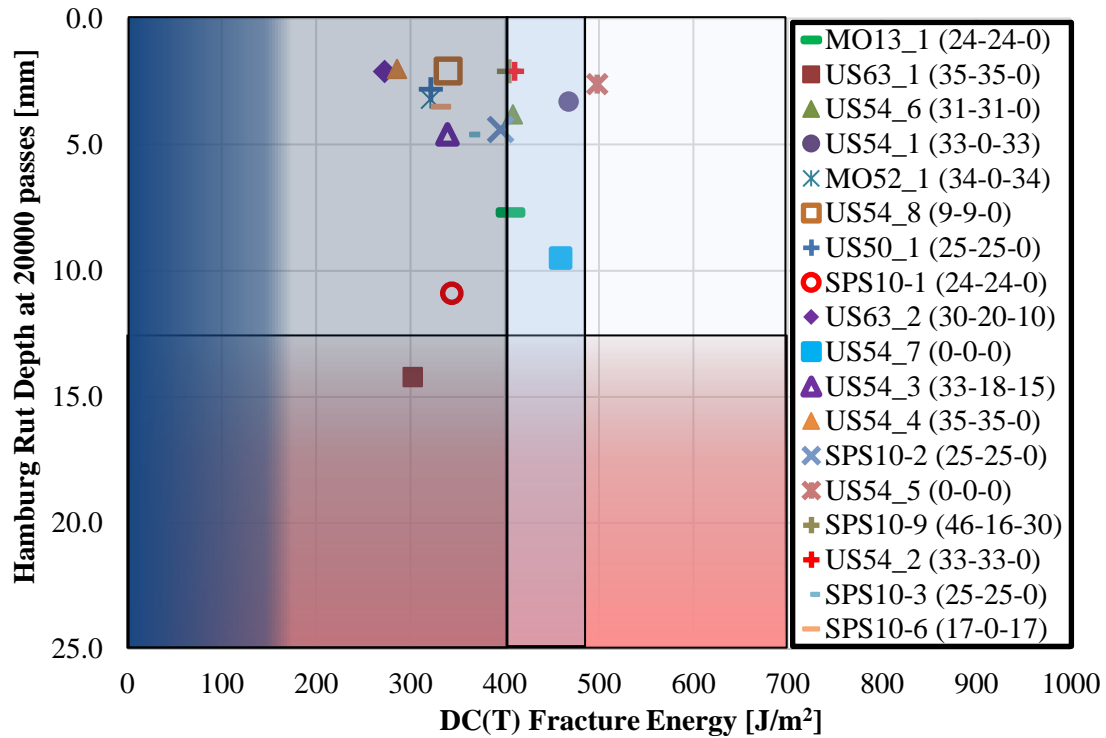


Figure 5-22. Hamburg-C(T) plot for Missouri field cores

This plot allows the simultaneous evaluation of rutting and cracking behavior. Some useful trends that can often be observed when viewing data in this form are:

- The best overall performing mixtures will appear in the upper-right corner of the diagram (low rutting depth, high fracture energy). These can be considered as high total energy mixtures; i.e., rut and crack (or damage) resistant. These are high toughness mixtures, and the best candidates for surfacing materials especially in demanding climates and for high traffic volumes.
- Mix variables that increase net total energy in the mix and thus move mixtures in the direction of the upper-right corner of the plot include:
 - Higher quality binder (low temperature susceptibility, higher useful temperature interval, or UTI), degree of polymer modification
 - Higher quality aggregate (stronger, more angular, better bond with asphalt)
 - The presence of crack interceptors or rut mitigators, such as fibers, rubber particles, and even RAS (but only if properly used)

Other salient features of the plot include:

- Binders with different grades but similar UTI tend to move a mixture along a binder tradeoff axis, or roughly diagonal lines moving in the upward-left or downward-right direction, for

stiffening and softening, respectively.

- Pure stiffening elements, such as RAP, tend to move points upward and to the left.
- Pure softening elements, such as rejuvenators, tend to move points downward and to the right.
- Binders with higher UTI, where the grade bump is on the high temperature grade, tend to move points mainly upward, but also slightly to the right due to the benefits of polymer in intercepting cracks.
- Binders with higher UTI, where the grade bump is on the low temperature grade, tend to move points mainly to the right, but also slightly upward, again, due to the benefits of polymer in intercepting cracks.
- Data points that appear in the undesirable middle-to-lower-left portion of the plot are sometimes those that contain RAP and insufficient binder bumping, and possibly poor bond, where the RAP tended to cause lower DC(T) values, and the nature of the RAP-virgin material combination led to a moisture-susceptible mix with high Hamburg rut depth value.

A number of interesting findings can be extracted from the results of Missouri field cores (Figure 5-22), including:

- The best performing mix overall was US54_5, which is a virgin mix with a relatively high UTI binder (PG 64-22 H, with a UTI of 98.3). It has a gold-colored asterisk symbol, and is the furthest data point to the upper right.
- The next two best performing mixtures were:
 - SPS10_9: An innovative mix, containing 46% ABR, with 16% binder replacement from RAP, and 30% from RAS, along with PG46-34 binder, with a relatively moderate UTI (86.4), and;
 - US54_1: Comprised of 33% ABR, all coming from RAS, and PG58-28 binder
- Two poor-performing mixes in the Hamburg-DC(T) space contained RAS and exhibited stripping in the Hamburg test, including:
 - US63_1 (Figure 5-18, Sample 2), with 35% RAS and PG58-28 binder. The results suggest that the mixture could have benefitted from a second binder bump (such as PG XX-34 binder) to improve DC(T) fracture energy, along with more effective measures to improve moisture sensitivity.
 - SPS10_1, with 24% RAP and PG64-22 H binder. The Hamburg results for this mix are shown in Figure 5-23 (Sample 2 data trace).

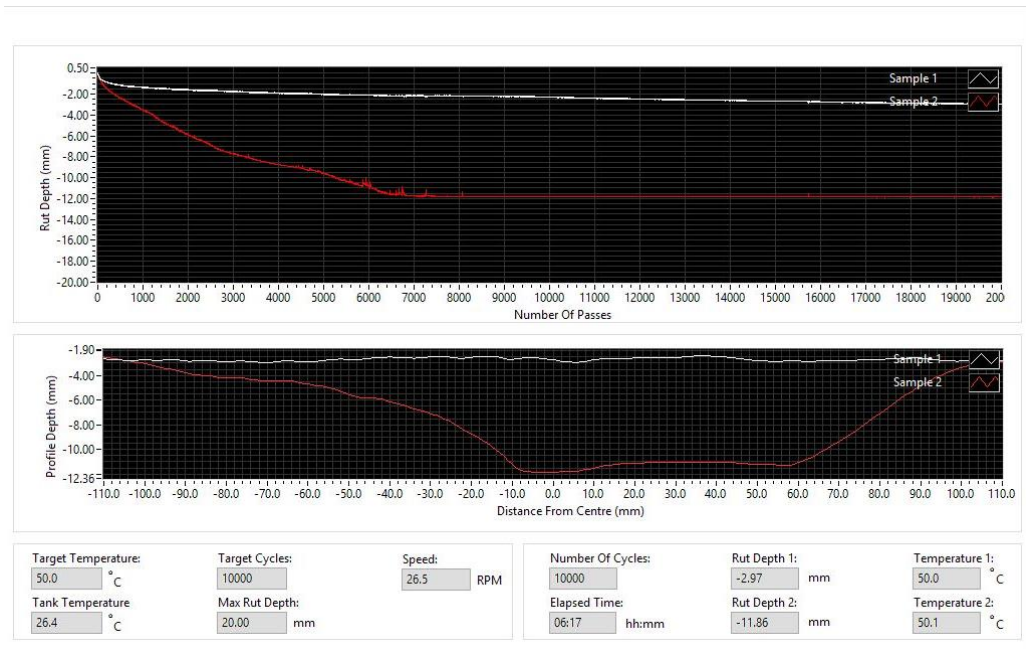


Figure 5-23. Moisture sensitivity in Hamburg test for SPS10_1 (Sample 2)

The thin core sample had a fast rutting rate, and possible stripping inflection, followed by a complete flattening and bottoming out in the Hamburg wheel track test at around 7,000 passes. The results also suggest that the mixture could have benefitted from binder bumping (softening) to improve DC(T) fracture energy, along with more effective measures to improve moisture sensitivity.

- A large cloud of mixtures had similar total energy on the Hamburg-DC(T) plot but with a range of mix stiffness. These mixes fell along a similar diagonal contour, spanning from the US57_7 mix (light blue square) to the US63_2 mix (purple diamond). The results suggest that these mixes have similar overall performance, with some performing better on the Hamburg relative to the DC(T) and vice-versa.

In order to further evaluate the study mixtures against performance thresholds, they were plotted using their 10,000 Hamburg wheel pass results (Figure 5-24), which is more appropriate for the moderate traffic levels experienced on the roadways sampled.

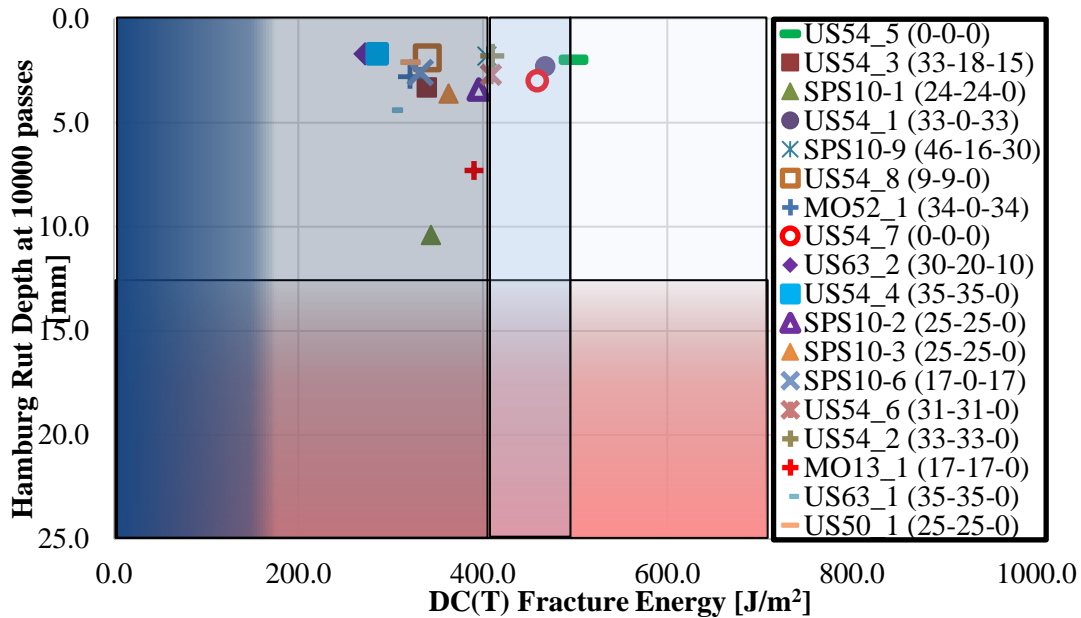


Figure 5-24. Hamburg-DC(T) plot for 10,000 Hamburg wheel passes

The short-term aged mix data points should ideally fall in the medium traffic passing zone, which is the box near the upper-right that contains the dark pink-colored asterisk symbol (US54_6), and two other symbols. This zone requires a minimum of 460 J/m² fracture energy and a maximum of 12.5 mm of rutting in the Hamburg test. The five field-aged mixtures can be judged against a slightly relaxed criteria for the DC(T), with a minimum long-term aging fracture energy threshold of 400 J/m² recommended. This adds the box just to the left of the aforementioned medium traffic zone box to the passing zone for field-aged mixes.

The 10,000 Hamburg-DC(T) plot led to the following conclusions:

- Three of the newly constructed mixes met both the high and low temperature medium traffic criteria. These were US54_5 (0-0-0), US54_1 (33-0-33), and SPS10_9 (46-16-20).
- A number of the remaining mixes appear to have the capacity (sufficient total energy) to meet both DC(T) and Hamburg criteria for medium-traffic volume roads, however, they will need a softer binder with similar UTI to pass the DC(T) test. This will shift the points downward, and to the right, and hopefully into the medium traffic passing zone. They could also be improved with a higher UTI binder, but that would be a more expensive option to improve the cracking performance of these mixes. For instance, it's possible that US54_2 (red + symbol) would only need a slightly softer binder or a small amount of rejuvenator to move the data point slightly down and to the right, into the medium traffic passing zone.
- One of the five field projects was in the appropriate zone for a field-aged mix. This was US54_7, a virgin mix constructed in 2003, which retained an impressive 459 J/m² of fracture energy even after 14 years of aging. As expected, the aged field core exhibited a low rut depth in the Hamburg.
- None of these mixes would be suitable for use on high-traffic volume facilities, unless a

higher UTI binder and perhaps additional measures were taken. Referring back to the 20,000 Hamburg results (Figure 5-22), which would be appropriate for high-traffic volume facilities, the use of a softer binder with a similar UTI would move the points in the diagonal direction of the US54_7 mixture and beyond (along that particular binder tradeoff axis line), which would cause a failure in the Hamburg test. Thus, the total energy of these mixes would need to be enhanced, which could be achieved by use of a higher UTI binder, stronger aggregates (or aggregate structure), and by the use of rut and/or crack mitigating materials (rubber, RAS pulp, fibers). Fortunately, high traffic volume facilities are usually comprised of stone mastic asphalt mixes (SMAs). SMAs benefit from hard rock, thick asphalt films, polymer-modified binder, and fibers, which give them an edge in meeting even stricter rutting and cracking criteria.

5.8. Creep Compliance Tests

5.8.1. DC(T) Creep Compliance

DC(T) creep compliance master curves were generated for all of the sections using DC(T) creep test data obtained at three different temperatures (0°C, -12°, and -24°C). Figure 5-25 and Figure 5-26 show the master curves for US54 field cores and plant-produced mixes, respectively.

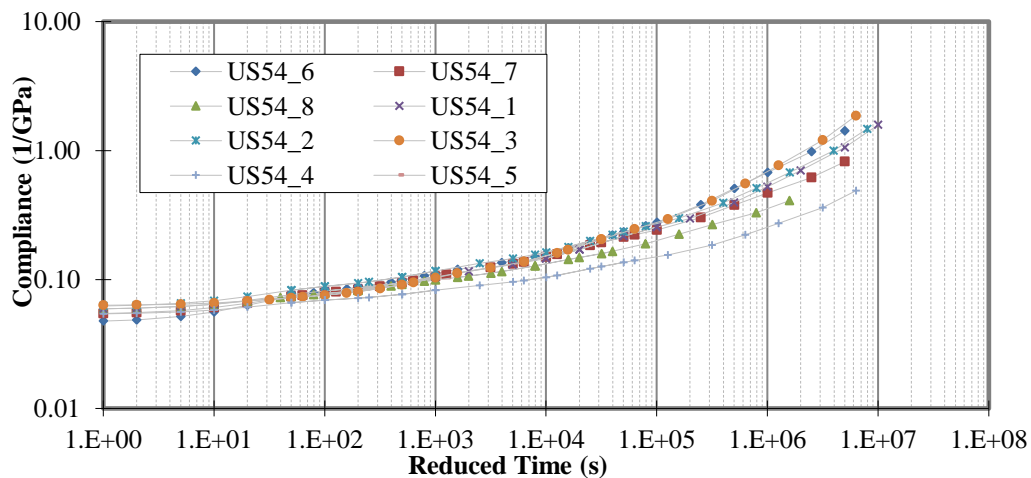


Figure 5-25. Generated DC(T) master curves for field cores

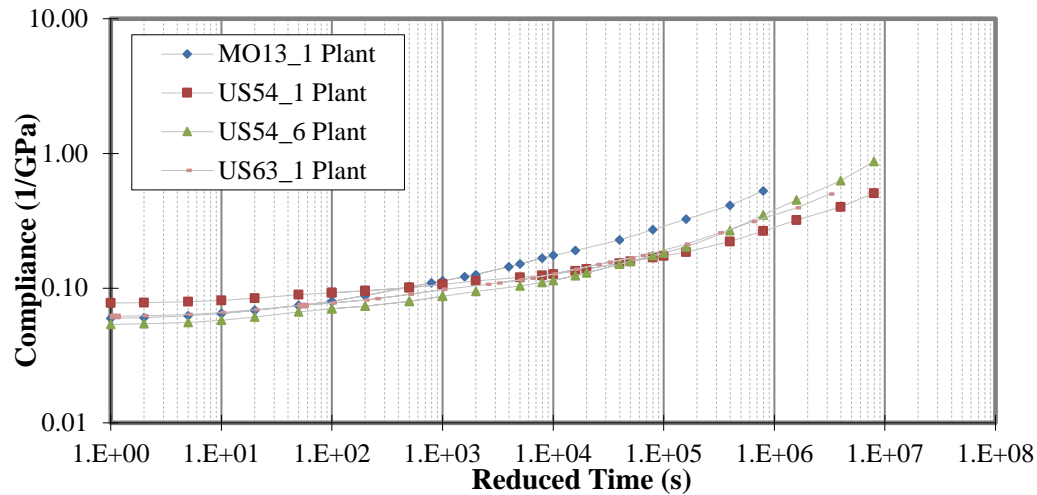


Figure 5-26. Generated DC(T) master curve for plant mixtures

A reference temperature of -24°C was used. Some interesting findings include:

- The stiffest mix (lowest creep compliance) was the US54_4 mix, which contains 35% RAP. This corresponds to the fact that this mix was in the most brittle position on the Hamburg-DC(T) plot.
- Another stiff mix in terms of creep compliance was US54_8, which contained a PG70-22 binder and 9% RAP.
- One of the most compliant mixes, US54_3 contained a softer PG58-28 binder. Interestingly, this mix also contained 33% ABR. Similarly, the second most compliant mix, US54_6, had 31% ABR and PG58-28 binder. This suggests that, like fracture energy, the low-temperature viscoelastic properties of recycled mixes can be acceptable, provided that the virgin binder is appropriately selected.
- By comparing Figure 5-25 and Figure 5-26, it appears that creep compliance may be strongly affected by reheating of the samples, as the plant mix creep compliance for corresponding sections was significantly lower than the field core result.

The primary motivation for running creep compliance tests at low temperatures includes the following:

- For complex materials such as modern, heterogeneous recycled materials, it is not clear if simple cracking tests such as the DC(T) and I-FIT will be sufficient for completely characterizing and controlling cracking properties for all mixes investigated. This is because fracture tests are mainly focused on material response to overstressing, or the resistance side of the equation. However, creep compliance, material coefficient of thermal expansion and contraction, and temperature cycling magnitudes combine to create the driving side of the equation (i.e., stress development). The structural configuration, i.e., layering of the pavement, and other environmental and material factors will affect thermal cracking.
- The aforementioned factors can be conveniently evaluated using the IlliTC thermal cracking

simulation model.

5.8.2. $ID(T)$ Creep Compliance

Figure 5-27 shows the master curve of IDT creep compliance performed on plant mixtures.

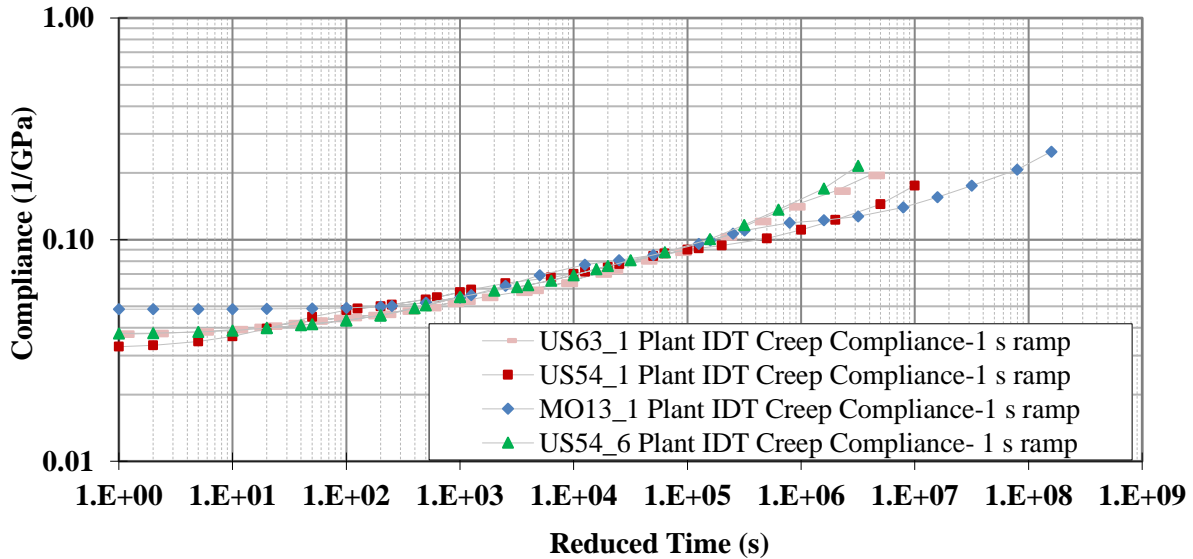


Figure 5-27. IDT creep compliance master curve for plant mixtures (Ref. Temp: -24°C)

Similar to DC(T) creep testing, IDT creep was carried out at -24°C , -12°C , and 0°C . This allowed for plotting the creep compliance at three different temperatures and by shifting the curves with respect to the creep compliance at -24°C , the master curves were constructed. At each temperature, the creep load was kept low in order not to damage the samples and obtain pure viscoelastic behavior. On the other hand, the response (vertical and horizontal deflections) under too low loading levels might be affected by noise and not be useful. Also, the 1 s ramp was chosen to shorten the ramp of the load as much as possible such that the assumptions of ideal step loading were not violated. As it can be seen in the log-log plot of IDT creep compliance (Figure 5-27), MO13_1 and US54_6 were the least compliant and most compliant mixtures in linear viscoelastic range, respectively.

Using a power law function to fit the creep compliance master curve data, the m-values were calculated and reported in Figure 5-28.

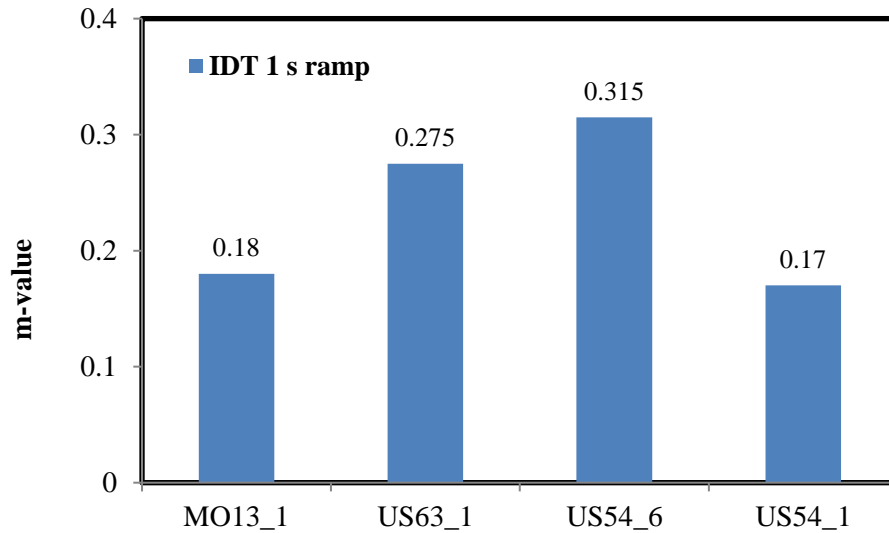


Figure 5-28. IDT and DC(T) creep m-values

As shown, US54_6, which was the most compliant mixture, had the highest m-value. This again indicates the flexible viscoelastic behavior at low temperatures. The Poisson's ratio, which is calculated using AASHTO T 322, is presented in Figure 5-29.

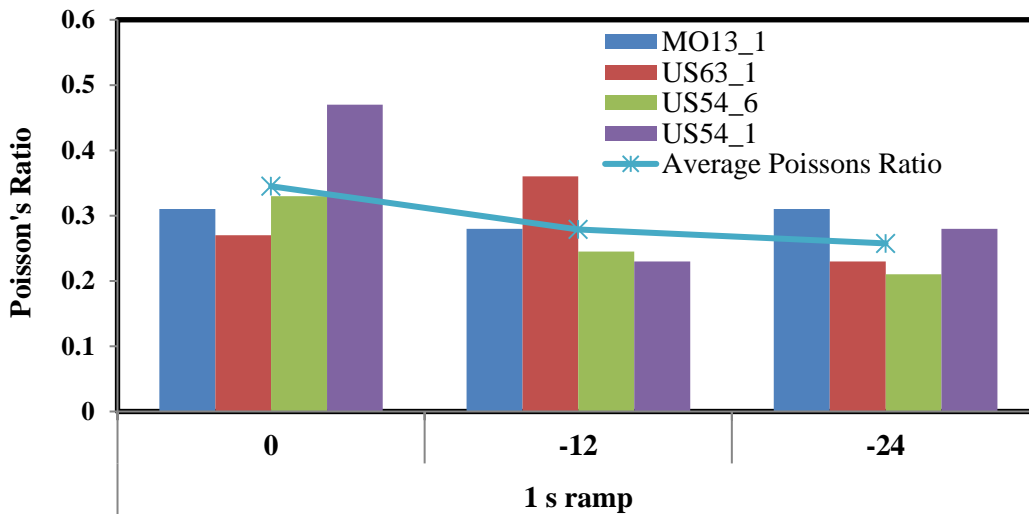


Figure 5-29. Poisson's ratio from IDT creep testing

As expected, as the temperature decreases, the Poisson's ratio becomes lower, indicating the lower lateral expansion when diametrically loaded.

5.9. ANOVA and Tukey Grouping Test

In this study, one-way analysis of variance (ANOVA) was performed to check if there is any statistical difference between the performances of sections under different tests. Minitab 2017

software was employed to run the statistical analysis for each of the DC(T) fracture, I-FIT, IDEAL, IDT, and Hamburg tests. Also, a significance level of 0.05 ($\alpha = 0.05$) was selected to investigate the null hypothesis, which states that all the treatment means (e.g., performance of mixture types in this case) are statistically the same. The 0.05 level of confidence is commonly used in statistical analysis, which indicates that there is a 5% risk of concluding that an effect exists when there are no actual effects existing. P-values lower than 0.05 reject the null hypothesis and provide statistical evidence that mixtures performed differently in the performance test. If the statistical test indicates that the performance of mixtures varies, the Tukey-Kramer method is used in order to compare the sections and rank them accordingly.

Table 5-6 presents the statistical analysis of the mixtures under each performance test.

Table 5-6. ANOVA test and Tukey-Kramer grouping for performance tests

Statistical parameter	DC(T) fracture	IDT	HWTT	I-FIT	IDEAL CT
Total DF	15	11	11	15	11
F-value	16.64	2.27	15.58	12.43	12.45
P-value	0.000	0.157	0.001	0.001	0.002
Section (Plant mix)	Ranking				
US54_1 (33-0-33)	A	A	A	B	B
MO13_1 (17-17-0)	A-B	A	B	A	A
US54_6 (31-31-0)	B	A	B	B	B
US63_1 (35-35-0)	C	A	B	B	B

Total Degree of Freedom (total DF=total number of replicates -1), F-value, and P-value are obtained from ANOVA test and presented in Table 5-6. As the significance level is set to 0.05, p-values of performance tests that are less than 0.05 imply the existing of significant difference in terms of performance between the studied sections. As mentioned before, four replicates for each section were tested under DC(T) fracture and I-FIT; while three replicates were tested in IDEAL-CT, IDT, and HWTT. As the P-value suggests, only IDT test could not distinguish the mixtures (P-value>0.05) and the ranking is accordingly the same all of the sections. The other performance tests could yield P-values higher less than 0.05, meaning that there was a statistically significant difference between the performances of at least two sections under the test. DC(T) fracture and Hamburg tests ranked US54_1 as the best performer, while MO13_1 ranked the best in the I-FIT and IDEAL-CT tests. It is also worth mentioning that DC(T) test could have three ranking levels (A, B, and C) while the other tests had a maximum of two ranking levels. This implies that DC(T) could more distinctly rank the performance of these four mixture types.

5.10. IlliTC Modeling

As a part of the SHRP A-357 project, researchers developed Fortran-based computer program TCMModel to predict transverse cracking in the pavement at different depths on an hourly basis. TCMModel used inputs from the indirect tensile (IDT) test, namely IDT strength, and IDT creep

compliance master curves, along with the mixture coefficient of thermal expansion/contraction (CTEC) to predict transverse cracking. The program used Paris law, a phenomenological power-type law, to predict the crack propagation in the asphalt mixtures by empirically linking the model's parameters with the IDT tensile strength and the slope of the creep compliance master curves. However, in the following decades, the asphalt paving industry moved rapidly toward sustainability by using recycled materials (recycled asphalt pavements [RAP] and recycled asphalt shingles [RAS]). Subsequently, it was seen that the over-reliance of TCMModel on the IDT tensile strength to predict cracking limited the precision of the model's transverse cracking results. During the same time, new tests were developed to measure the fracture energy of the asphalt mixture using a fracture mechanics-based approach, such as the DC(T) test. In light of those pertinent factors, researchers at the University of Illinois Urbana-Champaign developed a new transverse cracking analysis tool called IlliTC as a part of a national pooled funded study on low-temperature cracking. The framework of the IlliTC tool is simple and combines three types of files comprising data pertaining to climate, materials, and geometry of the pavement to be evaluated. The tool has a set of temperature profiles at various depths for some specified locations, calculated through Integrated Climatic Model (ICM) simulations. For material properties, the user inputs the tensile strength in MPa calculated from the IDT test or extracted from the DC(T) test, the DC(T) fracture energy in J/m^2 , raw creep data from IDT test, and either the mixture CTEC or the aggregate CTEC and mixture VMA. The tool creates a finite element mesh depending on the specified geometry (pavement depth) and uses cohesive zone elements in the mesh to simulate thermal cracking. Further, the tool employs a tactic of simulating one high level crack instead of multiple crack simulations to save computational time, and finally uses a probabilistic crack distribution model to compute the amount of transverse cracking from the single crack simulation. Field validation of this tool has been presented by Dave et al. (2013). Recently, Dave and Hoplin (2015) showed that IlliTC is sensitive to the variation in fracture energy of asphalt mixtures and shows a difference in transverse cracking of asphalt pavements when the fracture energy is varied by a value as low as $25 J/m^2$.

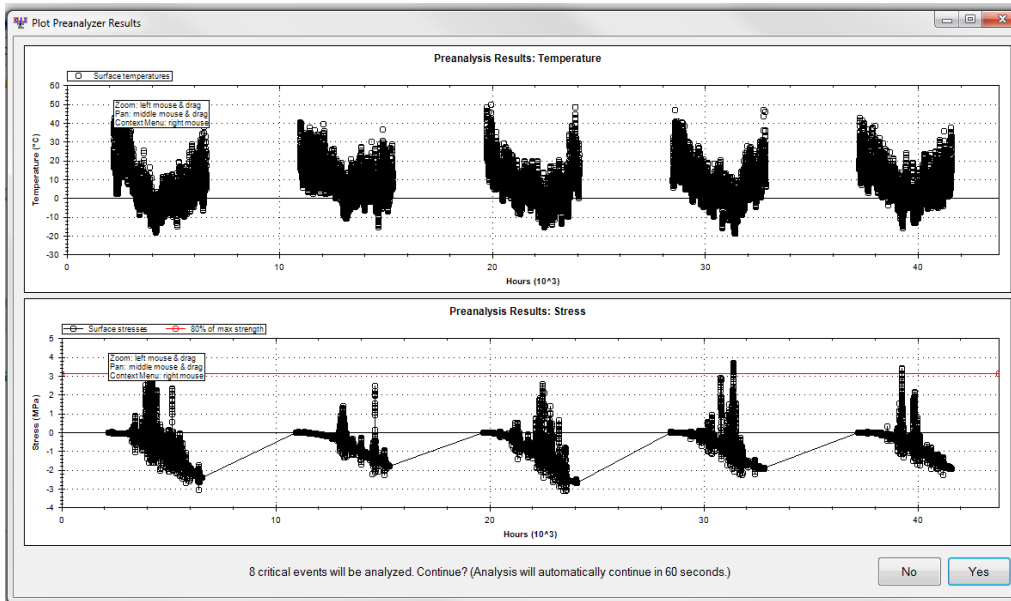
The inputs for the mixtures used for IlliTC modeling (e.g., DC(T) fracture energy, voids in mineral aggregates [VMA], and coefficient of thermal expansion and contraction) and the results from the computations are shown in Table 5-7.

Table 5-7. Summary of the inputs to IlliTC software

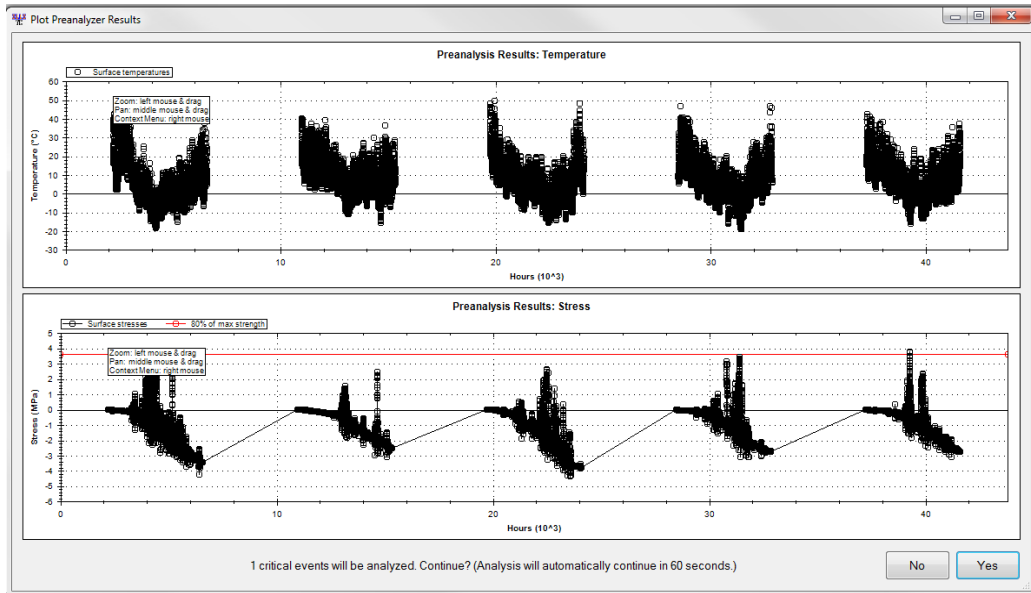
Section	MO13_1	US63_1	US54_6	US54_1
Fracture energy (J/m^2)	385	263	342	448
Mix VMA (%)	18.9	16.7	17.4	16.9
Mix CTEC ($mm/mm/^\circ C$)	3.00E-05	3.00E-05	3.00E-05	3.00E-05
IDT strength (MPa)	3.9	4.5	4.5	3.9
m-value	0.180	0.275	0.315	0.170
Critical events	8	1	3	0

The IlliTC results show the combined effect of mixture factors on the thermal cracking resistance of the mixtures. The US54_1 section has the best performance, possibly due to relatively high fracture energy. Considering the mixture fracture energies, US63_1 section might have been

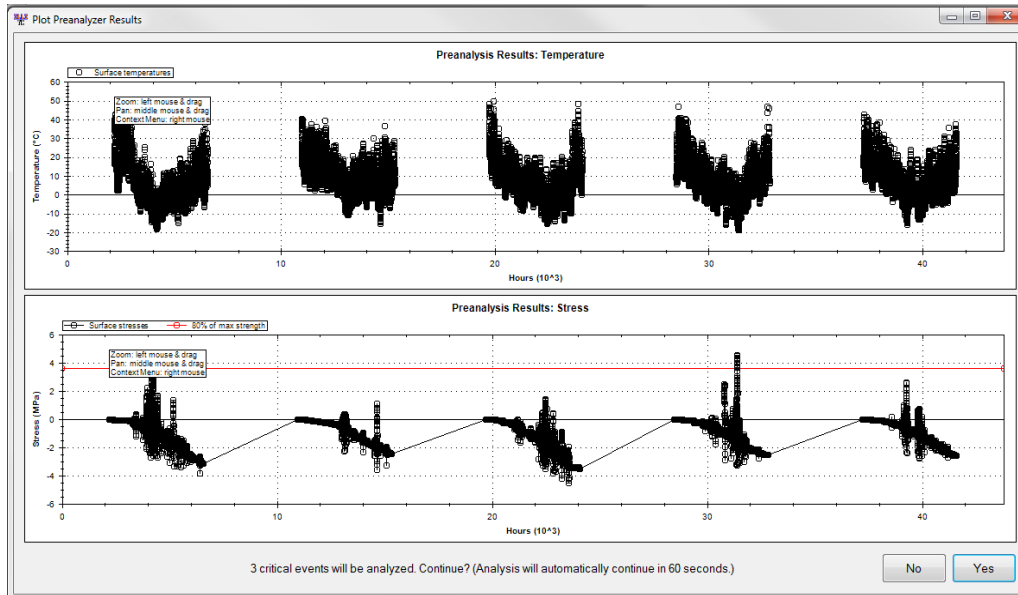
expected to perform the worst. However, the US63_1 section has high m-value that allows the mixture to relax the built-up thermal stresses, allowing it to last several winters as shown by the solitary critical event recorded in five years of simulation (Figure 5-30).



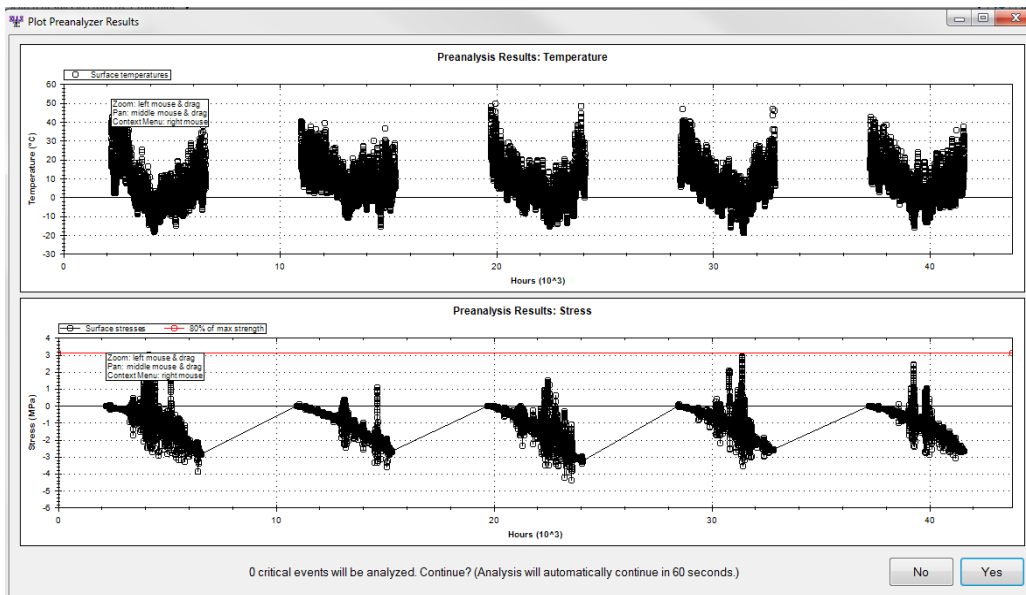
(a) MO13_1



(b) US63_1



(c) US54_6



(d) US54_1

Figure 5-30. IlliTC stress and temperature outputs, (a) MO13_1, (b) US63_1, (c) US54_6, and (d) US54_1

The US54_6 section, on the other hand, shows three critical events in the same time-frame, probably caused by relatively low fracture energy and a high mixture VMA. The MO13_1 section is the worst performer among the lot. The section has high VMA and low m-value, prompting high thermal stress accumulation over time. It is recognized by the authors that ideally correct mixture CTEC values should have been used keeping in mind the variety of stockpiles utilized in this study. However, it is a common practice for the mixture CTEC to be assumed as closely as possible on the basis of the aggregate stockpiles used in the mixture.

6. RUBBER DEMONSTRATION PROJECTS IN MISSOURI

6.1. Introduction

Ground tire rubber, or GTR, is gaining popularity as a recycled mixture component and performance-enhancing modifier in the Midwest US (Gillen 2007, Bressette et al. 2007, H. Zhou et al. 2014, Hicks et al. 1999; Han et al. 2016). The noticeable increase in usage has been driven by recent advances in production technologies, material specifications, modern asphalt mixture performance testing, and competition leading to reduced cost as compared to polymer modified asphalt mixes. According to an annual survey report, 100,000 and 50,000 tons of GTR modified asphalt mixture were produced in Missouri in 2012 and 2013, respectively (Hansen et al. and Copeland 2017). The use of modified asphalt rubber in Missouri dates back to the early 1990s when MoDOT placed four test sections with various modifiers along the westbound driving lanes of I-44 in Phelps County and several experimental features projects were undertaken along I-44 in Laclede County and US 71 in Cass County. The modifiers included two polymers (styrene-butadiene-styrene [SBS] and styrene-butadiene rubber [SBR]) and two crumb rubbers modifiers (coarse and fine); the experimental features projects included placing rubber modified asphalt concrete overlay (RMAC), which was a generic name for the patented Plus Ride system (dry-process rubber modification), and asphalt rubber concrete (ARC) overlay (wet process). Overall, MoDOT did not have a great experience with rubber modification during the 1990s, with the polymer-modified section outperforming all the rubber-modified sections and rubber-modified sections showing problems like stripping, low-severity transverse cracking and so on (Gopalaratnam et al. 1999). However, rubber-modified asphalt has been used with success in other states of the Midwest and the US, as reported by various researchers and DOTs (Lo Presti 2013).

In 2016, Illinois Tollway used an engineered crumb rubber (ECR) product called Elastiko, which is a dry-process ground tire rubber modified with a chemical treatment, in one of the test sections on I-88 near DeKalb, Illinois. Details of its laboratory performance measurements can be found elsewhere (Buttlar and Rath 2017). Overall, the ECR-modified mixture showed good high and low temperature laboratory performance. In addition, the ECR-modified mixture was reported to have enhanced workability and compactability, which addresses a previous difficulty in GTR (CalRecycle 2019). Following this, the dry process ECR-modified mix was deployed at a field trial undertaken on I-35 near Kansas City, Missouri, as a collaboration between Ideker, Inc., the University of Missouri-Columbia, MoDOT, and Asphalt Plus, LLC. Mix design verification by performance testing with ECR and control mixes, field sampling, and lab testing of plant samples were conducted by the University of Missouri-Columbia, in the MAPIL (Mizzou Asphalt Pavement and Innovation Laboratory).

6.2. Dry Process Rubber Demonstration Project: I-35, Kansas City, Missouri, Fall 2017

In fall 2017, preliminary lab tests were performed on laboratory-prepared (pugmill-mixed) samples to ensure that the ECR mix possessed similar performance characteristics as the control mixture. Two rounds of mixture testing were performed; round one used the original binder content in the control mixture design in the ECR mixes, and round two used the recommended

+0.2% binder increase to accommodate additional cracking resistance. Although mixture performance testing is still under development in Missouri, the following criteria were established for the demonstration project by the University of Missouri and MoDOT:

- Target minimum DC(T) fracture energy: 690 J/m²
- Target minimum I-FIT flexibility index: 6.0
- Target maximum Hamburg rut depth at 20,000 passes: 12.5 mm (<10 preferred)

A summary of mix performance tests conducted on the design mixtures with detailed results is summarized in Table 6-1 for the control SMA and new dry GTR SMA trials 1 and 2.

Table 6-1. Summary of mix design performance test results

Test	Criteria	Control		GTR results (two trials)			
		Result	Pass/Fail	Trial 1	Pass/Fail	Trial 2	Pass/Fail
DC(T)	690 J/m ² min	663	Fail	690	Pass	717	Pass
I-FIT	FI ≥ 6	18.4	Pass	7.1	Pass	13.8	Pass
Hamburg	Rut ≤ 12.5 mm	12.5*	Fail	6.7	Pass	11.8	Pass

*A measured value of 12.52 mm was recorded

In general, it was found that the new dry GTR mix design mixes had equivalent or superior performance to the polymer-modified control mixture. In fact, all of the GTR test results for the three tests and two trials were found to meet criteria (6-for-6, or 100% passing rate), while the control mix only met 1-of-3 criteria (33% passing rate). The test results followed logical trends. The second ECR trial (with the recommended 0.2% higher binder content), displayed more cracking resistance as measured by both the DC(T) and I-FIT, but at the expense of higher Hamburg rut depth. Although the trial 2 Hamburg result for the GTR mix was above the preferred maximum rut depth of 10 mm articulated by MoDOT, it was still better than the control mixture and met the requirement of 12.5 mm maximum rut depth. Since the 20,000 pass Hamburg test is deemed as conservative, the control mixture has been used successfully in the field without significant rutting under interstate traffic, and the ECR trial 2 mix was judged as suitable in the I-35 mainline surface mix trial.

Also of significance was the level of repeatability of the two cracking tests conducted. For the three rounds of testing (control plus two ECR trials), the DC(T) displayed a coefficient of variability (COV) of 9%, 1%, and 6%, with an average of 5% COV. On the other hand, the I-FIT test results had much higher COV levels of 27%, 53%, and 27%, with an average of 36%. In general, a COV level below 20% is desirable for asphalt mixture performance testing in order to have confidence in making relative comparisons between mixtures and in forming performance specifications.

Several hundred tons of the new Ideker ERC SMA mix design were laid on the final evening of paving in the fall 2017 as an initial trial. The contractor had no difficulty in mixing and compacting the ECR-modified mix in the cold weather (air temperatures fell into the 10°C (50°F) range toward the end of paving). The trial ECR mix was laid on an exit ramp for an

abandoned truck weigh station, and had variable layer thickness. Cores were obtained in an area where the ECR was placed as the bottom lift of a two-lift overlay, and had thicknesses in the 30–40 mm range, which is short of the optimal 50 mm thickness for most lab performance tests. That notwithstanding, a limited number of DC(T) fracture and Hamburg wheel track tests were performed on the obtained cores. DC(T) fracture energies were correct for thickness, using a thickness correction factor developed at the MAPIL. The results are summarized in Table 6-2.

Table 6-2. Summary of performance testing of fall 2017 test strip mixes

Test	Criteria	Control		ECR	
		Result	Pass/Fail	Result	Pass/Fail
DC(T)	690 J/m ² min	753	Pass	1156	Pass
Hamburg	Rut ≤ 12.5 mm	18.5	Fail	11.2	Pass

The as-constructed ECR was found to exceed the performance of the control mix in both the low-temperature DC(T) cracking test, and in the high-temperature Hamburg wheel track test, which agreed with mix design testing results. The as-constructed ECR mix outperformed the mix design test samples, with significantly higher fracture energy and slightly lower rut depth.

6.2.1. Binder Test Results

Superpave Performance grading tests were performed on the neat (unmodified) binder used with ECR, which was specified as PG 58-28, and the modified binder used in the control mix (specified as 64-22V). Figure 6-1 shows the continuous low temperature performance grade (LTPG), high temperature performance grade (HTPG) and useful temperature interval (UTI) for the two binders.

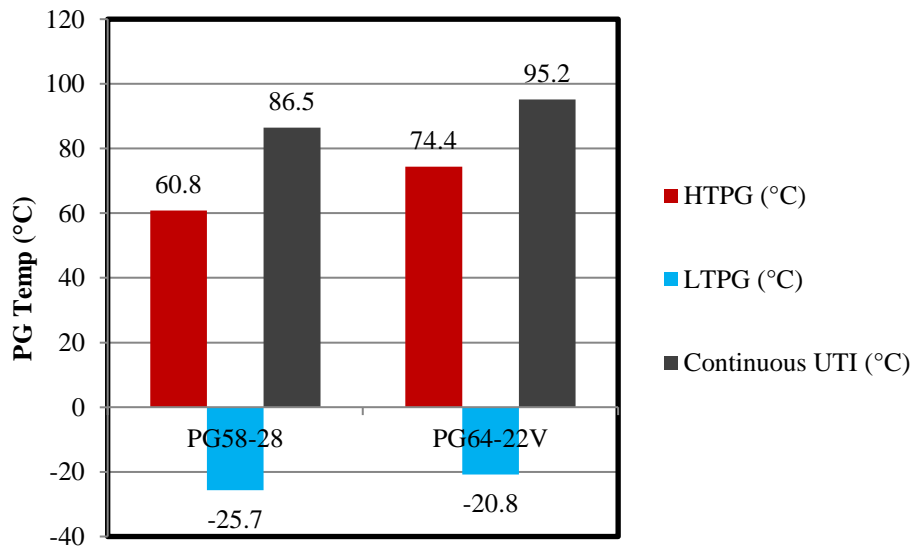


Figure 6-1. Summary of binder grading using DSR and BBR

According to Table 6-3, the continuous LTPG of 58-28 and 64-22V binders are -25.7°C and -20.8°C, respectively.

Table 6-3. Summary of BBR results on binders

Binder type	Temp. (°C)	Stiffness (60 s) MPa	S (60 s) MPa	COV %	m-value (60 s)	Mean m-value (60 s)	COV %	LTPG based on stiffness (°C)	LTPG based on m-value (°C)	ΔT _c (°C)
58-28	-12	128.6	125.5	8.2	0.34	0.34	0.9	-29.2	-25.7	-3.5
	-12	133.8			0.34					
	-12	114.0			0.34					
	-18	280.3	270.4	4.6	0.28	0.28	0.9			
	-18	256.4			0.28					
	-18	274.4			0.27					
64-22V	-6	90.7	90.2	0.8	0.35	0.34	1.6	-30.6	-20.8	-9.8
	-6	89.4			0.34					
	-6	90.7			0.35					
	-12	173.3	176.6	2.7	0.29	0.29	0.8			
	-12	182.1			0.29					
	-12	174.4			0.29					

Therefore, the LTPG of the binders is -22°C and -16°C, respectively, which is outside of the specified low temperature grades for this binder. Another factor used recently by researchers as an low temperature performance factor is ΔT_{cr} (Equation (10)). ΔT_{cr} is the difference between the LTPG based on creep stiffness criteria (S = 300) and m-value (m = 0.300) (Anderson et al. 2011). Highly negative numbers indicate an m-dominated binder, which have been shown to be more prone to field cracking. The 64-22V binder was found to have a highly m-controlled response, which may be due to the nature of the modifiers used in the binder.

$$\Delta T_{cr} = T_{cr}(\text{stiffness}) - T_{cr}(\text{m-slope}) \quad (10)$$

where

T_{cr} (stiffness) is the critical low temperature where S(60) = 300 MPa

T_{cr} (m-slope) is the critical low temperature where m(60) = 0.300

6.3. Dry Process Rubber Demonstration Project: I-35, Kansas City, Missouri, Spring 2018

Demonstration project oversight was provided by members of the University of Missouri MAPIL research team (led by Professor Bill Buttlar), representatives from Asphalt Plus (who supplied the ECR product and the ECR feeder system), and a MoDOT representative (Mr. Dan Oesch). The ECR feed system (Figure 6-2) was installed at Ideker’s Mosby asphalt plant, which can be completed in less than one day.



Figure 6-2. View inside ECR feeder unit showing pugmill-style agitation system

Installation of the feeder unit, which is very similar to an SMA cellulose fiber feeder unit, involves leveling and anchoring of the unit, installation of power to the unit, connection of the ~ 4 in. output hose to the lower portion of the drum plan (similar location as the fiber feed), and routing of the cable for the external feed rate output monitor to the asphalt plant control trailer (Figure 6-3).

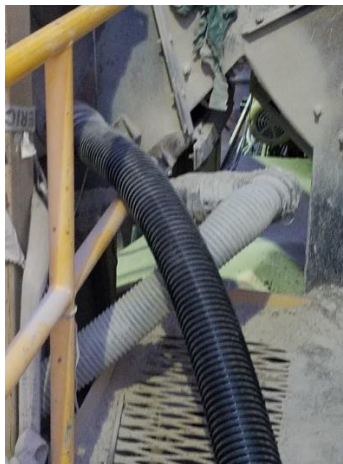


Figure 6-3. Connection of fiber and ECR-GTR hoses at similar location near bottom of drier drum

Similar to the Illinois Tollway contractor experience, the ECR mix demonstrated ease in compactability in the field and excellent release from trucks and paving equipment (Figure 6-4).



Figure 6-4. ECR SMA night paving on I-35 mainline in spring 2018

On the night of May 9, 2018, plant mix was sampled by filling the bucket of a front end loader from the surge silo and creating a sample pad in front of the plant's QC lab. Personnel from MAPIL, MoDOT, and Ideker filled more than 100 sample containers from this sampling pad for testing at the respective laboratories. A smaller team sampled the non-ECR control mix a few weeks later on May 21.

6.3.1. DC(T) Fracture Energy Test Results of Plant-Produced Mixtures

Figure 6-5 shows the average DC(T) fracture energy of four replicates tested at -12°C.

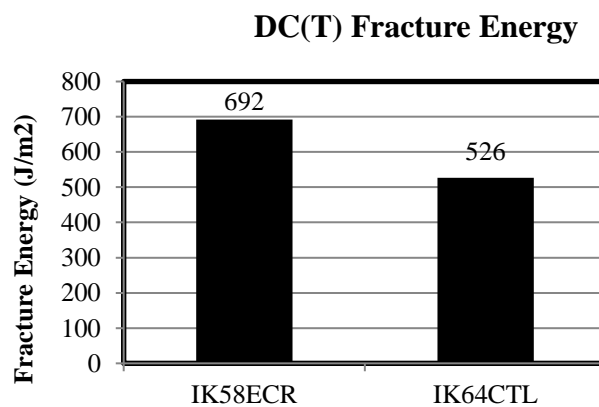


Figure 6-5. DC(T) fracture energy of SMA mixtures at -12°C for plant mixes

Similar to the design mixes, higher fracture energy was measured on the ECR-modified mixture as compared to the control SMA mixture. The ECR plant-produced mixture met the DC(T)

threshold for fracture energy, while the control mixture was approximately 25% below the recommended level of 690 J/m² for SMA mixes.

6.3.2. SCB Test Results

Similar cracking test trends were found in the IL-SCB, or I-FIT cracking test (Figure 6-6).

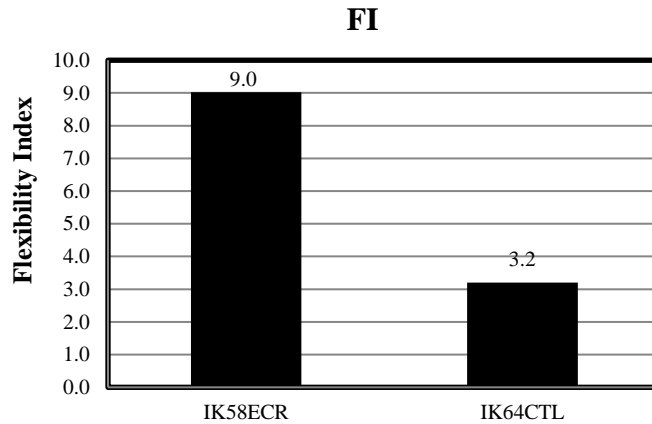


Figure 6-6. SCB cracking test results for SMA mixture at 25°C

Unlike the lab testing results, the ECR plant-produced mixture was found to be significantly more crack resistant at intermediate temperature as compared to the control mix. In the case of the plant-produced mixture, the ECR mixture exceeded the recommended threshold of 6, with an average value of 9.0, while the control mix was nearly 50% below the threshold (FI = 3.2).

6.3.3. IDEAL Test Results

In winter 2018, the IDEAL cracking test equipment was installed at MAPIL. Due to its convenience and potential use as a quality control test, the sampled mixtures were subjected to the IDEAL cracking test. The results of the IDEAL tests are provided Figure 6-7.

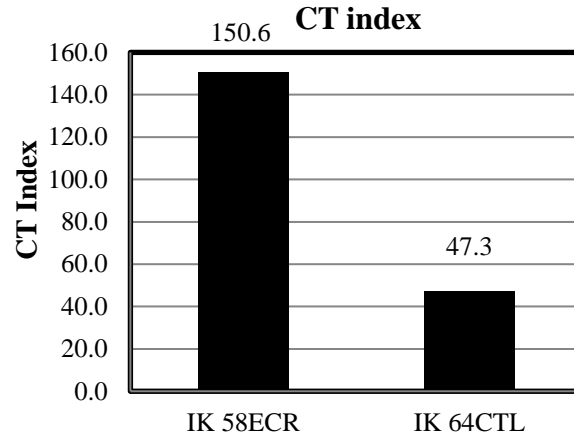


Figure 6-7. IDEAL cracking test results for SMA mixtures at 25°C

Early literature suggests a minimum CT index of 145 for SMAs (Zhou 2018) to control cracking at intermediate temperatures. The IK58ECR was found to have the highest CT index (150.6), while the IK64CTL was measured to have a much lower CT index of 47.3 (Figure 6-7). Consistent with the DC(T) and I-FIT, the ECR mix was found to have superior cracking resistance as compared to the control mix, and meets recommended performance test criteria, while the control mix falls well short.

6.3.4. Hamburg Wheel Tracking Test Results

Hamburg wheel tracking test (HWTT) was performed with 20,000 passes and at 50°C, which is recommended for high traffic levels. Figure 6-8 shows the rut depths accumulated under the HWTT for the three tested sections.

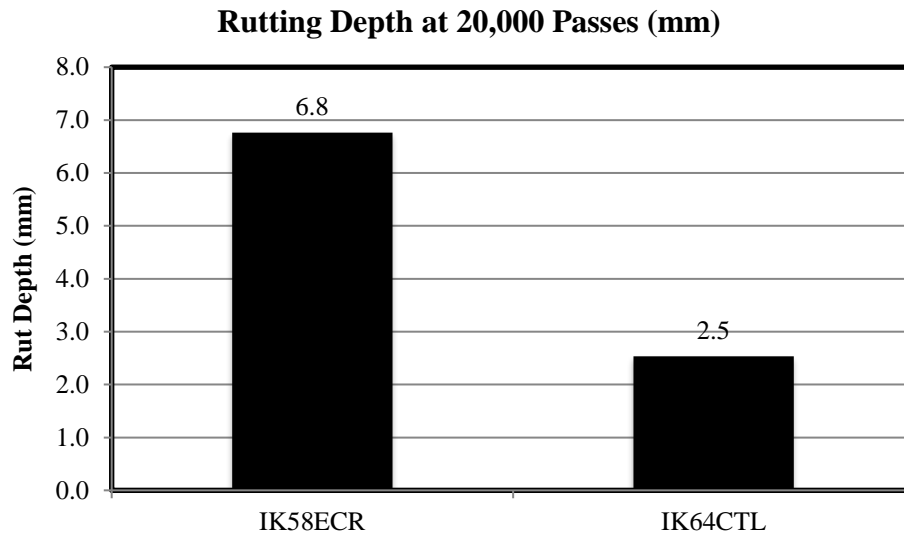


Figure 6-8. Hamburg wheel track test results for SMA mixtures at 50°C

Both plant-produced mixes, ECR and control, performed much better than the lab mixes, and easily met the maximum rut threshold of 12.5 mm. Consistent with cracking test results, the ECR mix was found to be less stiff than the control mixture. Accordingly, the rut depth in the ECR mix was measured at 6.8 mm, while the control mix had a very low Hamburg rut depth of 2.5 mm. Overall, it can be concluded that the ECR mix had a better balance of cracking and rutting test performance characteristics, meeting all three crack test criteria, along with rut criteria. On the other hand, the control mixture only met rutting criteria, while falling considerably short of cracking criteria in all three tests.

6.4. Summary and Conclusions

In this research, the effect of using ECR in the dry process was investigated in SMA mixtures on I-35 near Kansas City, MO. A softer base binder (PG58-28) was used in the ECR-modified mixture, while PG64-22V (polymer modified binder) was utilized in the control SMA mixture. Different mixture cracking tests including DC(T) fracture energy (low temperature), SCB (I-FIT), and IDEAL tests (intermediate temperature) were performed to evaluate the potential use of ECR in SMA mixtures in Missouri. The major findings from this study are as follows:

- Overall, ECR outperformed the control SMA mix in both the mix design and the field trial study phases.
- In the design phase, ECR mixes had superior DC(T) fracture energy and rutting resistance, while the control mix had a higher flexibility index.
- In the design phase, both ECR trial mixes (differing in asphalt content by 0.2%) met the DC(T), I-FIT, and Hamburg criteria (6-of-6 test results met criteria), while the control mix met only 1-of-3 criteria.
- In the production phase, the ECR mix met 4-of-4 criteria, including far superior crack test results in each of the three tests investigated (DC(T), I-FIT, and IDEAL), while the control

mix met only 1-of-4 criteria.

- Overall, the ECR mix was found to have a better balance of cracking and rutting performance than the control mix.
- Similar to the experience on the Illinois Tollway and in Georgia, the ECR, dry GTR process was found to be relatively straightforward to produce, and easy to lay down in the field. It also showed excellent release characteristics, easily sliding out of delivery trucks and with minimal adherence to other production and construction equipment.
- ECR functions as a warm mix additive, providing easier compaction at lower mat temperatures.
- Given the performance test results obtained, ease of construction, and potential cost savings to the contractor, and in turn, to the state of Missouri, it is recommended that the new dry GTR processes be specified for use in Missouri. The following are recommended for the ECR specification:
 - A binder bump following the manufacturer's recommended level of 0.1% binder addition to a control mix design per 5% of ECR used (by weight of binder).
 - Mixture performance testing in lieu of Superpave or MSCR binder requirements, which are judged as more predictive than binder tests results. In addition, binder testing of GTR-modified binders is cumbersome, and its correlations to field performance are questionable. Preferably one rutting and one cracking mix performance test should be specified.
 - The DC(T) is believed to have the best correlation to low temperature cracking, is the most repeatable, and has the most field performance data available to date. The I-FIT uses a smaller sample size and less expensive equipment, but has a much higher variability as measured by COV. The IDEAL test has little field data in the Midwest, but has a very low test cost and is by far simplest to perform (and the only test suitable for the QC phase).

7. FIELD PERFORMANCE EVALUATION

7.1. Field Sections Studied and Investigated in this Chapter

This chapter investigates field sections that were constructed prior to 2016. These sections are summarized in Table 7-1.

Table 7-1. Field sections with significant time in service

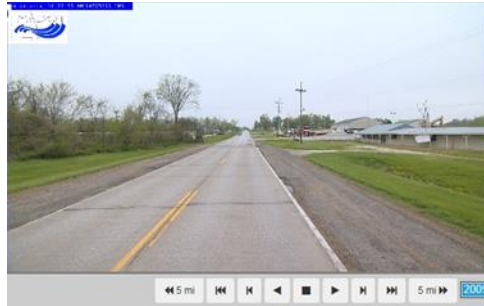
Section # (%ABR total - % by RAP - % by RAS)	Constr. year	Virgin binder grade	Asphalt content	ABR (%)	%ABR by RAP	%ABR by RAS
MO52_1 (34-0-34)	2010	PG64-22	4.8%	33.5	0	33.5
US54_8 (9-9-0)	2006	PG70-22	5.6%	8.6	8.6	0
US50_1 (25-25-0)	2011	PG64-22	5.0%	24.6	24.6	0
US63_2 (30-20-10)	2008	PG64-22	5.6%	29.9	19.9	10
US54_7 (0-0-0)	2003	PG64-22	6.2%	0	0	0

Table 7-2 shows the latest field performance measures available for these sections, as of the year 2017.

Table 7-2. Performance measures in 2017 for field sections

Section # (%ABR total - % by RAP - % by RAS)	Constr. year	IRI (in./mi)	Paser rating	ARAN rut depth (mm)	Visual observations
MO52_1 (34-0-34)	2010	91	4.0	7.1	Mainly joint reflective cracking
US54_8 (9-9-0)	2006	64	5.5	2.0	Block cracking developing
US50_1 (25-25-0)	2011	61	6.5	2.2	Very little distress
US63_2 (30-20-10)	2008	78	4.5	1.5	Dense block & thermal cracking
US54_7 (0-0-0)	2003	53	7.5	3.0	Very little distress after 14 years

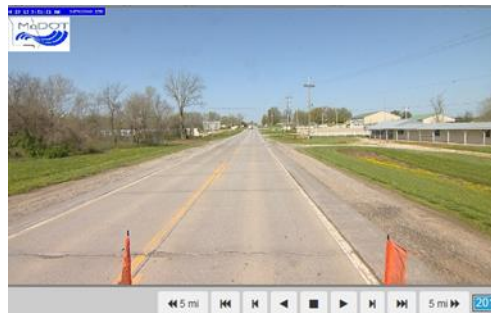
A series of photos selected from MoDOT's ARAN viewer portal are presented in Figure 7-1 through Figure 7-5 for each section.



(a) Pre-existing condition (2009)



(b) Condition just after paving in 2010



(c) Condition in 2013



(d) Condition in 2017

Figure 7-1. Series of ARAN photos for MO52_1



(a) Pre-existing condition (2005)



(b) Condition just after paving in 2007

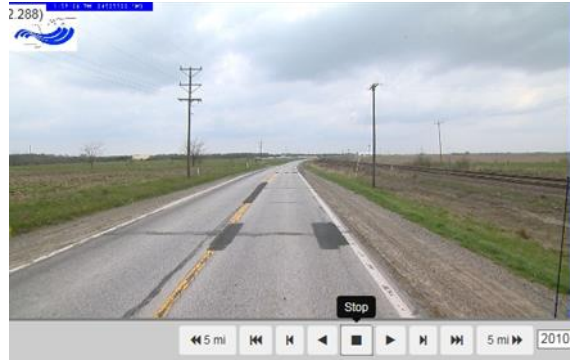


(c) Condition in 2013

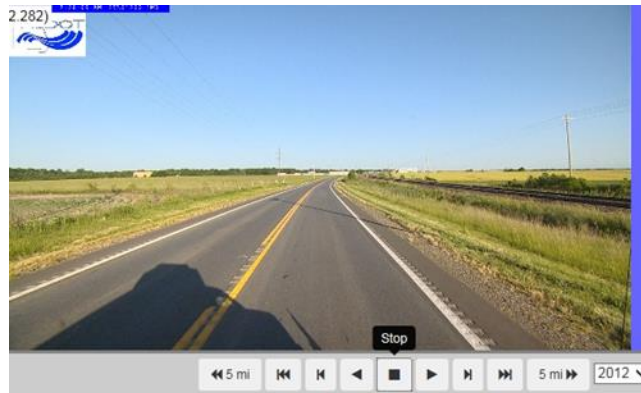


(d) Condition in 2017

Figure 7-2. Series of ARAN photos for MO54_8



(a) Pre-existing condition (2010)



(b) Condition just after paving in 2011



(c) Condition in 2017

Figure 7-3. Series of ARAN photos for MO50_1



(a) Pre-existing condition (2008)



(b) Condition just after paving in 2009

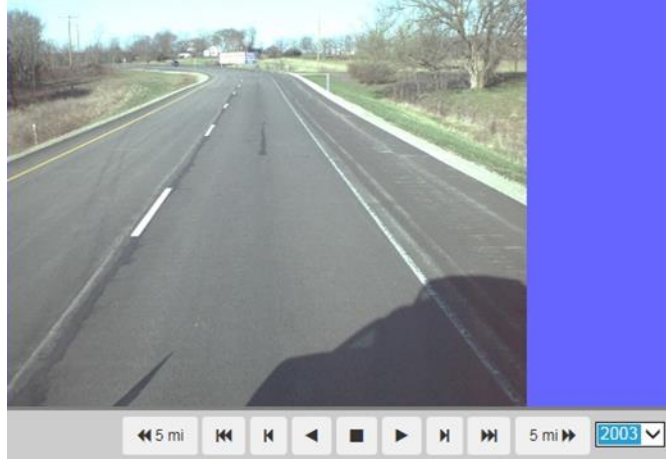


(c) Condition in 2014

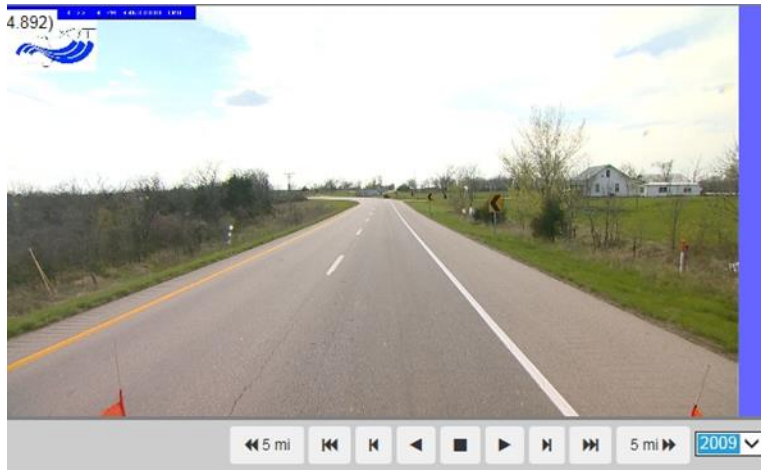


(d) Condition in 2017

Figure 7-4. Series of ARAN photos for MO63_2



(a) Condition just after paving in 2003



(b) Condition in 2009



(c) Condition in 2016

Figure 7-5. Series of ARAN photos for MO54_7

Where available, condition of the pavement is shown in the year prior to rehabilitation, after construction, during service, and at present.

7.2. Relation of Field Performance to Recycling Levels and Performance Tests

Table 7-3 summarizes the five field sections with respect to recycling levels, virgin binder grade used, and performance rating.

Table 7-3. Field section details vs. average deterioration rate

Section # (%ABR total - % by RAP - % by RAS)	Constr. year	Virgin binder grade	Asphalt content (%)	ABR (%)	%ABR by RAP	%ABR by RAS	Det. rate (rating/yr.)*	Visual crack rating (5=worst)**
MO52_1 (34-0-34)	2010	PG64-22	4.8	33.5	0	33.5	0.83	4
US54_8 (9-9-0)	2006	PG70-22	5.6	8.6	8.6	0	0.45	3
US50_1 (25-25-0)	2011	PG64-22	5.0	24.6	24.6	0	0.25	2
US63_2 (30-20-10)	2008	PG64-22	5.6	29.9	19.9	10	0.63	5
US54_7 (0-0-0)	2003	PG64-22	6.2	0	0	0	0.14	1

*Average deterioration rate in terms of change in PASER rating per year

**Average deterioration rate for cracking distresses, relative ranking

A deterioration rate was computed based on the average decline in PASER rating over the service life of the overlay. A second rating scale was developed based only on the cracking distresses observed (i.e., ignoring rutting and roughness), as shown in the final column. Clearly, the US54_7 section was the best performer, with a very low deterioration rate (still very little cracking after 15 years in service). This section contained no recycling, and also possessed a relatively high binder content for a 12.5 NMA mix (6.2%). The worst two performers were MO52_1 and US63_2, which had the highest recycling rates (34 and 30% ABR, respectively), but without any bumping/softening of the virgin binder grade.

Figure 7-6 and Figure 7-7 provide plots of PASER rating versus years in service, and IRI versus years in service, respectively.

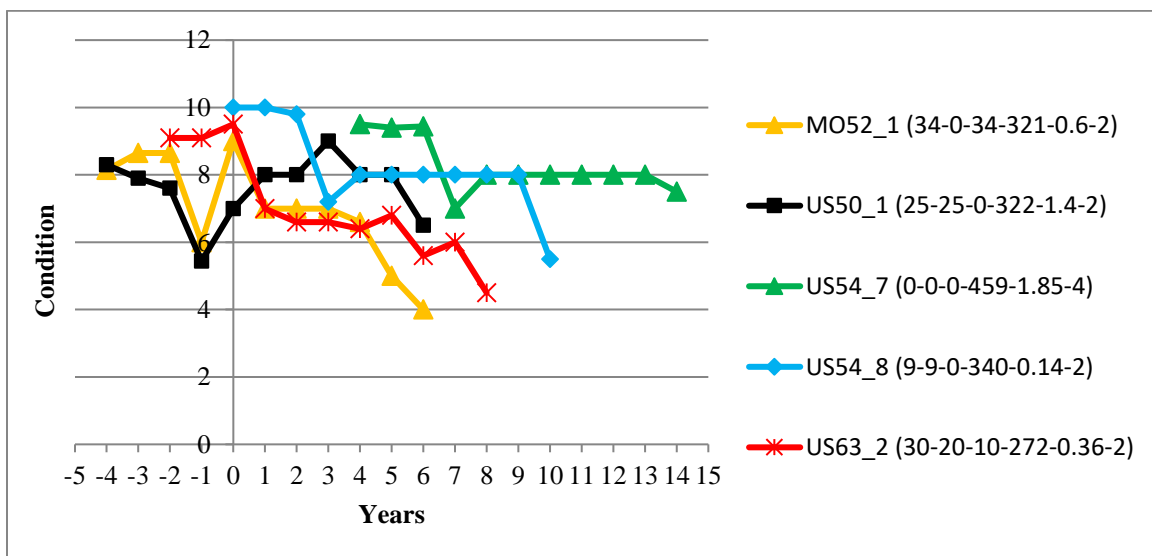


Figure 7-6. PASER rating vs. years in service

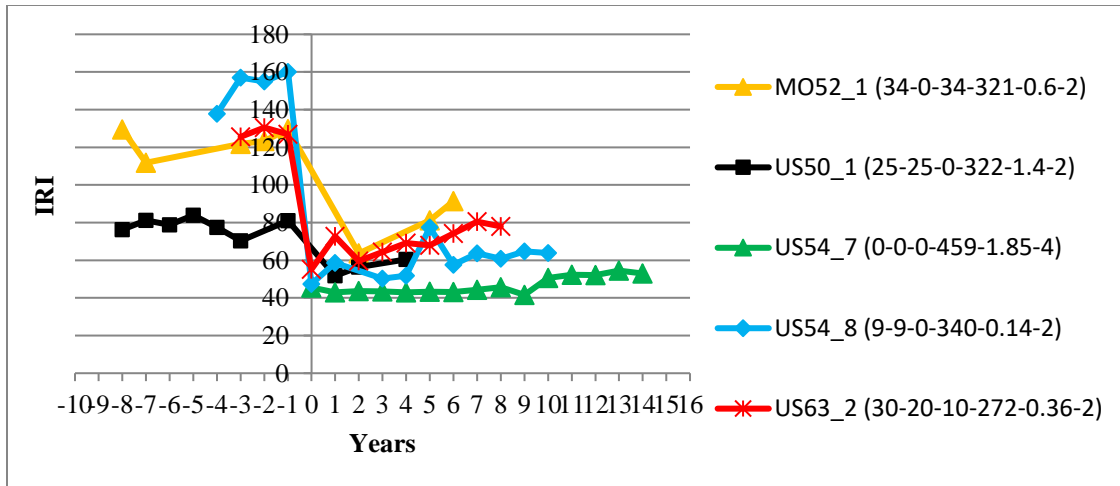


Figure 7-7. IRI vs. years in service

The legends on the plots display the recycling ABR breakdown, DC(T) fracture energy (in J/m²), and I-FIT FI.

The time of construction was taken as year zero for each section, and thus the condition of the pre-existing pavement is represented by negative year labels on the plots. Although fluctuations in the PASER and IRI data create some ambiguity, the overall deterioration rate and overlay performance can be reasonably assessed. These plots further demonstrate the relatively good performance of US54_7, and relatively poor performance of MO52_1 and US63_2. Identical rankings in terms of IRI and PASER deterioration rates are noted.

Table 7-4 provides a summary of field performance versus lab cracking performance tests.

Table 7-4. Field performance vs. lab cracking tests

Section # (% ABR total - % by RAP - % by RAS)	ABR (%)	Det. rate (rating/yr.) *	Deterioration ranking (5=worst)	Visual crack rating (5=worst) **	DC(T) Gf (J/m ²)	DC(T) rank (5=worst)	I-FIT FI	I-FIT Rank (5=worst)
MO52_1 (34-0-34)	33.5	0.83	5	4	321	4	0.6	3
US54_8 (9-9-0)	8.6	0.45	3	3	340	2	0.14	5
US50_1 (25-25-0)	24.6	0.25	2	2	322	3	1.4	2
US63_2 (30-20-10)	29.9	0.63	4	5	272	5	0.36	4
US54_7 (0-0-0)	0	0.14	1	1	459	1	1.85	1

*Average deterioration rate in terms of change in PASER rating per year

**Average deterioration rate for cracking distresses, relative ranking

Both tests correctly identified the best and worst performers of the five sections investigated. The DC(T) correlated the best with the visual cracking rating, rating three-out-of-five sections (the first fourth, and fifth best performers) in the correct ranking, with only a swap between the second and third ranked sections. The I-FIT matched the correct ranking of two-out-of-five sections for both the deterioration rate and visual crack ranking. The largest discrepancy between

DC(T) and I-FIT rankings was for section US54_8, where the DC(T) ranked this section as #2, while the I-FIT ranked it last (#5 of 5), whereas the correct ranking was #3 of 5.

Table 7-5 lists the Coefficient of Variation (COV) for the two performance tests for the field sections tested.

Table 7-5. Test averages and coefficient of variability for field sections

Section # (%ABR total - % by RAP - % by RAS)	DC(T) Gf (J/m ²)	DC(T) COV (%)	Avg. COV DC(T)	I-FIT FI	I-FIT COV (%)	Avg. COV I-FIT
MO52_1 (34-0-34)	321	3.8	16.4%	0.6	51.4	51.3%
US54_8 (9-9-0)	340	25.5		0.14	80.7	
US50_1 (25-25-0)	322	27.6		1.4	51.6	
US63_2 (30-20-10)	272	13.7		0.36	35.4	
US54_7 (0-0-0)	459	11.4		1.85	37.6	

The average DC(T) COV for the field sections was 16.4%, slightly higher than the overall COV for the 18 mixtures investigated (Table 5-3), but still within the recommended maximum COV range of 20%. On the other hand, the I-FIT test had an average COV of 51.3% for the field section evaluations. Higher COV values make it more difficult to draw inferences regarding statistical differences between means of sample populations to be compared (for instance, between testing parties), and create more uncertainty when comparing mean values against specification requirements.

Clearly, more tests sections are needed to further evaluate performance tests and specification limits needed to establish a balanced mix design approach for recycled materials. That notwithstanding, the results obtained herein show the strong possibility of arriving at a specification in the near future that would allow contractor innovation in designing modern, heterogeneous recycled mixtures.

8. SUMMARY, CONCLUSIONS, AND RECOMMENDATIONS

8.1. Summary

A comprehensive lab and field investigation was carried out to evaluate the performance of recycled asphalt mixtures in Missouri. This project was sponsored by the Missouri Department of Transportation, and carried out at the University of Missouri-Columbia. The project also served to meet the matching funds requirement for a related project carried out in the Midwest Transportation Center (MTC). Eighteen field sections were evaluated, including a number of sections from the recent Long-Term Pavement Performance (LTPP), Special Pavement Sections (SPS-10) project in Osage, Beach, Missouri, which was constructed in 2016. Good and poor performing sections dating back as far as 2003 construction were sampled and tested. Binder testing and mix performance tests were carried out on field cores and laboratory compacted specimens. The study focused on medium traffic volume Superpave mixes.

Some key observations made in the study include:

- Missouri has a long legacy of recycling innovation with RAP and RAS, and recently contractors are pushing the envelope even further by using high amounts of binder replaced with heterogeneous RAP, RAS, and GTR mixes, sometimes incorporating rejuvenators.
- The national rule of thumb, suggesting the use of softer virgin binder grades for binder replacement levels over 20%, appear to be validated based on lab and field test results. For ABR values above 30%, it appears that double grade bumping may be required.
- When ABR levels are properly balanced with a softer virgin binder, good lab and field performance measures were generally obtained.
- The Hamburg-DC(T) plot demonstrated the potential benefit of incorporating a small amount of RAS into a recycled asphalt mix design, provided that an appropriate virgin binder was selected.
- A very good performing field section was identified and tested in this study (US54_7). This section has performed very well after 15 years in service, and still has a low roughness (IRI=53), low rutting (3 mm) and a high PASER rating (7/10). This, along with performance of the other four test sections, tended to validate the recommended long-term aged DC(T) minimum threshold of 400 J/m², as the US54_7 section still possesses 459 J/m² of fracture energy, while the sections with relative fast deterioration rates had fracture energy values in the low 300 s or as low as 272 J/m², in a section with advanced block and thermal cracking (US63_2). The I-FIT results appear to suggest a threshold of around 1.0 for long-term flexibility index.
- The DC(T)-Hamburg plot showed insight toward the current state and future adjustments for Missouri recycled mixes, including:
 - Missouri recycled mixes are generally on the brittle side, although 3 of 11 newer mixes investigated met recommended Hamburg and DC(T) criteria.
 - Most mixes exhibit sufficient total energy to pass Hamburg and DC(T) recommended criteria without major changes in the aggregate structure, recycling level, or binder cost. Adjusting these mixes would simply involve the selection of a softer virgin binder grade, with a similar useful temperature interval (UTI), and therefore similar cost to the existing

- binder (which is normally PG 64-22 or PG 64-22H).
- Four mixes exhibited failing Hamburg results at 20,000 wheel passes, while two of these mixes also failed to pass the Hamburg test at 10,000 wheel passes (which is more appropriate for medium-volume roads). These mixes showed a clear stripping inflection point.
 - Most Superpave mixes in Missouri probably do not have sufficient total energy to meet the stricter requirements suggested for high-volume roads. This seems to validate MoDOT's recent move to SMA mixes for high traffic volume facilities.
 - Both DC(T) and I-FIT tests exhibited a good spread in test values obtained for the broad array of mixtures tested in this study. The I-FIT test exhibits a very wide range in values, with normalized test values ranging from nearly zero to 100%, while the normalized DC(T) fracture energy values ranged from about 60 to 100%.
 - The differences in test range for the DC(T) and I-FIT is accompanied by significant differences in test repeatability for these two cracking tests. The DC(T) showed an average coefficient of variability (COV) for all study mixes of 12.7%, and 16.4% for the five long-term aged sections investigated. The I-FIT test showed an average COV for all study mixes of 44.6%, and 51.3% for the five long-term aged sections investigated.
 - The DC(T) and I-FIT were both able to identify the best and worst performing section among the five field sections. The relative rankings suggest that the two tests are providing different crack measures for the asphalt tested. The DC(T) was most correlated to the rate of thermal and block crack development.

8.2. Conclusions

Based on the findings of the study, the following conclusions were drawn:

1. Missouri's practices for the responsible and effective use of recycled materials continues to improve over time. Recent mix designs demonstrate more appropriate balancing between recycled material levels and virgin binder selection, resulting in better performance tests results when compared to older recycled mix designs.
2. Opportunities exist for further improving recycled mix design methods and recycling optimization in Missouri, including:
 - a. Moving to higher ABR levels, by implementing mixture performance tests (balanced mix design);
 - b. Increasing the use of recycled ground tire rubber (GTR) in Missouri mixes, by using balanced mix design to certify mixes using new, more economical GTR recycling methods, and;
 - c. Researching the use of recycled materials in stone mastic-asphalt (SMA) designs.
3. The Hamburg-DC(T) plot can be used to quickly and effectively design and adjust recycled mixtures to meet rutting and cracking performance requirements. This may serve to reduce mix design iterations. When data is viewed holistically on this diagram, industry-wide trends can be observed, leading to new recommended practices and areas of opportunity.

8.3. Recommendations

Based on the findings of this study, the following recommendations are suggested:

1. More work is needed to further evaluate and fine-tune mix performance tests for use in balanced mix design, which is particularly important for modern, heterogeneous recycled mixes. This should include:
 - a. Sampling and testing of additional field sections, including a broad array of materials, recycling combinations, and project age;
 - b. Developing a reliability-based approach for setting performance test thresholds;
 - c. Considering adjustments to the Hamburg test to make it more performance-based and climate-based; i.e., making the test temperature related to climate and wheel pass requirements related to traffic level;
 - d. Working to improve the streamlining of and repeatability of mixture performance tests, and determining which tests are most appropriate for design, quality control, and quality assurance (not necessarily the same tests will be appropriate for QC).
 - e. Working toward a performance design approach for balanced mix design, where performance testing is given priority over mix volumetrics and ingredient specifications, rendering the designs as more innovative, less expensive, more sustainable, and more tied to performance.
2. More work is needed to evaluate GTR recycling, especially some of the new dry process techniques that are more economical, and more contractor friendly. Ongoing demonstration projects in Missouri should be included in future research.
3. A better physical understanding of recycling physics and chemistry is needed in order to arrive at even higher recycling amounts, in a confident manner. More binder and component characterization is needed, along with micromechanical modeling to better understand the interactions between recycled materials.

REFERENCES

- Anderson, R. M., G. N. King, and D. I. Hanson. 2011. Evaluation of the Relationship between Asphalt Binder Properties and Non-Load Related Cracking. *Journal of the Association of Asphalt Paving Technologists*, Vol. 80.
- Bazant, Z. P., and P. C. Prat. 1988. Measurement of Mode III Fracture Energy of Concrete. *Nuclear Engineering and Design*, Vol. 106, No. 1, pp. 1–8.
- Bressette, T., H. Zhou, A. Stonex., and R. G. Hicks. 2007. Asphalt Rubber and Its Potential Use in China. *Plan, Build, and Manage Transportation Infrastructures in China Congress 2007 (ISSTP)*, pp. 776–85.
- Buttlar, W. G., and P. Rath. 2017. *Illinois Tollway I-88 Ground Tire Rubber Test Sections: Laboratory Mix Designs and Performance Testing*. Illinois Tollway, Downers Grove, IL.
- CalRecycle. 2019. Rubberized Asphalt Concrete: Design and Specification Guide. RAC-103. Integrated Waste Mangement Board, California Department of Resources, Recycling, and Recovery, Sacramento, CA.
- Dave, E. V., Hoplin, C. 2015. Flexible pavement thermal cracking performance sensitivity to fracture energy variation of asphalt mixtures. *Road Materials and Pavement Design*, Vol. 16, pp. 423–441.
- Dave, E. V., W. G. Buttlar, S. Leon, B. Behnia, and G. H. Paulino. 2013. IlliTC—Low Temperature Cracking Model for Asphalt Pavements. *Road Materials and Pavement Design*, Vol. 14, pp. 57–78.
- Gillen, S. 2007. *Ground Tire Rubber(GTR) Asphalt Pavement Demonstration Project*. Illinois Tollway, Downers Grove, IL.
- Gopalaratnam, V. S., J. W. Baldwin, and W.-M. Cao. 1999. *Temperature-Dependent Performance of Polymer Concrete Wearing Surface System on the Poplar Street Bridge*. Missouri Department of Transportation, Columbia, MO.
- Han, L., M. Zheng, and C. Wang. 2016. Current Status and Development of Terminal Blend Tyre Rubber Modified Asphalt. *Construction and Building Materials*, Vol. 128, pp. 399–409. <https://doi.org/10.1016/j.conbuildmat.2016.10.080>.
- Hansen, K. R. and A. Copeland. 2017. *Asphalt Pavement Industry Survey on Recycled Materials and Warm-Mix Asphalt Usage: 2016*. National Asphalt Pavement Association, Lanham, MD.
- Hicks, R. G., J. R. Lundy, and J. A. Epps. 1999. *Life Cycle Costs for Asphalt-Rubber Paving Materials*. Rubber Pavements Association, Tempe, AZ.
- Lo Presti, D. 2013. Recycled Tyre Rubber Modified Bitumens for Road Asphalt Mixtures: A Literature Review. *Construction and Building Materials*, No. 49, pp. 863–881. <https://doi.org/10.1016/j.conbuildmat.2013.09.007>.
- Marasteanu, M., W. Buttlar, H. Bahia, and C. Williams. et al. 2012. *Investigation of Low Temperature Cracking in Asphalt Pavements National Pooled Fund Study*. Minnesota Department of Transportation, Minneapolis, MN.
- Mohammad, L. N., M. A. Elseifi, A. Raghavendra, and M. Ye. 2015. *Hamburg Wheel-Track Test Equipment Requirements and Improvements to AASHTO T 324*. Final Report for NCHRP Project 20-07/Task 361, Transportation Research Board, Washington, DC.

- Ozer, H., I. L. Al-Qadi, J. Lambros, A. El-Khatib, P. Singhvi, and B. Doll. 2016. Development of the Fracture-Based Flexibility Index for Asphalt Concrete Cracking Potential Using Modified Semi-Circle Bending Test Parameters. *Construction and Building Materials*, No. 115, pp. 390–401.
- Paris, P. C., and F. Erdogan. 1963. A Critical Analysis of Crack Propagation Laws. *Journal of Basic Engineering*, No. 85, pp. 528–533.
- Zhou, F. 2018. “IDEAL Cracking Test for QC / QA and Associated Criteria.” *Texas A&M Transportation Institute*.
- Zhou, F., S. Im, L. Sun, and T. Scullion. 2017. Development of an IDEAL Cracking Test for Asphalt Mix Design and QC/QA. *Road Materials and Pavement Design*, Vol. 18, pp. 405–427.
- Zhou, H., S. Holikatti, and P. Vacura. 2014. Caltrans Use of Scrap Tires in Asphalt Rubber Products: A Comprehensive Review. *Journal of Traffic and Transportation Engineering (English Edition)*, Vol. 1, No. 1, pp. 39–48. [https://doi.org/10.1016/S2095-7564\(15\)30087-8](https://doi.org/10.1016/S2095-7564(15)30087-8).

**THE INSTITUTE FOR TRANSPORTATION IS THE FOCAL POINT FOR TRANSPORTATION
AT IOWA STATE UNIVERSITY.**

InTrans centers and programs perform transportation research and provide technology transfer services for government agencies and private companies;

InTrans manages its own education program for transportation students and provides K-12 resources; and

InTrans conducts local, regional, and national transportation services and continuing education programs.



**IOWA STATE
UNIVERSITY**

Visit www.InTrans.iastate.edu for color pdfs of this and other research reports.